A Shape-Based Approach for Image Retrieval in Healthcare Information Infrastructure

O.O. Olugbara

July 2008

DECLARATION

I declare that this thesis was written by me and that the work contained herein is my own except where explicitly stated otherwise in the text. This work has not been submitted for any other degree at any university, institution of higher learning or professional qualification.

Oludayo Olufolorunsho Olugbara

Signature

Date

DEDICATION

Those who seek justice suffer injustice, those who seek injustice enjoy the pleasure of the world for a transient period, but the Almighty God is the LORD of justice.

To the famous UNILORIN 49+,
for our indissoluble togetherness and tenderness and for the future of our country together.

To my late lovely mother Aina Olugbara, she left three of us, Bose (8), Dayo (6) and Dele (2) when we were still very young.

To Taiwo Oloruntoba-Oju (PhD),
for his steadfastness and unbending deportment against pervasive prejudice.

ACKNOWLEDGEMENTS

The LORD is good, a stronghold in the day of trouble, and he knoweth them that trust in him, Nahum 1:7.

First, I would like to thank the Almighty God, without his steadfast love, enduring mercy, unflinching support and divine fortification, I could not achieve anything. The love of God for me and my family is stoutly appreciated.

Next, I would like to thank my ebullient supervisor, Prof. Mathew, O. Adigun, director of center for mobile e-services for development. I am very fortunate to have had him as my supervisor. He prepared me well from the beginning of my career as an academic and I am completely favored working under his supervision. My heartfelt gratitude goes to him for his intellectual contribution to improve the quality of this work. His constructive criticisms and general comments encouraged and enabled me to assiduously work. I also wish to particularly thank him for all the reference materials that he gave me freely and for taking his time and effort to scrupulously edit this thesis at different stages of its development despite his tight schedule.

I would also like to express my thanks to my co-supervisor, Sunday, O. Ojo, professor of computer science and head of department. He initiated many of the ideas in this work and provided very useful insights from a broad spectrum and deep understanding of many problem areas. More importantly, he has always been available to help me throughout the research process and I enjoy his maximum support and unremitting love.

I would like to acknowledge my deepest appreciation to Prof. T.C. Moyo for taking his time and effort to meticulously edit the final draft of this work. Comments and amendments suggested by him were duly incorporated to improve the quality of this work.

I would like to thank many great professors and researchers across the world that provided assistance during the course of this study. I would like to particularly thank Michael, J. Aramini of Massachusetts Institute of Technology (USA), Chunming, Li of Vanderbilt University (USA), Li Wang of Nanjing University of Science and Technology (China), Joseph, P. Hornak of Rochester Institute of Technology (NY), Jovisa Zunic of Exeter University (UK). I still rely on many comments and e-materials they provided to support this work. I appreciate the help from Borland International (USA) at the implementation stage of this work. I would like to thank Professors, I. Foster (USA), S. Jaehnichen (Germany), J. Bishop (South Africa), W. Hall (UK), W. Tichy (Germany), N. Shabolt (UK), C. Bishop (UK), A. Philips (UK). The lectures and materials they provided at 4^{th} IFIP WG 2.4 summer school in Cape Town, South Africa tremendously helped me to timely complete this study. I thank the managements of South Africa National Research Fund (NRF), Center of Excellence for mobile e-services and IFIB WG 2.4 for the scholarships they gave to me.

I would, furthermore, like to thank Professors, J.A Gbadeyan, M.A. Ibiejugba, T.S Ibiyemi, S.O. Oduleye, P. Akinyanju, Drs. R. Ndom, O.A. Taiwo and J.O. Omolehin for their words of encouragement when I was experiencing a tough time. People say tough time never lasts, but tough people do. I particularly thank my gemstone, Cecilia Temilola Olugbara for her sumptuous love, relentless endurance, unwavering support and inexorable encouragement during the trying periods. I earnestly thank my lovely father, Chief Joshua Olugbara for the struggle he went through to ensure that we grow up to be successful. I also would like to thank my elder sister, B. Adeleke, her husband, Pastor Z. Adeleke, as well as my younger brothers, Dele Olugbara, Femi Olugbara and Dada Olugbara for continually loving me, even when I did not meet up to expectation. I would like to thank my charming friends, Brothers T. Oluwafemi, S. Bankole and Sister T. Oluwafemi for their unvarying support, encouragement and prayers, which strengthened me to finish this work.

Thanks to all members of the center for mobile e-services for development for their love and assistance throughout my study. In particular, Drs. S.S. Xulu, A. Kwake, Mr. P.F. Neil, Miss N. Mdletshe, E. Jembere, T.C. Nyadeni, P. Mudali and A. Ipadeola showed enormous love to me throughout my stay on campus. I sincerely appreciate diverse contributions from many of my colleagues. Space limitation does not allow me to explicitly mention their names. God will continue to love all of you in Jesus' name. Finally, I would like to thank my spiritual fathers, Bishop D. Oyedepo, Bishop T. Aremu, Rev. F. Ajiboye and Pastor B. Mackenzie, for the grace that they showed throughout my study.

But there is a spirit in man: and the inspiration of the Almighty giveth them understanding, Job 32:8.

TABLE OF CONTENTS

LIST OF TABLES

LIST OF FIGURES

LIST OF ABBREVIATIONS

AID	Additional Image Description
ANOVA	Analysis of Variance
ASSERT	Automatic Search and Selection Engine with Retrieval Tools
BMP	Bitmap Image
CAD	Computer Aided Diagnostics
CBIR	Content-Based Image Retrieval
CEV	Contour Evolution
CNED	Connectivity Number Edge Detection
CPU	Central Processing Unit
CSC	Colour Space Conversion
CSF	Cerebrospinal Fluid
CSSD	Curvature Scale Space Description
CT	Computer Tomography
DBMS	Database Management System
DICOM	Digital Imaging and Communication in Medicine
DFP	Density Histogram of Feature Points
DFPP	DFP Plots
DSS	Decision Support Systems
DT	Delaunay Triangulation
DTR	Decision Tree
E-Commerce	electronic Commerce
E-Healthcare	Electronic Healthcare
EP	Expected Precision
FD	Fourier Descriptor
FDB	Feature Database
GBF	Global Binary Fitting
GID	General Image Description
GD	Grid-based Descriptor
GM	Gray Matter

GUISET	Grid-based Utility Infrastructure for SMME Enabling Technology
HMM	Hidden Markov Model
HRCT	High Resolution Computer Tomography
IBI	Image Binarization
IBR	Image Bases Reasoning
IBM	International Business Machine
IDB	Image Database
IRMA	Image Retrieval in Medical Applications
IRS	Image Re-Sampling
JPG	Joint Photographic Expert Group
K-Fold CV	K-Fold Cross Validation
K-NN	K-Nearest Neighbour Search
LBF	Local Binary Fitting
LDL	Latent Dirchl et al. Location
LoG	Log of Laplacian
LOOCV	Leave One Out Cross Validation
MARS	Maritime Mobile Access and Retrieval System
MATLAB	Mathematical Laboratory
MBR	Minimum Bounding Rectangle
MGE	Mobile Grid Environment
MI	Moment Invariants
MLP	Multi-Layer Perceptron
MoM	Mean of Mean
MPEG	Moving Picture Experts Group
MRI	Magnetic Resonance Imaging
NA	Not Applicable
NCI	Non-Classification of Images
ND	Number of Retrieved Documents
NMC	Non-similarity Measurement Contents
ND	Number of Retrieved Document
NR	Number of Retrieved Relevant Document
NSTC	National Television System Committee

PC	Personal Computer
PACS	Picture Archiving and Communication System
PCA	Principal Component Analysis
PCI	Pre-Classification of Images
PMCC	Product Moment Correlation Coefficient
PRECALL	Precision and Recall
PRR	Probability of Relevance
QBE	Query by Example
QBIC	Query by Image Contents
QBS	Query by Sketch
QBT	Query by Text
QOS	Quality of Service
RBIR	Region Based Image Retrieval
RDB	Relational Database
RDBMS	Relational Database Management System
RF	Relevance Feedback
RGB	Red, Green and Blue Colour space
ROI	Region of Interest
SMC	Similarity Measurement Contents
SMME	Small, Medium and Micro Enterprise
SVM	Support Vector Machine
TPVA	touch-Ponit-Vertex-Angle
VLS	Variational Level Set
VRB	Vector Re-Sampling
WM	White Matter
WWW	World Wide Web
ZMD	Zernike Moment Descriptor

Abstract

This study investigated some models and techniques that would help build shape-based image retrieval with an improved accuracy. As an initial step, a modular prototype system, called BrainSearch was implemented and used to demonstrate the utility of our algorithms and techniques on brain Magnetic Resonance Imaging (MRI) characterization and their suitability for image retrieval. The system supports retrieval based on shape similarity, a single keyword image annotation and five brain MRI classes. The BrainSearch system was realized to make it easy to test retrieval performance and to expedite further algorithm investigation. This was made possible by the implementation of region-based Local Binary Fitting (LBF) active contour, Density histogram of Feature Points (DFP) shape representation and k-Nearest Neighbor (k-NN) classifier.

Then we performed a series of experiments to evaluate the performance of BrainSearch utilizing different retrieval techniques. Results generally showed that (a) region-based DFP shape representation is better than edge-based DFP shape representation, whether pre-classification of images is used or not, (b) retrieval technique that uses pre-classification of images gives better results than retrieval technique that uses non-classification of images, no matter the DFP shape representation used, (c) the pre-classification of images cannot improve edge-based DFP shape representation better than when region-based DFP alone is used, and (d) the pre-classification of images as well as factors, like shape representations and similarity measures, improve retrieval performance of BrainSearch system. Overall, the hybrid combination of LBF active contour, DFP shape representation and k-NN classifier is promising for the retrieval of brain MRI.

Chapter 1

Introduction

Digital image databases have seen an explosive growth in recent years, because of the advances of computing and multimedia technologies. These advancements allow the construction and archiving of images with low cost and as a result, the size of image databases is increasing daily. Image retrieval, popularly referred to as content-based image retrieval is an emerging technology that allows a user to retrieve relevant images in an effective and efficient manner. Digital imaging has extensive applications in our daily lives and it is being used for several applications. Examples of imaging applications are in museums for archiving important images and manuscripts from art gallery and museum management. Many useful applications of imaging are found in security for tracking an intruder, crime prevention, law enforcement and object recognition in digital forensic.

Many useful applications of image retrieval can also be found in weather forecasting, fabric and fashion design, trademark and copyright database management, picture archiving and communication systems, military, biomedical imagery and home entertainment. The success of biometric technology can directly be linked to the usefulness of imaging and the progress, so far recorded in image processing field. The strength of the newly emerging multimedia application lies in its ability to efficiently process images. More images are used daily in hypertext markup language and extendible markup language documents on the world-wide-web to convey meaningful information. In particular, image retrieval is potentially useful in discovering brain activation patterns, in classifications and in diagnoses by comparing observed patterns with those of known diseases, leading to clinical applications.

The storage, manipulation and analysis of the contents of digital images are essential requirements for the next generation of healthcare information infrastructure. The aim of this infrastructure is to bring timely health information to support communication among healthcare decision makers and communities at large. Among several healthcare services that can be provided with the aid of the emerging grid technology for ubiquitous access, image classification and diagnosis services are important. The ubiquitous access and retrieval services enable the storage, retrieval, analysis, management, manipulation and sharing of all kinds of healthcare specific digital images. The healthcare community is currently exploring collaborative approaches for managing image data and exchanging useful knowledge. Image retrieval in healthcare applications allows for supporting clinical decision-making. It also eases distributed management of clinical data and scenarios for integration of image retrieval access methods into picture archiving and communication systems as well as healthcare information infrastructure.

However, retrieval results of the existing image retrieval systems are generally not satisfactory due to the weak connection between low level image features and high level image semantics. Moreover, traditional text-based description requires images to be manually annotated. This can be a very time-consuming task that is cumbersome, error prone and prohibitively expensive. Additionally, images can have contents that texts alone cannot adequately convey. Thus, due to the rich content of images, traditional text-based retrieval methods can be complemented with efficient and effective image retrieval algorithms and techniques to enhance medical diagnosis and therapy planning.

In this research work the use of active contour, DFP shape representation and k-NN classifier to realize a prototype shape-based image retrieval system was investigated. The system was used to demonstrate the utility of these methods on brain MRI characterization and their suitability for image retrieval in healthcare applications.

1.1. Problem Statement

The problem of retrieving similar images from database of images is a long standing issue. In particular, efficient content-based image retrieval in the medical domain is still a challenging problem (Selvarani & Annadurai, 2008). Due to the weak connection between image features such as shape, texture and color and the semantics of images, the majority of the existing image retrieval systems suffer from poor retrieval rate. This problem is generally referred to as the semantic gap. Image retrieval approaches based on low level concepts naturally have some inherited problems for human perceptual recognition. Humans recognize images based on high-level concepts such as texts and keywords and they typically query images by their semantics. Alternatively, high level concepts alone are not sufficient for image retrieval, because images can contain important information that texts cannot reveal.

Another very important problem in image retrieval is the need for suitable similarity measures and image representations that can lead to an improved retrieval rate. In particular, variations can occur among semantically similar objects in medical images such as MRI, x-ray, ultrasound, digital radiography, digital subtraction angiography, computerized tomography and positron emission tomography scans, which have direct reliance on medical diagnosis and intervention. These variations can cause serious problems for an image representation method, making it difficult to conceive a measure for similarity in image retrieval. Hence, it would be prudent to have approaches and techniques for improving retrieval results in healthcare applications. The main problem being investigated in this study is how to improve the retrieval rate of an image retrieval system suitable for brain MRI retrieval. Based on this, the research questions considered are stated in the next section.

1.2. Research Questions and Hypothesis

The problem statement for this study directly leads to the following main research question. *How can the performance of image retrieval algorithms and techniques be practically improved for healthcare applications?* Derived from this question are three important research sub-questions. The first sub-question raises the awareness that image representation can have significant effects on retrieval results. For example, many of the existing image representation methods are not invariant to transformations, such as scaling, rotation, translation, occlusion and affine transformation, thereby leading to poor retrieval results. The problem of adequate image representation remains an open issue (Zhang, et al., 2001), hence the need to investigate:

(a) *How can image pattern be represented such that contextual information and other important image characteristics are retained in the representation?*

Moreover, image features and similarity measures should be suitably chosen to improve retrieval results. The second sub-question is also an open issue (Smeulders, et al., 2000; Zhang, et al., 2001; Lehmann, et al., 2003):

(b) Which are the important features of an image and similarity measures that can be used in the image retrieval process so that the discovered image is visually and semantically meaningful?

The image retrieval algorithms and techniques obviously need to be evaluated so as to demonstrate their usefulness. The evaluation of image retrieval systems is an important issue in image retrieval research (Muller, et al., 2004). This leads to the third research sub-question, an open hypothesis (Wang, et al., 2001), which is reformulated in this study as the following null hypothesis. There will be no significant difference between the performances of an image retrieval system that uses pre-classification of images and an image retrieval system that uses non-classification of images. The research question below would have been answered already by the time the null hypothesis is tested.

(c) Will pre-classification of images improve retrieval results of an image retrieval system?

1.3. Research Aim and Objectives

The aim of this study is to develop algorithms and techniques to improve *performance of an image retrieval system in healthcare applications.* The specific objectives of this research are to:

(a) develop algorithms and techniques to improve the performance of image retrieval system, understand the representation of image pattern and investigate the characterization of images,

(b) test and evaluate the performance of the algorithms and techniques developed in (a) above, and

(c) investigate what is the impact of pre-classification on the retrieval system.

1.4. Significance of the Study

The significance of this study lies in how image retrieval algorithms and techniques can be improved to advance the proposed image retrieval functionality in Grid-based Utility Infrastructure for Small, Medium and Micro Enterprise (SMME) Enabling Technology (GUISET) (Adigun, 2006). GUISET is a scientific apparatus created to facilitate the study of application and service components in a Mobile Grid Environment (MGE). It proposes e-Commerce, e-Healthcare, e-Agriculture and e-Tourism applications as part of its suite of service-oriented on-demand applications. GUISET initiative, being the niche research project of the Department in which this work was carried out, has the goal of empowering rural communities with a technology that can boost their social and economic factors. We strongly believe that imaging science presents a compelling case of opportunities where GUISET can offer a significant benefit to healthcare communities. Moreover, a GUISET architecture that is equipped with image retrieval functionality will enable communities to share common imaging database and services for algorithm comparison and validation. The technology will assist rural clinicians to manage large quantity of data by providing reliable assistance to diagnosis and therapy planning through medical image analysis.

As a result, this effort will enhance GUISET architectural framework in a number of respects. First, GUISET provides a multimodal user interface used by application and services, which will now include having image object service request input interface. Whenever an image object service request is given to GUISET resource broker as input, it should be able to discover relevant images that are similar to example image presented. Thus, the functionality of GUISET is enhanced through image retrieval service provisioning. Second, the e-Commerce product transaction that GUISET technology targets will be enhanced by providing image communication services to complement textual inputs. With this enhanced functionality, an image database of e-Commerce products can be maintained within the GUISET framework, so that the image of a product being sought by a prospective buyer can be given to the resource broker, which will in turn request from image retrieval services agent to obtain the best match product from the database.

In particular, e-Commerce services involving trading in art works will greatly benefit from such enhanced functionality of GUISET. Given this potential for enhanced functionality, the GUISET framework should support image analysis, mining and retrieval in the context of use, be it e-Commerce or e-Healthcare. Image retrieval service provisioning is, therefore, proposed for GUISET to provide more intriguing functionalities and services in both e-Commerce and e-Healthcare applications. This will facilitate the realization of the objective of GUISET, which is to support automatic creation and management of multiple utility computing services in a shared infrastructure. Figure 1.1 shows the GUISET architectural framework incorporating the general image retrieval system for e-Commerce and the specific image retrieval system for brain image retrieval services being proposed in this study. The healthcare information infrastructure that supports image retrieval fits appositely into the infrastructure layer of GUISET with its 3-layer architecture. The resources at middle layer will enable image retrieval services to be supported as utility services. The multi-modal interface layer will enable the image retrieval services to be provided on multi-target devices.

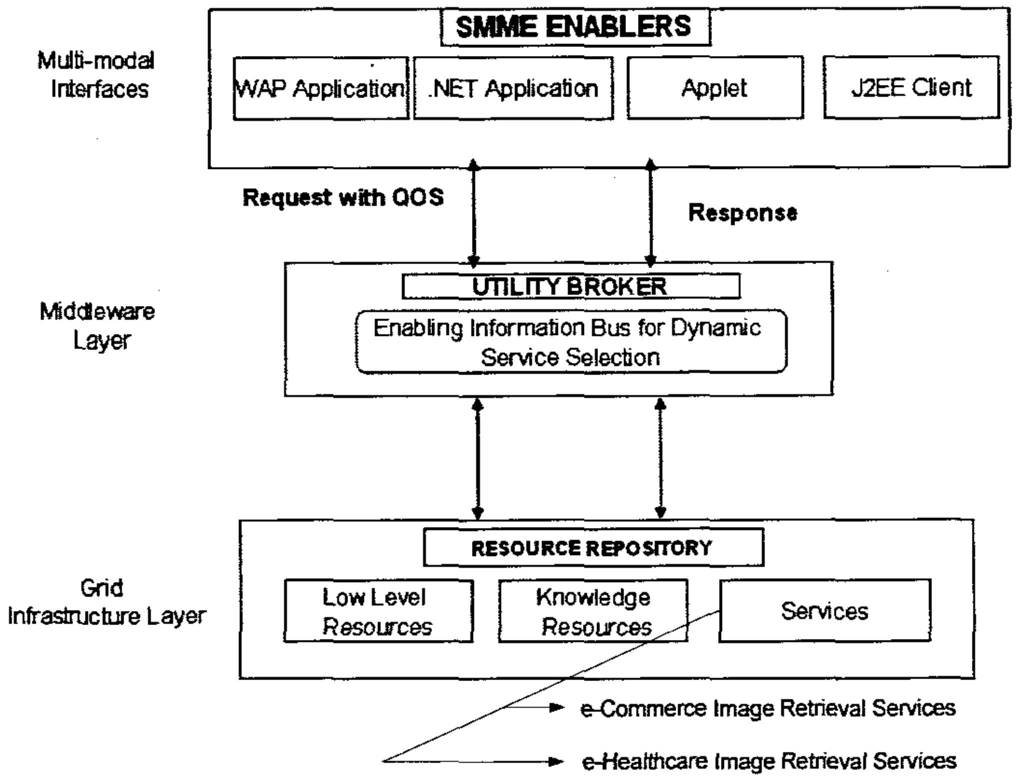

Figure 1.1: The GUISET architecture

1.5. Research Methodology

To realize the objectives of this study, image retrieval was formulated as a classification problem in which similar images were associated with known class labels. The queried image was then assigned a class label with the majority votes among some k number of images. This requires training a classifier such as k-NN to learn to recognize known class labels of the training examples and then use this knowledge to predict the correct class label for a new example image presented as a query to the retrieval system. Basically, image classification is different from image retrieval, because similarity between objects is class specific and can be inferred from the training data. A new image sample has to be assigned to the most similar of a number of available labeled training image examples. Alternatively, image retrieval is generally concerned with a weaker concept of image proximity based on a generic or non-class specific measure. A large collection of images is searched for images that are similar to a given query image. Both image retrieval and image classification directly rely on the notion of similarity computation and image representation. The k-NN algorithm uses one keyword annotation for the feature vector, five image classes for classification and Paradox database for image indexing. The Jensen polynomial was used to demonstrate the possibility of computing a unique shape index from edge-based and region-based shape features.

The input image is first converted to grayscale image if the input image is colored. The input image is then re-sampled to a fixed dimension of 72 x 72 using high-resolution cubic spline interpolation to achieve scale invariance in shape representation. The image shape feature was segmented using region-based LBF active contour and DFP was used for the extraction of the segmented shape. Then we modified DFP algorithm to count image pixels that lie on rectangles that fit into minimum bounding rectangle of the segmented objects rather than taking a count of the entire image pixels, giving a shape feature vector of size 72 for image representation. The shape feature vector was further reduced to dimension of 36 using our vector re-binning technique, resulting into 50% additional storage gain. Edge information was extracted from the evolved region-based shape feature of the input image using connectivity-number based edge detection algorithm for binary images. The extracted shape features (edge or region-based features) were then stored in a Paradox database for all the images in the database. The computation of the ranking list of similar images to the query image was based on six similarity measures, namely, Chi-test statistics, Quadratic form, Histogram intersection, Procrustes shape, Pearson correlation and Bray Curtis.

The effectiveness of the foregoing choice of method was demonstrated by experimentation. A series of experiments was conducted to evaluate the performance of an image retrieval system that uses a classification technique against when a non-classification technique was used. Classification accuracy and intuitive-PRECALL measurements were used to evaluate retrieval results when the techniques of pre-classification of images and non-classification of images were used respectively. A statistical technique, called analysis of variance was used to analyze retrieval results to test for statistical significant.

The uniqueness of this study is first in the choice of solution method, which deviates from conventional retrieval approach of text-based retrieval when trying to bridge the semantic gap problem. Rather, we elected the artificial intelligence approach to image retrieval in which a classifier was trained to learn to recognize keywords or class labels of images. Later, this knowledge was used to predict the correct class for a new example image presented as a query. Another uniqueness of this study is that it seeks to produce a hybrid of peculiar algorithms and techniques, such as active contour, DFP shape representation and k-NN classifier on brain MRI characterization and their suitability for image retrieval. This then provides the opportunity to add our voice to a recent discovery that shape can be very useful when used for medical image indexing and retrieval (Antani, e t al., 2004). We believe that improvement on current algorithms and techniques for image representation in a certain way could yield retrieval systems to discover images that are more visually meaningful than existing systems do. Hence, our approach is to introduce some methods such as classifiers equipped with learning capabilities that will improve existing algorithms and techniques for image retrieval.

1.6. Preliminary Work

The primary motivation for this study was to develop efficient healthcare information infrastructure to assist rural healthcare practitioners to remotely use grid resources and services to diagnose brain diseases and as well prescribe medications. As a result, an information infrastructure framework for integrating utility grid computing and wireless body area network for healthcare service provisioning was described (Olugbara, et al., 2007a). The architectural and requirements engineering frameworks of the infrastructure were described (Olugbara, et al., 2007b, Olugbara, et al., 2007c). One of such services to be provided by the infrastructure is medical diagnostics and therapy planning using examples of previous cases diagnosed for similar diseases. A preliminary study on readiness assessment of healthcare information infrastructure was conducted to determine e-Healthcare readiness status of healthcare practitioners, public and patients from communities associated with two healthcare facilities in Uthungulu Health District of KwaZulu/Natal, a South African province. The result of the pilot testing showed that (a) readiness with acceptance and use appeared to be the most important attribute, followed by structural and then engagement, while need-change is the least important, (b) healthcare practitioners agreed to be e-Healthcare ready, but the public and patients fairly agreed, and (c) attitude of healthcare practitioners is a function of their preference for technology usefulness to ease of use. Theoretical framework for the model was drawn from change management, information technology acceptance and use as well as innovation adoption theories. Results of the study showed that healthcare practitioners, public and patients are willing to accept the use of healthcare information infrastructure technology (Ojo, et al., 2008). The application of Pearson *correlation coefficient for similarity measurement and* case-based reasoning to a strategy game (Olugbara, et al., 2007d) has also influenced this study. Pearson correlation coefficient is among similarity measures evaluated in this study. Moreover, k-NN classifier and case-based reasoning are useful artificial intelligence techniques for generally solving classification problem.

1.7. Thesis Contributions

To support the hypothesis that pre-classification of images will improve retrieval results in image retrieval systems and to ultimately provide answers to the research questions formulated in this study, we have:

(a) demonstrated that a hybrid combination of LBF active contour, DFP shape representation and k-NN classifier is promising for brain magnetic resonance image retrieval,

(b) *improved on the existing general image retrieval architecture* by adding onto it a new shape-based image retrieval algorithm that works with different image processing methods and techniques,

(c) demonstrated the improved way in which the various algorithmic techniques are combined to realize our algorithm for image retrieval,

(d) demonstrated the use of Jensen polynomials for computing shape index directly from DFP shape representation and some geometrical properties such as orientation, eccentricity and image profiles,

(e) created mechanisms to evaluate a number of similarity measures and then determine effects of these measures on retrieval results of the BrainSearch implementation prototype. The effectiveness of the whole approach in improving retrieval results was evaluated via the prototype system.

1.8. Synopsis of the Rest of the Thesis

The remainder of this thesis is briefly outlined as follows. Chapter 2 gives the overview of our methods for improving retrieval results of an image retrieval system. In particular, a shape-based image retrieval algorithm with annotation and a system performance evaluation technique for comparing retrieval results are described. Chapter 3 discusses related works that have influenced the current study. We categorized some existing image retrieval systems based on the identified image processing steps and common management techniques they employed for image retrieval. Chapter 4 discusses design issues for the realization of our algorithms and techniques. Additionally, we developed an indexing technique for shape-based index computation from DFP shape representation using Jensen polynomials. Chapter 5 describes our image retrieval prototype system used to implement the image retrieval experiments designed to determine the factors that affect retrieval system performance. Chapter 6 describes the evaluation experiments, results and explains interpretations of the results of the image retrieval experiments performed. A statistical method based on analysis of variance for hypothesis testing is described for determining whether one image retrieval system is better than another retrieval system. Chapter 7 concludes, by summarizing the results of the experiments performed. Finally, we show how the objectives of this study were perceptibly met. Then we give a conclusion, contributions of the study to knowledge and state our future work in image retrieval research.

Chapter 2

Overview

This chapter briefly gives an overview of the work carried out to realize the aim and objectives of this study. The general approach that ultimately led to the development of our algorithms and techniques for brain MRI retrieval for healthcare information infrastructure is descriptive and comparative. The research artifacts were subjected to conceptual mathematical analysis and proof of concept.

We applied a number of algorithms and techniques from the fields of image processing, computer vision, artificial intelligence and statistics to accomplish the task of improving image retrieval results. Furthermore, new algorithms and techniques were developed for DFP shape representation. We demonstrated how Jensen polynomials could be used to compute a unique shape-based index key directly from some geometrical properties, such as orientation, eccentricity and image profile as well as from DFP shape representation. We also evolved a technique for evaluation of an image retrieval system based on intuitive-PRECALL and classification accuracy. The results generated by the retrieval system that used different retrieval techniques were then analyzed using analysis of variance (ANOVA). Retrieval system evaluation is an important work in image retrieval research, because different systems use different algorithms and techniques for the task of image retrieval.

As a result, it is difficult to evaluate image retrieval systems. Our approach was based on the fact that any retrieval system can be evaluated by allowing it to compute a set of solutions to a given problem using different solution techniques. Then all the solutions computed by this system are then compared to determine the best solution among all possible solutions. This is an effective approach to retrieval system evaluation rather than trying to evaluate a number of systems operating under diverse conditions. We then described the essential steps involved in our algorithms and techniques for the task of image retrieval. In addition, we also described our model of retrieval system evaluation and then applied the model to evaluate results generated by our prototype system for brain MRI retrieval to show the effectiveness of our algorithms and techniques.

2.1. Efficient MRI Retrieval Rationale

Medical image analysis is often regarded as a complex task that requires a human expert to make extensive use of the knowledge of anatomical and imaging techniques to arrive at a suitable decision. Specifically, the automatic and accurate segmentation of brain MRI remains a persistent problem (Lin, et al., 2004a, Lin, et al., 2004b). Several reasons are responsible for the difficulty in automatically and accurately segmenting MRI. First, there are large anatomical variations from person to person and the most important problem is that radiographs are projection images and thus, contain superimposed structures (Park, et al., 2003). Second, MRI intensities of different tissue classes can overlap, that is MRI contains intensity in-homogeneity. Third, there is acquisition noise in MRI and the presence of partial volume effect (Pham & Prince, 1999). As a result, seeking suitable algorithms and techniques to segment, index and retrieve MRI from database of images is an important issue in image retrieval research.

Generally speaking, to address the problem of improving image retrieval results, a single methodological approach is not sufficient. This is because there are a number of important considerations that can significantly affect retrieval results. These include among other factors (a) similarity measure to use for a given application, (b) segmentation method to apply and (c) management of semantic gap problem. Different solutions have been proposed for different image retrieval tasks, since a general solution is not feasible. The methods applied in this study can be classified into the following categories, namely, (a) shape modeling and feature extraction, (b) database approach for image data management, (c) instance-based learning for image retrieval and (d) retrieval system performance evaluation.

2.2. Efficient Shape Model Computation

Our method for shape model computation uses generic shape-based algorithm for image retrieval. The algorithm involves taking an input image through a number of image processing steps to extract shape features. It is able to process colored images as well grayscale images with respect to shape feature extraction, it can handle images of large dimensions and can easily be adapted to other applications where shape feature is considered important. The algorithm begins by first checking if colored image is passed as input. If a colored image is detected, conversion to a grayscale image takes place. This is an important stage of the algorithm, because processing grayscale images is exceptionally faster than processing colored images and moreover the generality of the algorithm is first achieved at this stage. Furthermore, there are a number of well established efficient algorithms and techniques in image processing field for grayscale image processing. Then, our algorithm compares the dimensions of the input image against fixed dimensions to decide whether re-sampling should take place or not. In this study, all input images are re-sampled to fixed image dimensions of 72 x 72. Re-sampling an image to a lower dimension achieves computational time efficiency and dimension reduction, because few pixels are eventually being processed. At the segmentation phase, the algorithm uses the evolved contour to binarize the input image. The algorithm then decides whether the user wants a region or edge extraction. Based on the user's choice, an appropriate shape model (region or edge) is computed. Both shape models will be visually displayed for the user to see, but only the model chosen will be returned in the histogram vector shape representation.

The processing steps in our algorithm are derivatives of the design criteria discussed in chapter 4. These involve image re-sampling using high resolution cubic spline interpolation function (Parker, et al., 1983), image segmentation using region-based LBF active contour (Li, et al., 2007), edge extraction using Connectivity-Number Edge Detection (CNED) algorithm for binary images (Zhang & Wang, 2005) and shape representation using DFP shape representation (Tran & Ono, 2003). Figure 2.1 briefly summarizes the essential steps of our algorithm for computing shape models. The most important components of the algorithm as it can be seen from figure are segmentation and shape models computation, because they cannot be avoided.

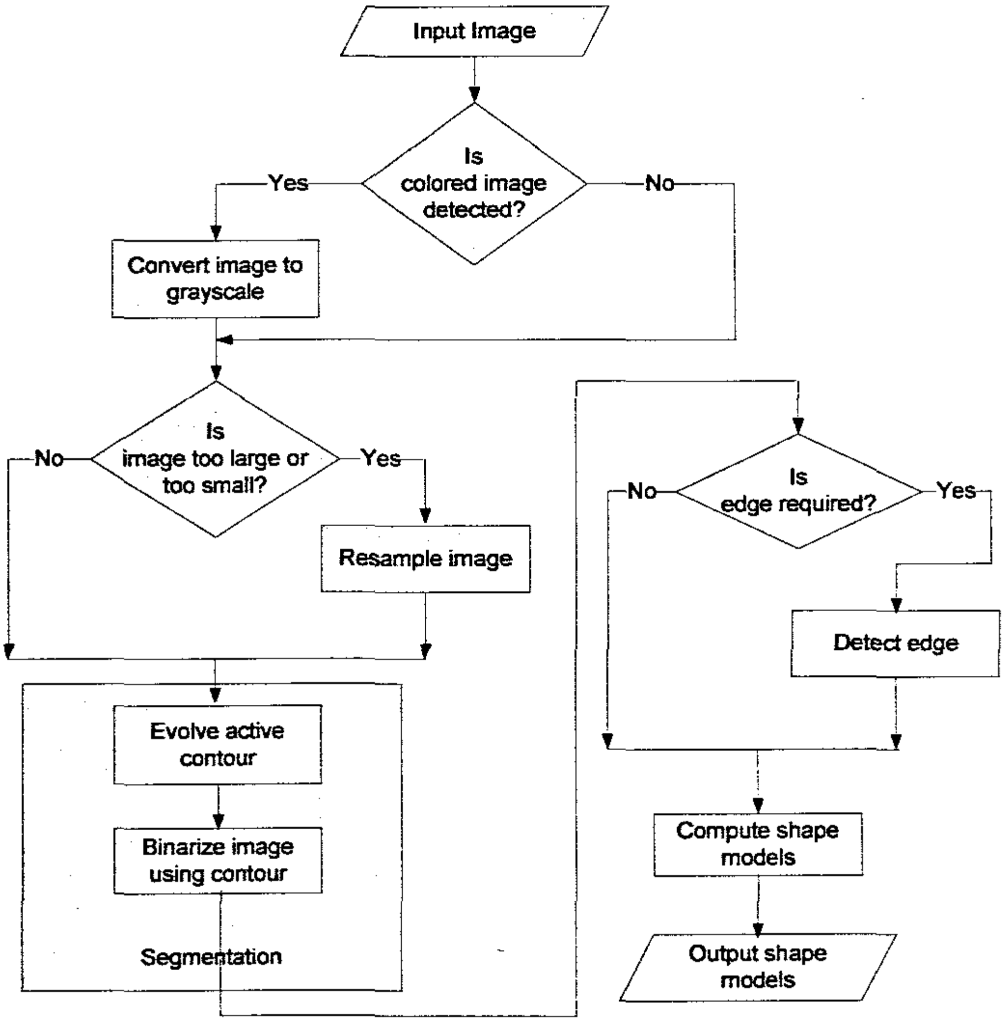

Figure 2.1: Algorithm for computing shape models

LBF active contour was applied in the image segmentation phase to segment the input image into regions of interest. The method has the advantage that binarization of an input image is easily accomplished. By simply assigning white color to those pixels smaller than 0 and black color to those pixels not smaller than 0, an image with black background and white foreground is created. So in our algorithm, curve evolution and binarization phases are combined into a single process of segmentation. Binarization is necessary, because many useful results on binary image processing that can be readily re-used to simplify the computational task of image retrieval are available in the literature. Moreover, many shape descriptors work effectively on sets of binary images, thus, we exploit the advantages of binary image processing techniques.

Then we used CNED algorithm to extract edge information from binary objects obtained after segmentation. CNED algorithm is simple, easy to use and utilizes fewer pixels for edge computation when compared to 4-directional Sobel, which is a popular edge detection algorithm. Then DFP shape representation algorithm is used as an efficient image representation technique. The DFP has several advantages, first it is computationally efficient and simple to describe. Second, it is histogram-based and histograms are invariant to translation and rotation around the viewing axis and vary slowly with changes of view angle, scale and occlusion (Park, et al., 1999). Moreover, DFP has been shown to be faster than Delaunay triangulation for large number of feature points. Additionally, DFP is insensitive to small change in the feature points set and thus, conforms well to the human vision and is invariant to translation, scale and rotation (Tran & Ono, 2003). If the edge points of the shape region are used instead of the entire region points, DFP computation becomes exceptionally fast, but its effectiveness need to be tested and compared with that of region-based DFP. We report on the effectiveness of DFP algorithm in chapter 6 when used for both edge and region-based shape representations.

2.3. Relational Database for Image Indexing and Accessing

Our method for access to Image Database (IDB) based on shape retrieval combines two useful techniques, namely, (a) to represent image by a suitable information structure and (b) to use this structure in the paradigm of conventional Relational Database Management System (RDBMS). A RDBMS provides several advantages, which include fast access, simple representation and efficient indexing scheme.

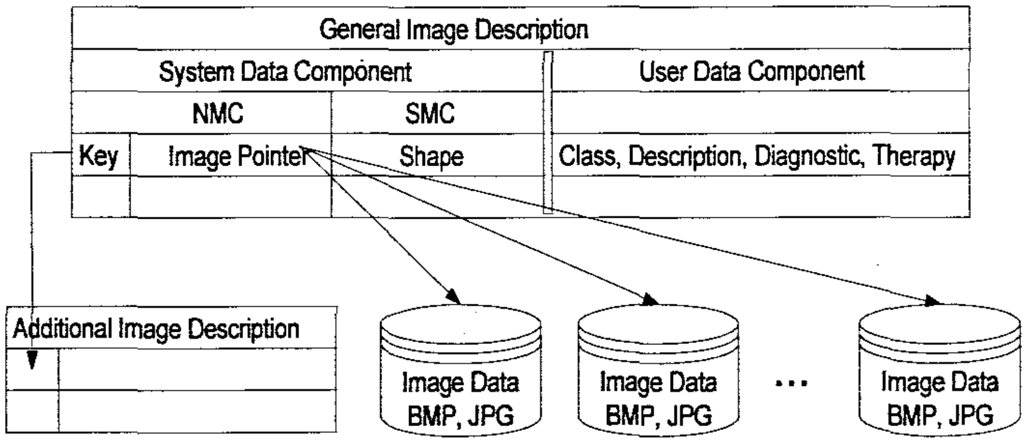

Figure 2.2: Logical scheme of BrainSearch IDB

Figure 2.2 shows a simplified logical scheme of the IDB of our prototype image retrieval system, called Brain image Search (BrainSearch). A Relational Database (RDB) method was adopted for indexing, archiving and accessing images in database. The BrainSearch system wss used to implement image retrieval experiments described in chapters 5 and 6. The system was written in Borland C++ Builder 6 and Paradox, a relational DBMS was used for data management. The IDB of BrainSearch system was organized as a General Image Description (GID), which is also called Feature Database (FDB) table of pointers to the actual image (BMP, JPG) that are stored outside the Paradox database in separate database locations. This allows for easy integration with the existing systems such as Picture Archiving and Communication System (PACS) by directly accessing images stored in different database locations. This is one of the three solutions proposed by Traina, et al. (2003) for integrating a CBIR system with existing applications. Additionally, GID table references Additional Image Description (AID) tables that are generated and used by the system for internal processing.

The GID has two sets of components, namely, system image data and user image data components. The user image data component describes the image data information supplied by the healthcare expert. This information includes the image description like mild Alzheimer disease, the diagnosis that can be administered for a patient with this type of disease, the required therapy and the class the disease belongs to like degenerative disease. These are high-level concepts used by the system for decision support. The system image data component further splits into Similarity Measurement Contents (SMC) and Non-similarity Measurement Contents (NMC). SMC are the image feature vectors such as DFP shape representation used to compute similarities between images. Finally, the NMC are features used by the system to aid internal processing. These include the GID table's primary key for uniquely locating an image representation in the table and the image pointer that connects an image representation to the actual image stored externally to the table. Image pointers need not be unique, because different regions of the same image can be extracted, represented and stored in the image database. However, we uniquely compute image index from DFP shape representation using Jensen polynomials.

2.4. Image Annotation for Efficient Retrieval

Our algorithm shown in Figure 2.1 can be used to efficiently extract a low level shape model from an input image. However, this algorithm does not solve the semantic gap problem, because a high level concept is not taken into cognizance. To solve the semantic gap problem, the algorithm was combined with image annotation scheme. In our method, only the annotation and post-processing components of the general annotation system (Tsai & Huang, 2008) were used. This is because the segmentation and feature extraction components of the general annotation system are already part of our algorithm.

Figure 2.3 shows an improved algorithm with keyword annotation that was implemented in this study for semantically meaningful image retrieval task. The annotation component of the algorithm was implemented using the k-NN classifier (Mitchell, 1997; Bustos, et al., 2005), thus the system performs a k-NN query to classify image feature vector and identify the image as normal, degenerative, infectious, stroke and tumor. K-NN search is an effective instance-based learning technique that computes the similarities of images in the database and the example image and returns k most ranked neighbors of the example image. The output of the system is the class that the example image was predicted to belong as well as the images similar to the example image. The parameter k is usually supplied by the user, thus making the system interactive.

Finally, an important characteristic of an effective retrieval system is that it gives maximum relevant information and withholds maximum irrelevant ones. The retrieval algorithm with annotation (Figure 2.3) developed in this study returns only the images predicted to belong to the same semantic category as the query image, similar to the approach proposed by Wang, et al. (2001). Additionally, the class that the query image is predicted to belong to is also given as output.

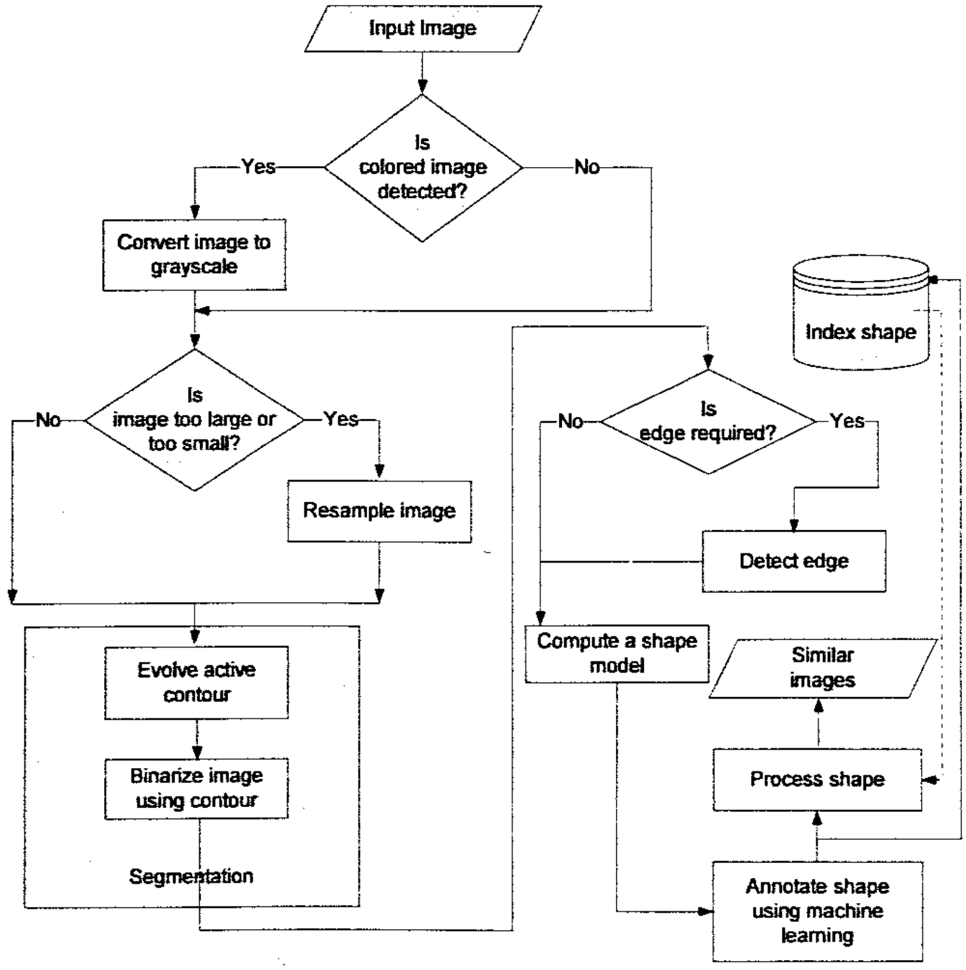

Figure 2.3: Algorithm with annotation for image retrieval

2.5. Evaluating Retrieval System Performance

We describe our model of image retrieval system evaluation and the general significant of system evaluation. The main reasons to evaluate or compare retrieval results are to know (a) how well the system work, (b) whether one technique is actually better than the other and (c) under what conditions is one technique better than the other. This will provide a basis for further investigation. As a result, the evaluation of retrieval results is an important issue in image retrieval research and information retrieval in general. The evaluation of a retrieval system can generally be investigated at several levels, namely, (a) processing, which involves time complexity and space efficiency evaluation of the algorithms and techniques used by the system, (b) search, which involves effectiveness of results produced by the retrieval system and (c) system, which involves evaluating user satisfaction of the retrieval system. The focus of this study is on evaluating search results of an image retrieval system. Generally, a retrieval system with high performance will always give maximum relevant information and withhold maximum irrelevant information.

Figure 2.4 shows an evaluation model for comparing results of a retrieval system that uses different retrieval techniques. The model requires that a prototype retrieval system be implemented to generate results based on pre-classification of images, PCI(s) and non-classification of images, NCI(s) techniques as functions of shape representation denoted by the parameter s. These results are then compared to determine, which retrieval technique gives a better result among the two techniques. Given a query image and database of images, the model system ranks the database images according to a status retrieval value or a similarity measure. The retrieval techniques PCI(s) and NCI(s) were respectively evaluated using classification accuracy (Cihlar, et al., 1998) and intuitive-PRECALL (Raghavan, et al., 1989) based performance judgment and results are statistically judged using ANOVA to test for significant difference. Classification accuracy and intuitive-PRECALL measurements appropriately measure the performance of an image retrieval system that uses PCI(s) and NCI(s) techniques respectively. Thus, to compare retrieval results based on PCI(s) and NCI(s), both techniques were brought to a common ground by using classification accuracy and intuitive-PRECALL measurements respectively. That is, intuitive-PRECALL based on the number of retrieved documents (ND) measures the performance of a retrieval system, which uses NCI(s) and classification accuracy measures the performance of a retrieval system, which uses PCI(s). Then the mean intuitive-PRECALL and mean classification accuracy over all queries are computed. In this study, ND directly corresponds to number of retrieved images. Thus, effective comparison of retrieval results was achieved by bringing both NCI(s) and PCI(s) techniques to a common ground using mean intuitive-PRECALL and mean classification accuracy respectively.

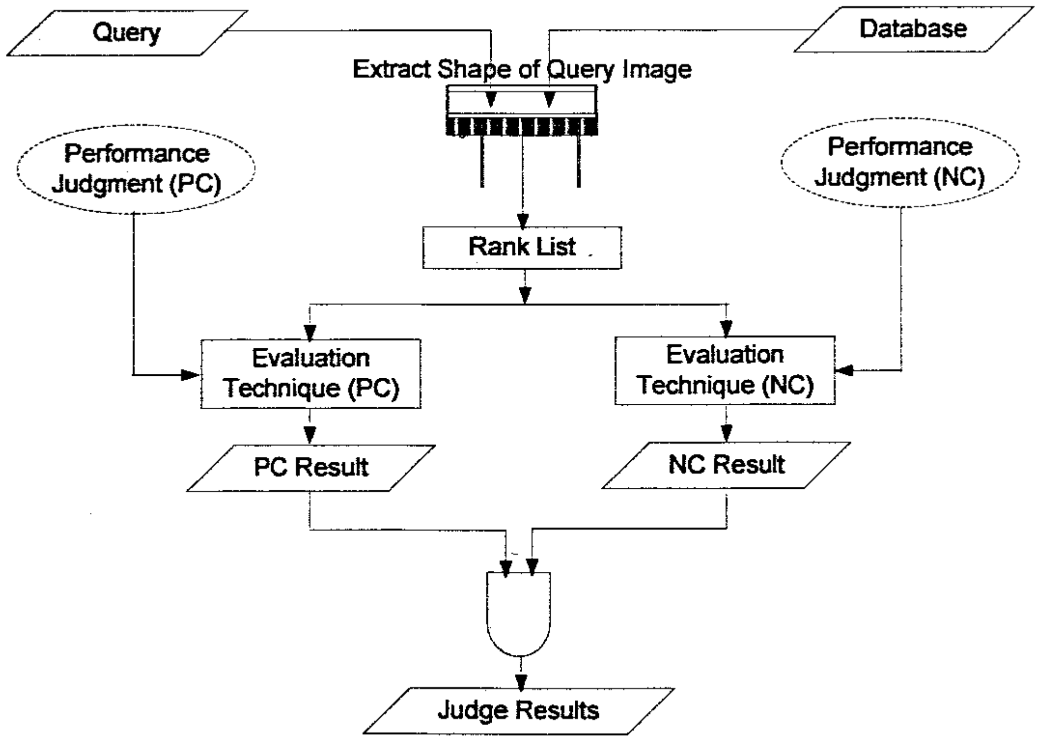

Figure 2.4: Comparing retrieval results

Figure 2.5 shows vertical, horizontal and cross comparison techniques for comparing different retrieval results. Accordingly, there are essentially six different possible evaluations, that is, (a) PCI(E) versus NCI(E), (b) PCI(R) versus NCI(R), (c) PCI(E) versus PCI(R), (d) NCI(E) versus NCI(R), (e) PCI(E) versus NCI(R) and (f) PCI(R) versus NCI(E). The parameters E and R correspond to edge-based DFP and region-based DFP respectively.

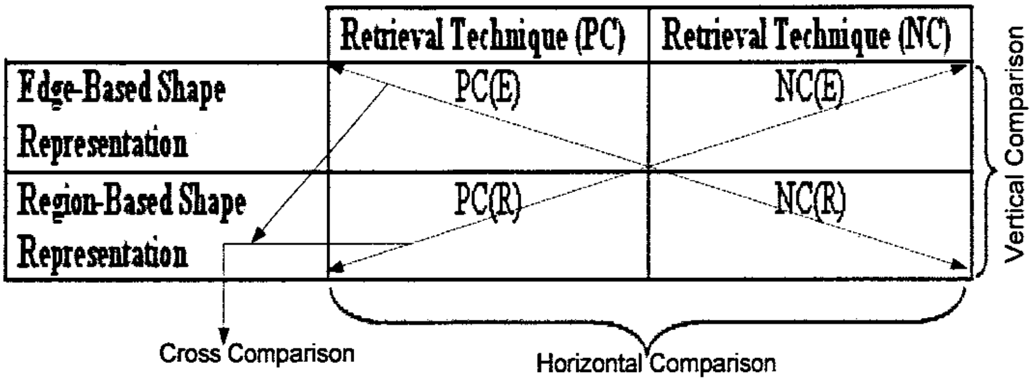

Figure 2.5: Retrieval comparison techniques

2.5.1. Vertical Comparison

Given two shape representations s_1 and s_2, the goal of this comparison was to compare retrieval results obtained by applying PCI(s_1) and NCI(s_2) to the representations respectively. This comparison does not tell us, which retrieval technique is better, but gives information about which, similarity measure and number of retrieved images will be better used for PCI(s) or NCII(s). This also allows for the evaluation of the effects of these factors on retrieval results and to determine whether there are significant interactions among factors.

2.5.2. Horizontal Comparison

Given a particular shape representation s, the goal of this comparison was to find out if PCI(s) will be better than NCI(s). It is also possible to determine, which similarity measure and number of retrieved images give the best retrieval result. This comparison does not tell us if PCI(s) is better than NCI(s) for an arbitrary s-based shape representation.

2.5.3. Cross Comparison

Given two shape representations s_1 and s_2, the goal of this comparison was to improve on the comparison described in 2.5.2 by determining if PCI(s) is better than NCI(s).

Chapter 3

Related Work

This chapter describes the related works with specific focus on healthcare applications domain to distinguish our study from others. As a result, we categorized related works into several groups of image processing steps and the associated management techniques. Seven similarity measures, namely, Minkowski-form distance, Chi-test statistics, Quadratic form, Histogram intersection, Procrustes shape, Pearson correlation and Bray Curtis as well as performance evaluation techniques, namely, precision, recall and their combinations are discussed. Evaluation of retrieval results is an important issue that many previous works have not considered due to the difficulty in evaluating retrieval systems, which use different algorithms and techniques. Our approach to evaluation is unique and considers choosing between alternatives algorithms and techniques for image retrieval task. We begin our discussion from the description of image retrieval problem to healthcare applications of image retrieval.

3.1. The Image Retrieval Problem

Image retrieval is the task of efficiently searching for similar images from an image database. Usually, the query to the image database can be of various types, namely, Query-by-Text (QBT), Query-by-Sketch (QBS) and Query-by-Example (QBE). This study focuses on query-by-example, because QBE is an efficient and effective way to initiate a request to image database. QBE process is simple and gives more perceptually meaningful results when compared to other query types. Figure 3.1 gives an illustration of the general task of image retrieval from a given image database. A query image is taken through some image processing steps to extract a shape feature, which is then matched against features in image database to produce a list of similar images to the query image. Accordingly, a query to image database is defined using any of three query types, namely, QBT, QBS and QBE and similar images are then retrieved from image database.

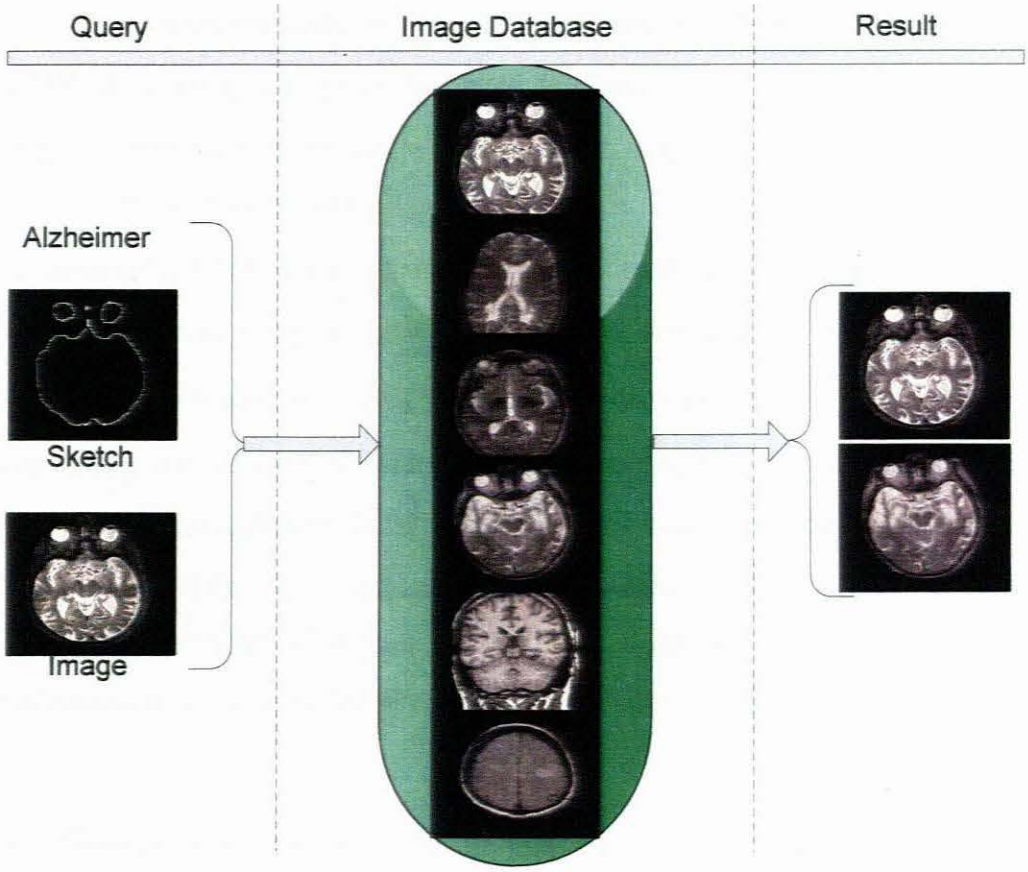

Figure 3.1: Image retrieval illustration

QBE is formally defined as: let B be an image database with $B = \{X_i \mid i = 1, 2, ..., n\}$ where X_i is an image represented by a set of features $X_i = \{X_{ij} \mid j = 1, 2, ..., m\}$. Since a query, Q, is also an image, it follows that $Q = \{Q_j \mid j = 1, 2, ..., m\}$. Whenever a query, Q, is defined on B, the image, X_k that satisfies the condition $\rho(Q, X_k) \leq \tau$ is returned as an answer to the query, where τ is a threshold value and ρ is a measure of similarity between two images being compared. Generally, a similarity measure is a function of the form:

$$\rho : I \ x \ I \rightarrow \mathbb{R}^{+}$$

where I is the image space and $\mathbb{R}^{+}$ is a positive real number space. Small values of ρ give an indication of strong similarity and high values give an indication of weak similarity between two images.

There are basically two types of similarity queries, namely, range and k-NN. A range query (Q,τ) for some tolerance $\tau \in \mathbb{R}^{+}$, reports all images from the database that are within the distance τ to Q, that is,

$$(Q,\tau)=\{b \in B \mid \rho(b,Q) \leq \tau\}$$

Alternatively, k-NN query reports k images from B that are closest to Q, that is, k-NN returns a set $B' \subseteq B$ such that $|B'|=k$ and for all $b \in B'$ and $a \in B-B'$, it is true that $\rho(b,Q) \leq \rho(a,Q)$. The notation $|B'|$ stands for the cardinality (i.e. number of instances of an entity) of B'. If τ is chosen such that $\tau = \min\{\rho(a,Q) \mid a \in B-B'\}$, k-NN query reduces to the range query. The problem, therefore, is how efficiently can we search for similar images in database? Our approach to this problem uses a number of image processing techniques to improve retrieval results for healthcare applications.

3.2. Content-Based Image Retrieval Systems

The goal of CBIR systems is to operate on collections of images so as to extract similar images in response to visual queries. CBIR systems use image features such as color, texture, shape, motion, spatial layout and their combinations. The visual features of the database images are usually extracted and described by multi-dimensional vectors, which form a feature database used for retrieval purpose. The user usually provides the retrieval system with an example image that can be a sketched figure or a text that represents the taxonomy of the image being searched for in the database. The system then changes the example image provided into an internal feature vector representation. The similarities between the feature vector of the example image and those of the database images are then computed and retrieval is performed for similar images. The general view is that all image retrieval systems mainly differ in the image features they use as well as the similarity measures and the search structures they employ. The common ground for all of them is to automatically extract image features by using some image processing techniques to manipulate image pixel values and to define an efficient rule for comparing images for similarity.

The first group of our categorization of image retrieval systems has to do with techniques for improving image representation. The majority of the existing techniques try to reduce feature space dimension so as to speed up search process. The dimension reduction methods either try to scale images to lower dimensions or extract the most significant components from the images or then build up an index on the reduced feature vector. The second group of our categorization investigates efficient techniques for image segmentation into objects of interest. There are a number of segmentation techniques available in the literature and all of them can be classified into global, region and block segmentation techniques. Our third categorization has to do with the issue of image classification. Generally, as mentioned in chapter 1, image classification is different from image retrieval, but classification is a useful technique for improving retrieval results. Image classification provides a good technique to complement low level image features with high level semantic constructs so as to improve retrieval results. Our fourth group categorization addresses the important issue of similarity computation. The concepts of both image retrieval and image classification strongly rely on similarity measurement. This measurement provides a useful means to determine how closely similar are two images and it is an important step in image processing and computer vision. Our last categorization addresses the important issue of system evaluation, which is based on statistical and information retrieval techniques to determine how effective a retrieval system is, in terms of solutions computed. The evaluation of retrieval quality is an important issue and retrieval systems need to be compared to identify good techniques. This can advance the field and opens up avenue for further investigation. Table 3.1 shows our categorization of image processing steps and management techniques for these processing steps. Sixty different image retrieval systems developed from 1997 to 2006 were then documented using our categorization scheme.

Table 3.1: Processing steps and management techniques

S/No	Processing Steps	Management Technique
1.	**Image Feature Representation**	
1.1.	Features descriptor	Color, texture, shape and Hybrid image features.
1.2.	Shape descriptor	Contour (edge) and region-based descriptors.
1.3.	Feature vector dimension	Very low (1-12), Low (13-60), Medium (61-120), High (121-512), Very High (>512).
2.	**Image segmentation**	
2.1.	Objects extraction by segmentation	Global, Region, Block and Hybrid technique.
3.	**Image Classification**	
3.1.	Image classification-based retrieval	Relevance Feedback (RF), Support Vector Machine (SVM), Bayes, Hidden Markov Model (HMM), Multi-Layer Perceptron (MLP), k-Nearest Neighbor (k-NN), Template, Decision Tree (DTR), Latent Dirchl et al. Location (LDL) and Hybrid classifier.
3.2.	Annotation image using keywords to define image semantics	1, 2, 3, 4, 5, >5 keywords defining image semantics.
3.3.	Define Image classes	Very low (1-10), Low (11-20), Medium (21-50), High (51-100), Very High (>100) image classes.
3.4.	Management of image dataset	Corel, WWW, Kodak Photo, Others, Hybrid datasets.
4.	**Similarity Computation**	
4.1.	Ranking of similar images	Euclidean, Histogram intersection, Cosine distant, Procrustes shape, Quadratic form, Earth Movers distance, Chi-test statistics.
5.	**Retrieval System Evaluation**	
5.1.	Evaluate performance	Recall and Precision.

3.3. Image Retrieval Approaches

Many earlier CBIR systems exploited a combination of low-level image features such as color, texture and shape to retrieve images. However, their retrieval performance is generally not satisfactory due to the weak connection between low-level features and the semantics of images, which is referred to as semantic gap (Sun & Ozawa, 2005). In order to reduce the semantic gap, many image retrieval approaches have been proposed in recent years for the derivation of semantic information from images. These approaches generally fall into three main categories, namely, relevance feedback, statistical classification and region-based retrieval.

A relevance feedback (Su, et al., 2003; Urban, et al., 2003), sometimes called a user-in-the-loop approach allows a user to interact with the retrieval system by providing useful information regarding the images, which the user believes to be semantically relevant to the query. Based on the user's feedback, the model of similarity measure is dynamically updated to give a better approximation of the perception similarity. However, such a retrieval approach can add extra burden to a user when complex control is provided. For example, in healthcare applications, an expert may not have the time to assist an application by interactively supplying relevant information that can aid the system to improve performance.

A statistical based classification approach (Vailaya, et al., 2001; Sheikholeslami, et al., 2002; Li & Wang, 2003) pre-processes database images by grouping images into semantic categories, so that semantically adaptive indexing methods can be applied to each category. However, a major difficulty in statistical classification is the selection of proper training dataset to incorporate the rich semantics of a large image database. In healthcare domain where ground truth data exists, this is not a serious problem. Thus, statistical classification techniques become practically useful in healthcare applications.

Region-Based Image Retrieval (RBIR) systems (Zhu, et al., 2000; Carson, 2002) segment images into Regions of Interest (ROI) that correspond to semantic objects. This is not the case in conventional CBIR that indexes each image in the database by the image features and the system retrieves images that have similar features to the example image. In RBIR systems, the retrieved images are based on the similarity between regions and they extend CBIR systems to a situation where a user may like to retrieve images based on information about their regions.

There are two basic approaches for edge detection, namely the gradient and the Laplacian. The gradient-based method detects the edges by looking for the maximum and minimum in the first derivative of the image. The Canny and Sobel are two popular operators that perform a 2D spatial gradient measurement of an image. Laplacian and Log of Laplacian are two popular filters based on Laplacian edge detection approach. The Laplacian edge detection method searches for zero crossing in the second derivative of an image to find edges. The Laplacian uses a convoluted mask or filter to approximate the second derivative, unlike the Sobel method, which approximates the gradient. Additionally, the Laplacian uses one filter for the second derive in both x and y directions while Sobel uses two filters, one for x and y direction. However, because the Laplacian filter approximates a second derivative measurement on the image, it is very sensitive to noise.

A review of 60 image retrieval systems from 1997 to 2006 is documented in this study. Figure 3.2 shows the distribution of approaches used by 60 image retrieval systems to segment objects in images. The majority of the systems use block technique for image segmentation. In particular, 24 systems use block-based technique, 19 systems use region-based technique and 16 systems used global technique to segment images and only 1 system uses a different technique, which is denoted Not Applicable (NA).

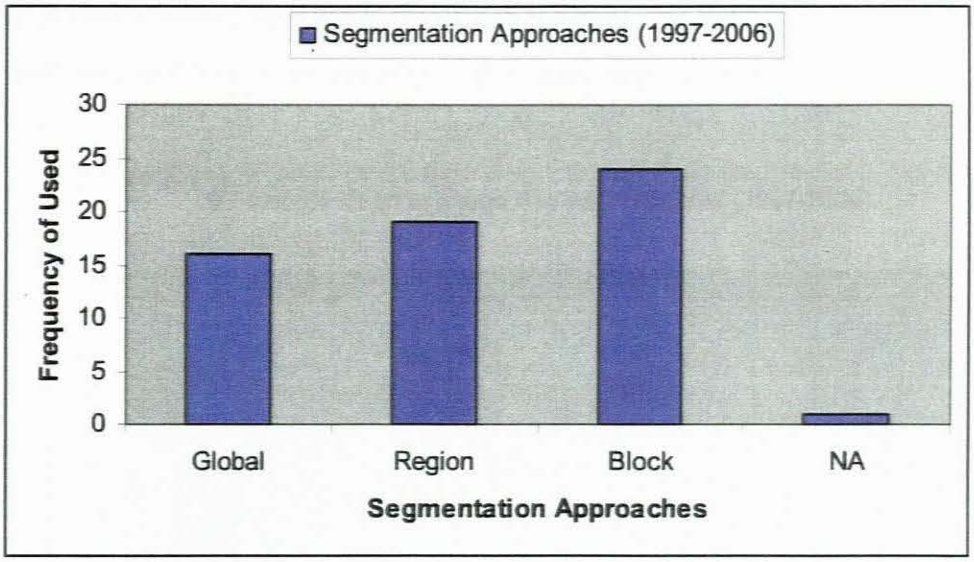

Figure 3.2: Distribution of segmentation approaches used by retrieval systems

3.4. Low-Level Visual Features

Low-level visual features used in CBIR systems can be generally categorized into three classes, namely, (a) primitive features, such as color, texture, shape, (b) logical features, such as identity of objects and (c) abstract features, such as significance of scenes being depicted. Figure 3.3 shows the distribution of image features used by 60 image retrieval systems documented in this study. Accordingly, many of the retrieval systems use a combination of image features. In particular, 37 systems use a combination of features, 14 systems use color features, 5 systems use texture and 3 systems use shape for image retrieval. Among those systems that use shape feature alone (Igbal & Aggarval, 2002; Dimov, 2003; Wong & Hsu, 2006), none considered healthcare applications to demonstrate the effectiveness of their retrieval systems. In terms of feature space dimensions used by these systems for image representation, the majority of the systems either use low or high feature space dimensions. Figure 3.4 shows the distribution of feature space dimensions used by 60 image retrieval systems. In particular, 15 systems use low feature space dimensions, 15 systems use high feature space dimensions, 6 systems use medium feature space dimensions, 5 systems use very low feature space dimensions and 5 systems use very high feature space dimensions.

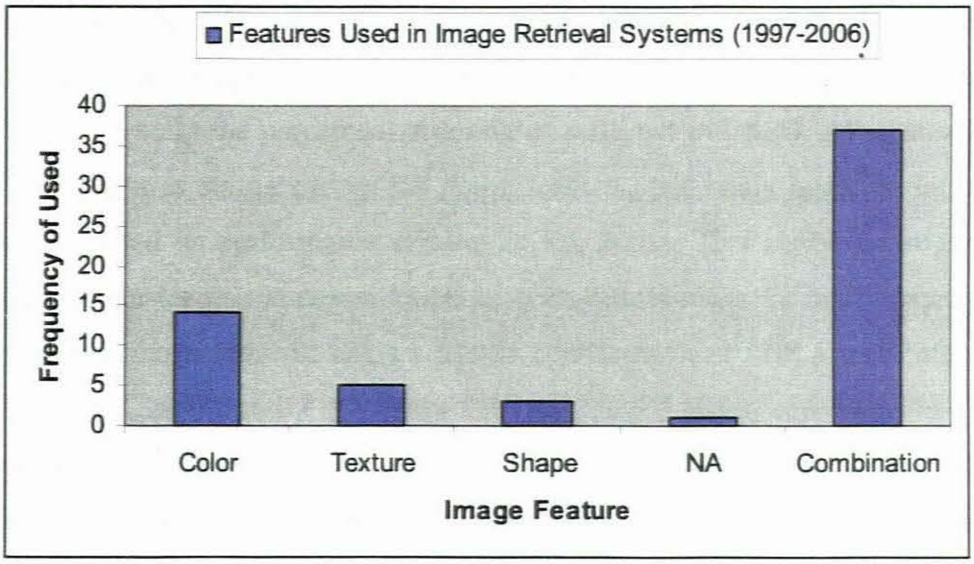

Figure 3.3: Distribution of image features used by image retrieval systems

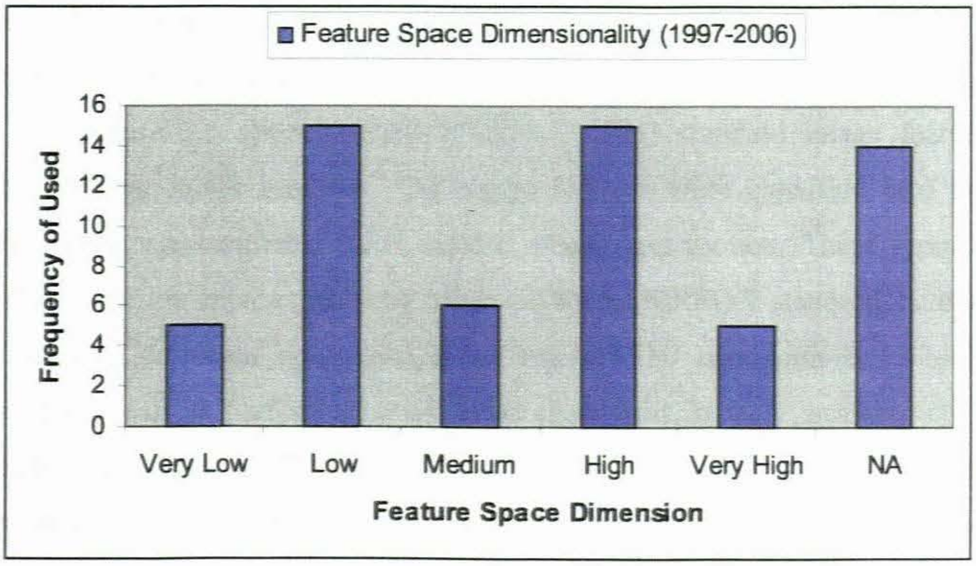

Figure 3.4: Distribution of feature space dimensions used by retrieval systems

The MPEG-7 proposed Curvature Scale Space Descriptors (CSSD) (Mokhtarian, et al., 1996) for contour-based shape description and Zernike Moments Descriptors (ZMD) (Kim & Sung, 2000) for region-based shape description. In terms of affine invariance, robustness, compactness, low computational complexity, ZMD gives good retrieval results and is better than CSSD, but lacks the perceptual meaning as reflected in CSSD. Alternatively, CSSD captures strong perceptual shape features, but many negative factors have affected its performance (Zhang & Lu, 2001). This study investigates both contour-based and region-based shape representations for brain magnetic resonance image retrieval using a hybrid combination of LBF active contour (Li, et al., 2007) and DFP (Tran & Ono, 2003) shape representation to improve retrieval results. LBF active contour is robust and can handle images such as MRI with intensity in-homogeneity. DFP is invariant to basic transformations such as rotation and translation. A hybrid combination of these two techniques for image representation will likely improve retrieval results. Our approach focuses on healthcare applications domain, but it generally extends to similar areas, where shape representation alone is considered very important.

Figure 3.5 shows MPEG-7 (Bober, 2001) standard image features proposed for image retrieval. The image features were classified into four main categories, namely, color, texture, shape and motion. Three types of color extraction approaches were proposed by the MPEG-7 standard, namely, histogram, dominant color and color layout. The histogram–based color extraction can be performed using three algorithms, namely, scalable color, color structure and GOF/GOP. Three different approaches for texture feature extraction as proposed by the MPEG-7 standard are texture browsing, homogeneous texture and edge histogram. The shape extraction can be performed using contour and region approaches. Finally, MPEG-7 standard proposed four different approaches for motion extraction, namely, camera motion, motion trajectory, parametric motion and motion actions. As indicated in the figure we investigated both contour and region based shape descriptors.

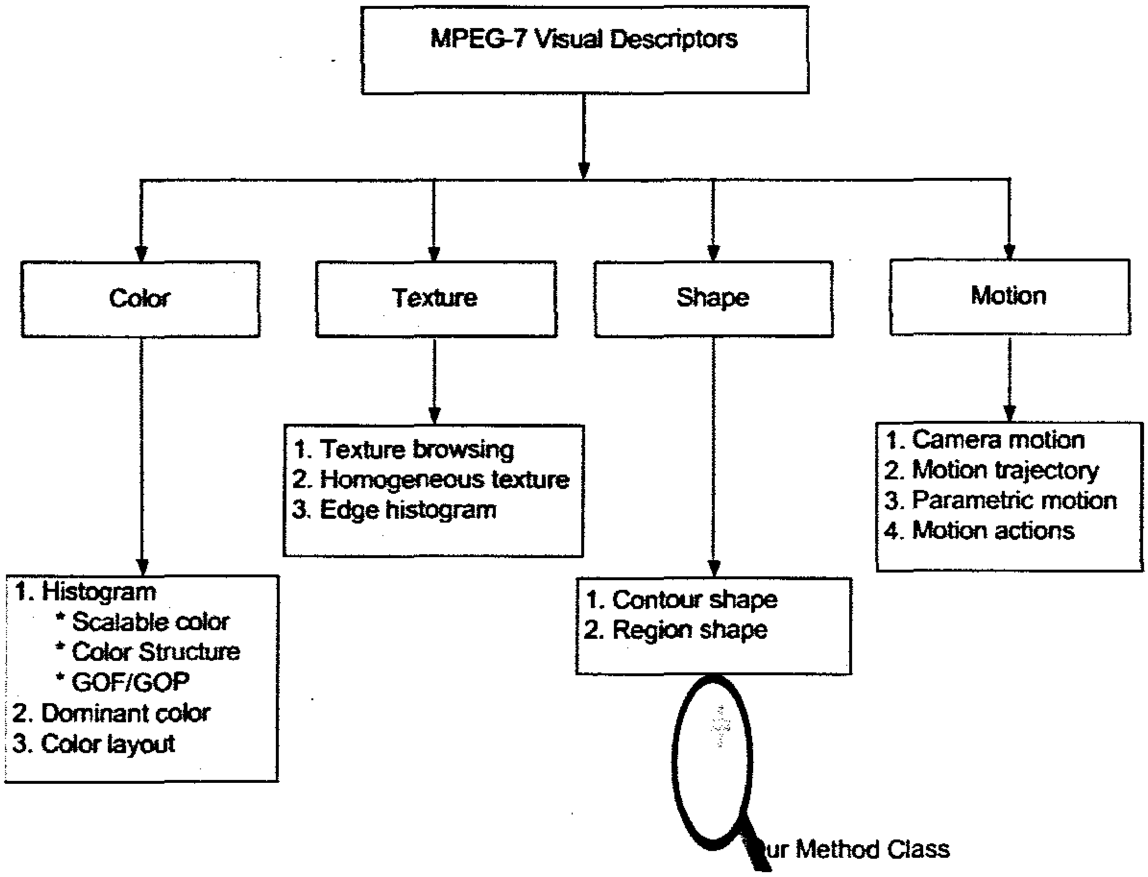

Figure 3.5: MPEG-7 visual information descriptors

3.5. Shape Feature Representation

This study investigated shape-based image retrieval for integration into healthcare information infrastructure. The shape of an image can be defined as the geometric information in an object when basic transformations such as rotation, translation and scale effects are removed. That is, an important characteristic of a good shape feature representation for an object is invariance to Euclidean transformations. A shape is an important cue used by humans to discriminate visual objects along with other features like color, texture and motion. However, compared to most image features, shape is easier for a user to describe in a query, either by sketch or by example. A query is usually given by example and it is unrealistic for a common user to conveniently sketch or describe an image as a query for features other than shapes. Consequently, shape is likely to give better human perception than many other image features.

The state-of-the-art methods for shape description are generally categorized into edge-based, which include rectilinear shapes (Jagadish, 1991), polygonal approximation (Arkin, et al., 1991) and finite element models (Sclaroff & Pentland, 1995). The second important category of shape description methods is the region-based, which include the Fourier descriptors (Persoon & Fu, 1977) and the statistical moments (Hu, 1962). The most successful representations for these two categories are Fourier Descriptor (FD) and Moment Invariants (MI).

Fourier descriptors describe the shape of an object with the Fourier transform of its edge pixels. The Fourier descriptors are obtained after applying Fourier transform on the edge pixels usually represented by a shape signature. The Fourier transformed coefficients are called the Fourier descriptors of the shape. An appropriate shape signature is essential for obtaining a good shape descriptor. A shape signature using centroid distance function was shown to outperform other shape signatures in shape based retrieval (Zhang & Lu, 2001). In Fourier shape descriptor, lower frequency coefficients describe the general shape property, while higher frequency coefficients reflect shape details. Usually, to achieve rotation invariance, the phase components are discarded and only the amplitudes of the complex coefficients are used. Translation invariance is inherently obtained from the contour representation. Scale invariance is achieved by dividing the magnitudes by the first component $|FD_0|$ of the descriptor. Generic Fourier descriptor (Zhang & Lu, 2002) is a region-based method and the shape descriptor is usually extracted from spectral domain by applying 2D Fourier transform on polar raster sampled shape image. Shape analysis using Fourier transform is supported by well developed and well understood Fourier theory. However, it is not desirable to directly acquire shape features using Fourier transform, because the acquired features are not rotation invariant. A modified polar Fourier transform was proposed by treating the polar image in polar space as a normal 2D rectangular image in Cartesian (Selvarani & Annadurai, 2008).

Moment invariants are used for shape representation and they are based on probability density functions such as expectation, variance, covariance and skewness. The moment invariants can be used for scale, position and rotation invariant object identification. However, moment invariants have high computational costs, because the features are computed on the entire region and low discrimination power (Tran & Ono, 2003). The moment invariants method can also break down for images, which are rotationally symmetric as the seven Hu invariant moments will be zero (Prokop & Reeves, 1992). Additionally, higher order moments have been shown to be more vulnerable to noise (Teh & Chin, 1988), thus making their use undesirable for object identification. Finally, the study reported by Shen & Ip (1998) compared invariant moments with a set of moments based on wavelet basis function. They concluded that when using Hu's moments, even a slight discrepancy in the image can cause a problem in discriminating between two similar objects.

Other shape descriptors include circularity, eccentricity, orientation, Euler number, profiles, areas, perimeter and convexity (Ang, et al., 1995), grid-based (Sajjanhar & Lu, 1997), Zernike Moments Descriptors (ZMD) (Kim & Sung, 2000), Delaunay Triangulation (DT) (Fang & Piegl, 1993), Touch-Point-Vertex-Angle (TPVA) (Safar, et al., 2000), Curvature Scale Space Descriptor (CSSD) (Mokhtarian, et al., 1996) and Hausdorff distance (Rucklidge, 1997). Safar, et al. (1999) compared four shape representation methods, namely Fourier Descriptors (FD), Grid-based Descriptors (GD), Delaunay Triangulation (DT) and TPVA sequence. They discovered that the precision of the FD is poor while GD, DT and TPVA are much better. There was no significant difference in the precision of the GD, DT and TPVA. But, the performance of DT is highly dependent on the technique used to find the feature points of object. Similarly, Zhang & Lu (2001) compared four shape descriptors, FD, GD, CSSD and ZMD. They concluded that in terms of affine invariance, robustness, compactness, low computational complexity, ZMD and FD are better than CSSD and GD. The ZMD lacks the perceptual meaning as reflected in FD and CSSD, but retrieval results favor its performance. The CSSD captures strong perceptual shape features, but many negative factors have affected its performance. A grid-based descriptor is suitable for cases where very similar shapes are required. New shape descriptors have been recently proposed, examples include shape matrix (Sheng & Xin, 2004), shape content (Belongie, et al., 2002) and DFP (Tran & Ono, 2003), which we have investigated along with region-based LBF active contour for both region and edge-based shape models computation.

3.6. Measuring Images Similarities

This study investigates Minkowski-form distance, Chi-test statistics and Quadratic form along with four new measures, namely, Histogram intersection, Procrustes shape, Pearson correlation and Bray Curtis for similarity computation. The purpose is to discover, which of these measures is more suitable for brain MRI retrieval and whether there will be significant difference between these measures. First, we need to describe these measures and show some adaptation carried out in this study. Secondly, we need to describe some areas where these measures have been used so as to demonstrate the difference between our study and others.

Image retrieval and classification are two important computer vision problems that directly rely on the concept of similarity measurement. A similarity measure is a critical component used to rank database images according to their similarity with the query image. Usually, the matching of the query image with database images is inexact, returning a list of images judged to be similar to the query image. The definition of similarity measure is based on three important design decisions, namely, (a) a feature space representation has to be chosen. A simple feature vector is often used for feature space representation; (b) the distribution of feature values is estimated. A histogram representation is usually chosen as a suitable nonparametric estimate of the feature distribution and (c) a similarity measure to compare two histograms is selected. Preliminary bench-mark studies have confirmed that distribution-based similarity measures exhibit excellent performance in image retrieval, in unsupervised texture segmentation and in conjunction with a k-nearest neighbor classifier in color or texture-based object recognition (Rubner, et al., 2001). The results of comparison of nine different similarity measures, namely, Minkowski-form distance, Weighted-mean-variance, Kolmogorov-Smirnov distance, Statistic of the Cramer/Von misses type, Chi-test statistics, Kullback-Leibler divergence, Jeffrey-divergence, Quadratic form and Earth movers distance for color and texture showed that there was no measure with best overall performance, but the selection rather depends on the specific task (Rubner, et al., 2001).

Now we describe the important similarity measures investigated in this study so as to put our idea in a proper perspective. To begin, we let S(I, J) denote a similarity measure between the query image I and the database image J. Suppose further that $f_i(I)$ denotes the distribution of pixels in the i[th] bin of an image I. The following measures were investigated for shape-based similarity computation on brain MRI:

3.6.1. Minkowski-Form

Minkowski-form measure (Rubner, et al., 2001; Long, et al., 2003), sometimes called L_p-norm is used to calculate the similarity or distance between two images if each dimension of the image feature vector is independent of each other and is of equal importance. For n-dimensional feature vector, the Minkowski-form similarity measure is defined as:

$$D(I,J)=\left(\sum_{i=1}^{n}|f_i(I)-f_i(J)|^p\right)^{\frac{1}{p}} \qquad (3.1)$$

If $p=1,2,\infty$, the measure D(I, J) corresponds to L_1-norm, which is called Manhattan, L_2-norm, which is called Euclidean and L_∞-norm, which is called maximum distance respectively. The L_1-norm computes the sum of absolute distances, L_2-norm computes the square root of the sum of squared points distance and the L_∞-norm measures the maximal difference. That is, $l_\infty=\max_{1\le i\le n}|x_i-y_i|$. The Minkowski-form measure is one of the most widely used distance measure for image retrieval. The L_1-norm was proposed for computing the similarity between color images (Swain & Ballard, 1991; Stricker & Swain, 1994; Funt & Finlayson, 1995) and for texture feature in the Netra system (Ma & Manjunath, 1997; Ma & Manjunath, 1999). The

Euclidean measure was used in the Maritime mobile Access and Retrieval System (MARS) (Rui, et al., 1997) to compute the similarity between texture features and to compute the similarity for color and shape feature in the Netra system. The Blobworld (Carson, et al., 2002) used Euclidean metric for texture and shape features. Voorhees & Poggio (1988) used the L_∞-norm to compute the similarity between texture images.

3.6.2. Histogram Intersection

Histogram intersection (Swain & Ballard, 1991) is a special form of the L_1-norm for computing the similarity between color images. Basically, whenever the histograms are of equal size, the histogram intersection and the L_1-norm are identical. Let $H(I)$ and $H(J)$ be histogram distributions of two images I and J respectively. Suppose each histogram contains n bins, then the histogram intersection is defined as:

$$H(I) \cap H(J) = \frac{\sum_{i=1}^{n} H_i(I) - \sum_{i=1}^{n} \min(H_i(I), H_i(J))}{\sum_{i=1}^{n} H_i(I)} \tag{3.2}$$

The denominator of this measure normalizes the histogram intersection and makes its values lie between 0 and 1. The histogram is usually normalized so that it represents the image without regard to the image size. The similarity value closed to 0 gives an indication of strong similarity between images. Similarly, a value of 1 gives an indication that the two images are dissimilar.

3.6.3. Quadratic Form

Minkowski-form measure, equation (3.1) treats all bins of the feature histogram independently and does not account for the fact that certain pairs of bins correspond to features that are perceptually more similar than other pairs. This problem is partially addressed in the weighted histogram intersection (Park, et al., 1999) by the introduction of the weight terms. This is a partial solution because cross similarity between bins was not considered. To solve this problem, quadratic-form similarity (Hafner, et al., 1995) was introduced and this measure is defined as:

$$D(I,J)=\sqrt{(F_I-F_J)^T A(F_I-F_J)} \tag{3.3}$$

where $A=(a_{ij})$ is a similarity matrix and a_{ij} denotes the similarity between i^{th} and j^{th} bins. The vectors F_I and F_J list all the entries in $f_i(I)$ and $f_i(J)$ respectively and F^T is the matrix transpose of F. The cross-distance measure considers the cross-correlation between histogram bins based on the perceptual similarity of the colors represented by the bins. According to Hafner, et al. (1995), this method more closely corresponds to human judgment of color similarity. The set of all cross-correlation values are represented by a matrix A, which is called a similarity matrix. The $(i, j)^{th}$ element in the similarity matrix A for Red, Green and Blue (RGB) color space is given as:

$$a_{i,j}=\frac{\max(d_{ij})-d_{ij}}{\max(d_{ij})} \tag{3.4}$$

where d_{ij} is usually the l_2-norm between the color i and j in the RGB color space. In the case that quantization of the color space is not perceptually uniform, the cross term contributes to the perceptual distance between color bins. The quadratic-form measure has been successfully used in many image retrieval systems such as Query By Image Content (QBIC) (Flicker, 1995) for color histogram-based image retrieval. The quadratic-form measure has been shown to give perceptually more desirable results than the Euclidean measure and the histogram intersection as it considers cross similarity between colors. This study adapts Quadratic form for shape-based similarity computation by taking d_{ij} to correspond to the L_1-norm.

3.6.4. χ^2-test Statistics

χ^2-test statistics is conventionally used to test for the goodness of fit and tests of independencies of distributions. This measure was originally proposed by Puzicha, et al. (1999) for image segmentation and retrieval. Belongie, et al. (2002) proposed χ^2-test statistics to match two shape objects represented by shape contexts, where f(I) and f(J) correspond to the n-bin normalized histograms. The equation for χ^2-test statistics as used in this study is given as:

$$D(I,J)=\frac{1}{2}\sum_{i=1}^{n}\frac{(f_i(I)-f_i(J))^2}{f_i(I)+f_i(J)} \tag{3.5}$$

3.6.5. Procrustes Shape

Procrustes distance (Kendall, 1984) here denoted by $D^2(I,J)$ is a least-square type shape similarity measure that requires shapes with 1-1 point correspondence. The square Procrustes distance between two shapes f(I) and f(J) measures the sum of the squared Euclidean distances between corresponding points, after alignment and is defined as:

$$D^2(I,J)=\sum_{i=1}^{n}(f_i(I)-f_i(J))^2 \tag{3.6}$$

The shape representations f(I) and f(J) are assumed to be invariant to basic operations such as scaling, rotation and translation for this measure to effectively work. Antania, et al. (2004) generated the ground truth data on spine X-rays using the Procrustes shape similarity measure.

3.6.6. Bray Curtis

Bray Curtis (Jacobsen, et al., 1999), which is sometimes called Sorensen measure, is a normalization technique that is frequently used in environmental science, botany and ecology for similarity computation. The normalization is done using absolute difference divided by components summation. The Sorensen measure has a good property that if all coordinates are positive, the value it computes lie in the interval [0, 1]. This makes Sorensen measure worthy of investigation in this study, because DFP shape representation satisfies the positive constraint requirement. The zero Sorensen distance indicates exact similarity of the objects compared. The equation for Sorensen measure is given as:

$$D(I,J)=\frac{\sum_{i=1}^{n}|f_i(I)-f_i(J)|}{\sum_{i=1}^{n}(f_i(I)+f_i(J))} \tag{3.7}$$

3.6.7. Pearson's Correlation Coefficient

Pearson correlation coefficient, sometimes called cross-correlation or Pearson Product-Moment Correlation Coefficient (PMCC) (Spiegel, M.R., 1972) measures the extent to which two samples are linearly correlated. PMCC measures the strength and direction of a linear relationship between two variables. These variables are assumed to be interval, approximately normally distributed and their joint distribution is bivariate normal. PMCC has the properties that it does not depend upon the units of measurement and upon how variables are labeled. The measure takes on the values from -1.0 to 1.0. A value of -1.0 indicates a perfect inverse correlation, 0.0 is no correlation and 1.0 is a perfect positive correlation. We applied PMCC to similarity computation in this study by subtracting the absolute value of the value computed by PMCC from 1.0. Thus, low PMCC value gives an indication of similarity and higher value of PMCC means dissimilarity. Give that $f_a(I)$ is the mean value of $f(I)$, the formula for PMCC is given as:

$$D(I,J)=\frac{\sum_{i=1}^{n}(f_i(I)-f_a(I))(f_i(J)-f_a(J))}{\sqrt{\sum_{i=1}^{n}(f_i(I)-f_a(I))^2\sum_{i=1}^{n}(f_i(J)-f_a(J))^2}} \tag{3.8}$$

3.7. CBIR Storage and Access

We investigated the use of Jensen polynomials (Csordas, et al., 1990) for shape-based indexing. We demonstrated the effectiveness of Jensen polynomials to uniquely compute shape index from geometrical properties, such as orientation, eccentricity and shape profiles. We also apply Jensen polynomials on DFP shape representation to directly compute index from this representation. The Jensen polynomials application uses features that satisfy Turan's inequalities for index computation.

The storage and access methods for CBIR are important considerations for an interactive system to yield an acceptable response time. A general characteristic of CBIR systems is that they are developed over conventional Database Management Systems (DBMS), which provide fast data access methods for indexing. The interest in CBIR naturally arises towards approaches better adapted to the index access techniques of conventional DBMS (Dimov, 2003). A key image consists of the most essential information of a given image, structured in descending order into a one dimensional array of fixed length. Common storage methods used for CBIR systems are relational databases and inverted files (Squire, 2000). These methods used dimension reduction techniques or pruning methods to enable efficient and fast access to the data (Muller, et al., 1999). Principal Component Analysis (PCA) (Sinha & Kangarloo, 2002) is conventionally used for dimension reduction, because it is optimal and linearly maps input data to a coordinate space such that the axes are aligned to reflect the maximum variations in the data. The QBIC system uses PCA to reduce a 20-dimensional shape feature vector to two or three dimension (Flicker, et al., 1995). The dominant eigenvectors technique is becoming popular for feature representation after applying PCA algorithm. The dominant eigenvectors can then be used for indexing, but this can lead to information lost, since not all eigenvectors are used. Comparing Jensen polynomials application of shape indexing with PCA, in PCA if all eigenvectors are used for indexing, reconstruction of the image is possible. However, in Jensen application, shape cannot be recovered from indexes and it is only useful for cases where shape reconstruction is not required. This technique is still adequate for index computation, because image reconstruction is not an important consideration in this situation. We want an efficient access to database images for fast retrieval of similar images in a database.

Figure 3.6 shows the distribution of dataset used by 60 image retrieval systems. The majority of the systems that is, 27 systems use different kinds of datasets, 24 systems use Corel dataset, 4 systems use hybrid datasets, 3 systems use WWW dataset and only 2 systems use Kodak Photo dataset.

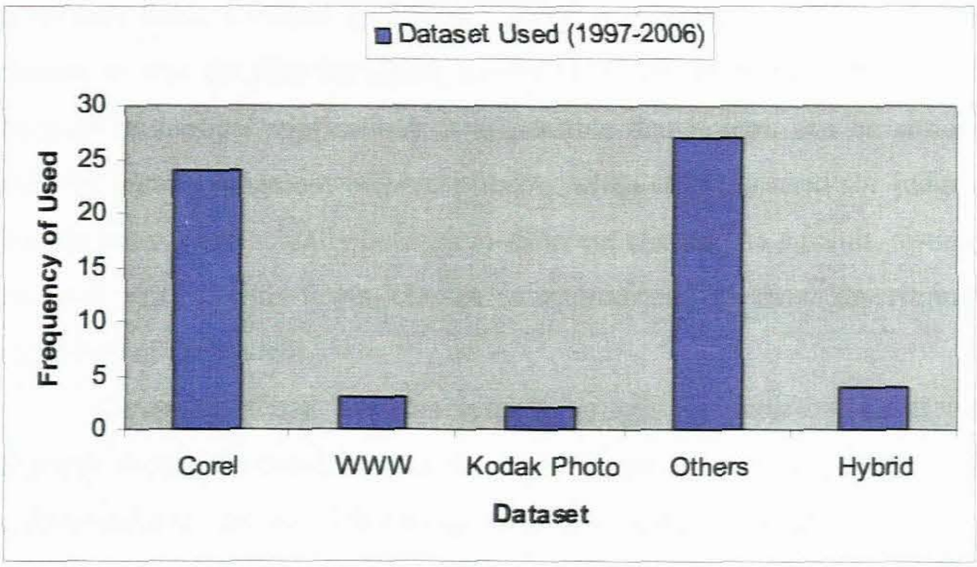

Figure 3.6: Distribution of dataset used by image retrieval systems

3.8. Image Semantics and Efficient Classification

Our classification-based image retrieval approach is similar to the approach proposed by Wang, et al. (2001) for improving image retrieval results. They posited that pre-classification of images will improve retrieval results. Their approach proposed to pre-classify images into high level semantic categories like graph or photograph, texture or non-texture, which are relatively simple to classify. After this classification, the retrieval system returns only the images belonging to the same semantic categories. In addition, region-based features similar to the approach in BlobWorld are used, but the region descriptions of the images are automatically matched. We propose in this study to pre-classify brain MRI into semantic categories, namely, degenerative, infectious, normal, stroke and tumor. The retrieval returns similar images belonging to any of these classes as well as the name of a class that the example image is predicted to belong. We then apply LBF active contour to segment the example image into region of interest. This makes our system different from that proposed by Wang, et al. (2001). We then set out to validate the hypothesis that pre-classification of images will improve retrieval results using our system. To validate this hypothesis, we allow our system to compute retrieval results using different techniques and then compare these results for significant difference using a robust statistical technique. We used very low, that is, 5 classes to test the discrimination capability of our retrieval system. This is because in medical applications, it is possible that images can be similar as seen by human judgment of perceptibility when shape is used for judgment, but the images can actually belongs to different classes. As a result, testing for retrieval results with fewer classes is appropriate to show discrimination capability of the system.

Generally, CBIR systems retrieve images by their low-level visual features. However, these features do not allow users to query images by their understandable high level semantics concepts. Image annotations, sometimes called image classification systems have been proposed to solve the inadequacy of conventional CBIR systems. Annotation systems aim at automatically annotating images with some controlled keywords to model user understandable high-level constructs. Machine learning techniques from artificial intelligence field of study are the tools used to develop the annotation systems that map the low-level visual contents to high-level semantics. Supervised machine learning techniques are particularly found useful to annotate images for efficient retrieval. These techniques learn correspondence between visual features and high-level image semantics and then use previously acquired knowledge to recommend an appropriate solution. Image annotation problem is generally formulated as classical image classification problem, where the image annotation system classifies visual features into some pre-defined classes (Antani, et al., 2002).

Figure 3.7 shows the distribution of image classification techniques used by 60 image retrieval systems. The majority of the systems that is, 20 systems use SVM, 8 systems use Bayes, 7 systems use k-NN, 6 systems use MLP, 3 systems use template, 2 systems use HMM and only 1 system use LDL. Figure 3.8 shows the distribution of number of classes used by the retrieval systems that use classification techniques. The majority of the systems that is, 27 systems use very low number of classes, 14 systems use low number of classes, 8 systems use medium number of classes, 7 systems use very high number of classes and 3 systems use high number of classes. Figure 3.9 shows the distribution of number of keywords used by the retrieval systems. The majority of the systems that is, 37 systems use a single keyword for semantic description of an image, 13 systems do not use keywords for semantic description, 6 systems use 5 keywords and more, 1 system uses 2 keywords and 1 system uses 3 keywords.

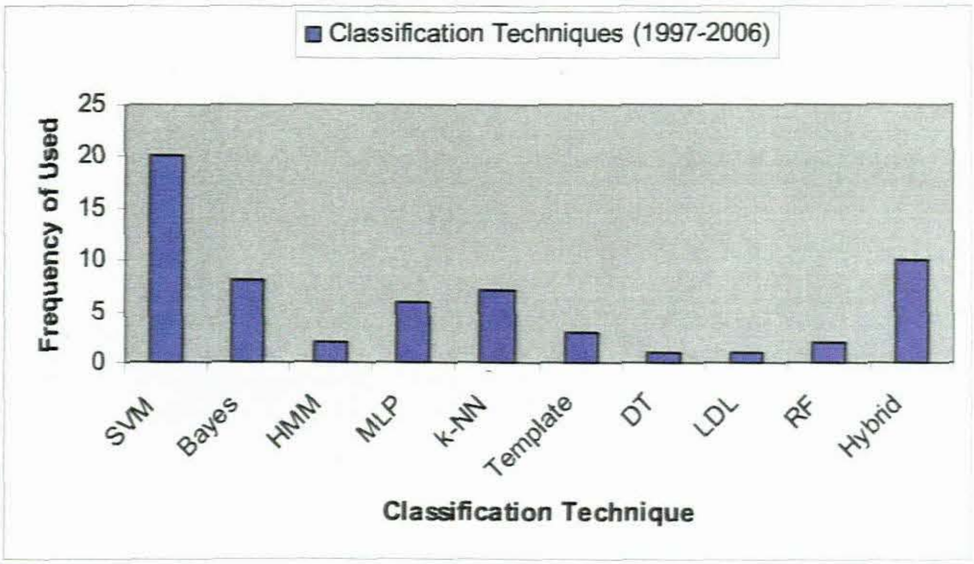

Figure 3.7: Distribution of classification techniques used by image retrieval systems

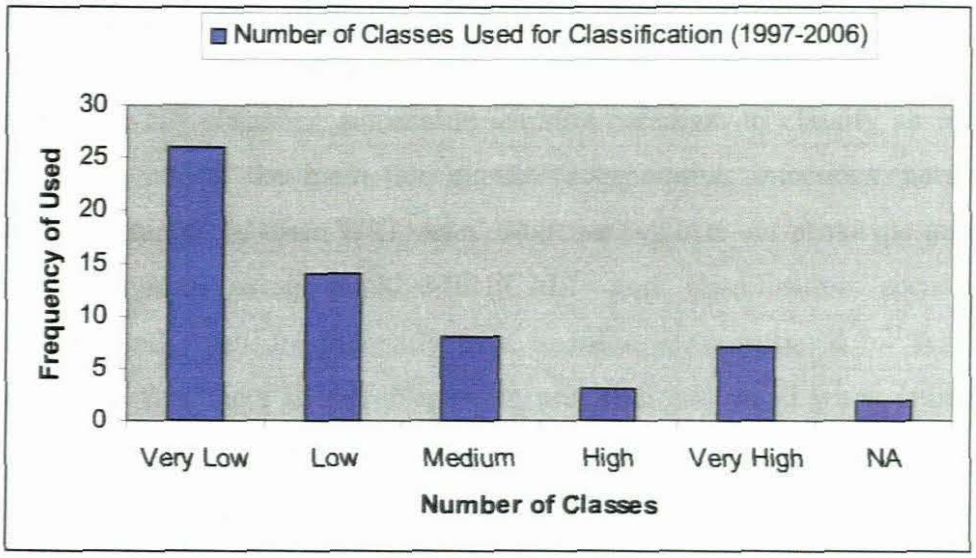

Figure 3.8: Distribution of classes used by classification systems

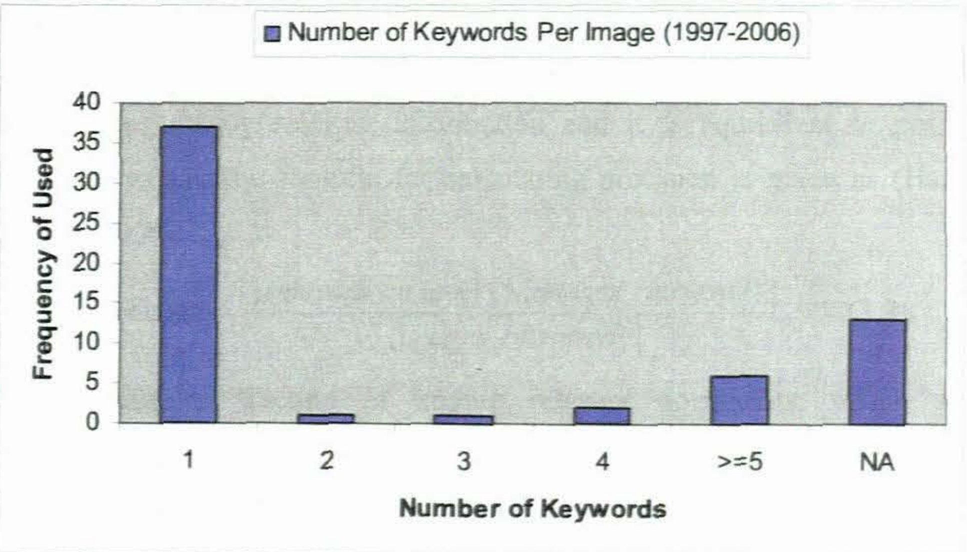

Figure 3.9: Distribution of keywords used by classification systems

3.9. Retrieval System Performance Evaluation

Our approach for improving retrieval results of an image retrieval system is based on k-NN classifier, a machine learning paradigm to classify an input image into one of the main five classes (degenerative, infectious, normal, stroke and tumor) of brain MRI. As a result, we evaluate our prototype image retrieval system using intuitive-PRECALL and classification accuracy. Precision and recall are popularly used in information retrieval for system evaluation. But, there is a problem with precision and recall when multiple queries are involved. We first describe the evaluation techniques based on precision and recall to prepare the ground for proper understanding of our evaluation methods described in chapter 4.

The performance of a retrieval system is generally measured using two common set-based measurements, namely, recall and precision. Precision quantifies fraction of retrieved documents, which are known to be relevant. It measures the ability of the search technique to retrieve top ranked documents that contains mostly relevant information and it is equivalent to positive prediction value. The formula for calculating precision is given as (Han & Kamber, 2006):

$$\Pr ecision = \frac{|\{relevant\ images\} \cap \{images\ retrieved\}|}{|\{images\ retrieved\}|} \qquad (3.9)$$

Recall quantifies fraction of known relevant documents, which were effectively retrieved. It measures the ability of the search technique to find the documents in the database that contain relevant information and it is equivalent to sensitivity. The formula for calculating recall value is given as (Han & Kamber, 2006):

$$\mathrm{Re}call = \frac{|\{relevant\ images\} \cap \{images\ retrieved\}|}{|\{relevant\ images\}|} \qquad (3.10)$$

Precision and recall have been used to evaluate retrieval systems returning a set of putative matches, where the number of matches is usually small relative to the database size. There is usually a trade-off between precision and recall, in which case, high precision returns relevant documents, but misses many useful ones as well. Similarly, high recall returns most relevant documents, but includes a considerably irrelevant one. This follows that an inverse relation exists between precision and recall. The ideal situation is how to simultaneously have high precision and recall values, which is a difficult problem. Traditionally, both precision and recall can be combined into a single measure of retrieval performance. The equation that gives the relationship between precision, recall, generality and fallout is (Raghavan, et al., 1989):

$$\mathrm{Pr}\,ecision = \frac{Generality \times \mathrm{Re}\,call}{Generality \times \mathrm{Re}\,call + (1 - Generality) \times Fallout} \quad (3.11)$$

The generality, G is the ratio of the number of relevant documents n in the collection to the number of documents in the entire collection N. Fallout of a retrieval system is the proportion of irrelevant documents retrieved. Mathematically,

$G = \frac{n}{N}$ and $Fallout = 1 - \mathrm{Pr}\,ecision$.

Another important measure in information retrieval and natural language processing that connects both precision and recall is the F_α - measure (van Rijsbergen, 1979). F_α - measure is a weighted harmonic mean of precision and recall. The formula for calculating this retrieval system performance measure is as:

$$F_\alpha = \frac{(1+\alpha^2) \times \mathrm{Re}\,call \times \mathrm{Pr}\,ecision}{\alpha^2 \times \mathrm{Pr}\,ecision + \mathrm{Re}\,call} \quad (3.12)$$

The non-negative real value α allows one to weight either precision or recall more heavily depending on which measure to be favored. As α increases, the weight of recall increases in the measure. If $\alpha = 1$, F_1 - measure is the mean of precision and recall. If $\alpha = 0$, F_0 - measure corresponds to precision. In most experiments, there is no particular reason to favor precision or recall, so most researchers use $\alpha = 1$ to have balance F_1 - measure (Hripcsak & Rothschild, 2005).

3.10. Classification System Performance Evaluation

Evaluation of classification results is an important process in image classification procedure. There are six different criteria for evaluating the performance of a classification technique, namely, accuracy, reproducibility, robustness and ability to fully use the information content of the data, uniform applicability and objectiveness (Cihlar, et al. (1998). But, in reality, no classification algorithm can satisfy all these requirements nor be applicable to all studies, due to different environmental settings and datasets used (Lu & Weng, 2007). Hence, many systems employing a classification technique often use classification accuracy for performance evaluation.

The technique used in this study for evaluating performance of a classification system uses the entire training data to select a classifier and estimate the accuracy of the system. A 5-fold cross-validation sampling technique was used to split the training dataset into disjoint subsets. The advantage of using this sampling strategy is that all the dataset examples are eventually used for the both training and testing. The purpose is to select a classifier such that the true accuracy is maximized. A small number of folds were used to reduce the computation time and to keep the variance of the estimator small. The accuracy estimate A_i of a classification system can be defined as:

$$A_i = \frac{|\{All\ images\ classified\} \cap \{\mathrm{Im}ages\ correctly\ classified\}|}{|\{All\ images\ classified\}|} \quad (3.13)$$

Classification accuracy evaluation generally includes three basic components, namely, sampling design, response design and estimation and analysis procedures (Stehman & Czaplewski, 1998). The selection of a suitable sampling strategy is a critical step (Congalton, 1991). Three main sampling strategies commonly used are (a) holdout set (Goutte, 1997), which is easy to compute, but has higher variance, (b) Leave-One-Out Cross Validation (LOOCV) (Guid, et al., 2004), which is easy to use for some classifiers and difficult for others and (c) k-Fold Cross Validation (k-Fold CV) (Goutte, 1997), which uses all data for both training and testing. The true accuracy estimate A is the average of the separate accuracy estimate A_i. This is given mathematically as:

$$A = \frac{1}{k}\sum_{i=1}^{k} A_i \tag{3.14}$$

3.11. Content-Based Medical Image Retrieval

The main goal of healthcare information infrastructures is to provide the needed information on time, at the right place and to the right persons so as to improve the quality and efficiency of care processes. Such a promising goal will definitely need more than a patient identity for query retrieval. Clinical decision support techniques such as image-based reasoning or case-based reasoning (Topel, et al., 2007) and evidence-based medicine (Bui, et al., 2002; Boissel, et al., 2003) can produce stronger needs for image retrieval. These can be valuable resources for supporting certain disease diagnosis and therapy planning, because previous similar cases or episodes of a diagnosis can be massively reused. Queries based on images demonstrate the usefulness of capturing images in electronic healthcare record (Katehakis & Tsiknakis, 2006). The importance of a query based on medical images and knowledge retrieval in healthcare applications domain was illustrated by Lowe, et al. (1998) and several other applications of image retrieval have been demonstrated (Cai, et al., 2001; Ogiela & Tadeusiewicz, 2001; Kuo, et al., 2002; Horsch & Thurmaur, 2003; Kherfi, et al., 2004; Muller, et al., 2004; Muller, et al., 2005). There are many neurological diseases such as Dementia that if a doctor wants to diagnose a symptom, he needs a series of images to diagnose or make a decision for therapeutic strategies (Su, et al., 2007). However, image-based queries can be expensive and time-consuming if a patient's charts, radiology reports and surgical pathology documents are to be manually reviewed. The Digital Imaging and Communications in Medicine (DICOM) (Stewart & Langer, 1998; Khludov, et al., 2000) is a standard for image communication in a distributed healthcare environment. Although DICOM can be used to store patient's textual information with the actual images, but a problem prevail with respect to standardization (Muller, et al., 2004). Content-based access to medical images for supporting clinical decision-making has been proposed to ease the management of clinical data and scenarios for the integration of content-based access methods into PACS (Muller, et al., 2004; Su, et al., 2007). As a result, the healthcare community has been exploring collaborative approaches for managing image data and exchanging knowledge (Dean & Solomonides, 2004; Rogulin, et al., 2004).

Applications of Decision Support Systems (DSS) in radiology and Computer Aided Diagnostics (CAD) for radiological practice have created a need for more powerful data management and retrieval techniques. An image retrieval system, as a tool for diagnostic aid has shown to improve the diagnostic quality (Aisen, et al., 2003). Image retrieval systems and image archives have been described as important economic and clinical factors in the hospital environment (Greenes & Brinklye, 2000; Kulikowski, et al., 2002). Several image processing methods and techniques have long been proposed for use in healthcare domain (Sarvazyan, et al., 1991; Pun, et al., 1994). Healthcare is a principal application domain for CBIR technologies, because of the increasing volumes of medical images generated on a daily basis in hospitals worldwide. Web-based interfaces to healthcare image databases were described (Frankewitsch & Prokosch, 2001). The Automatic Search and Selection Engine with Retrieval Tools (ASSERT) system classifies high resolution CT image of the lung (Shyu, et al., 1999). The Image Retrieval in Medical Applications (IRMA) system (Lehmann, et al., 2000; Lehmann, et al., 2004; Lehmann, et al., 2005) classify images into anatomical areas, modalities and viewpoints (Keysers, et al., 2003).

3.12. General Applications of CBIR in Healthcare

Four principal domains of healthcare, identified for use of CBIR methods and techniques, include teaching, research, diagnostics and automatic classification of images. In teaching domain for instance, lecturers can use large image databases to search for interesting cases to present to students. This can aid the understanding of the subject matter as many images are available for comparison. Research can immensely benefit from image retrieval methods and techniques. Researchers have more options for the choice of cases of interest to include into their research works and studies by allowing both text-based and visual access. Most medical applications of CBIR are centered on images produced in radiology departments.

The task of a pathologist when searching for reference cases supports the use of an image retrieval system instead of relying solely on reference books. Having efficient access to database images, therefore, will be of importance to a radiologist. As a result, we investigated algorithms and techniques that can improve retrieval results for healthcare applications. In particular, our study investigated the suitability and effectiveness of some image processing techniques for brain MRI. The choice of MRI is motivated by the difficulty in extracting objects from these images. The results of this study can aid the development of image retrieval systems for diagnosis of brain diseases as well as discovering useful patterns for the study of brain images.

3.13. Magnetic Resonance Imaging Applications

There are several approaches proposed in the literature to address the limitation of intensity based image classification and numerous MRI segmentation methods and techniques have been reported. Applications of image retrieval to MRI reported in the literature include MRI of the heart. In radiology, mammography is one of the most frequent application areas of MRI with respect to image classification and content-based search. The classification of High Resolution CT (HRCT) scans of the lung was described (Shyu, et al., 1999). Brain MRIs have been used to demonstrate image search algorithms (Mojsilovis & Gomes, 2002). The application of image retrieval to brain MRI using texture features extracted by wavelets transformations has been demonstrated (Traina, et al., 2003).

MRI is a useful technique in clinical practice to distinguish pathology tissue such as a brain tumor from normal tissue. MRI uses a powerful magnetic field, non-ionizing radiation (unlike CT scan and x-ray) in the radio frequency range and a computer to produce detailed pictures of organs, soft tissues, bone and virtually all other internal body structures. Detailed MRI allows physicians to better evaluate parts of the human body and certain diseases that may not be adequately assessed with other imaging methods such as x-ray, ultrasound or CT.

Fully automatic brain MRI segmentation and classification are of great relevance for research and clinical study of much neurological pathology. The accurate segmentation of MRI into different tissue classes, especially gray matter (GM), white matter (WM) and cerebrospinal fluid (CSF) is an important task. Moreover, regional volume calculations may bring even more useful diagnostic information. The quantization of gray and white matter volumes is of major interest in neurodegenerative disorders such as the Alzheimer disease, in movements disorders such as Parkinson or Parkinson related syndrome, in white matter metabolic or inflammatory disease, in congenital brain malformations or per-natal brain damage, or in post-traumatic syndrome and so on. Automatic segmentation of brain MRI, however, remains a persistent problem. Moreover, the automated and reliable tissue classification is complicated by the overlap of MRI intensities of different tissue classes and by the presence of a spatially smoothly varying intensity in-homogeneity, which is caused by either a non-uniform field or a non-uniform sensitivity (Homak, 2007). We investigated the use of region-based LBF active contour to segment brain MRI and tested the result in our prototype system to discover that LBF active contour is effective and suitable for brain MRI segmentation.

Chapter 4

Design Issues

The purpose of this chapter is to discuss the design issues considered for the realization of our objectives. There are a number of useful algorithms and techniques well developed in image processing, computer vision, artificial intelligence and statistics fields of knowledge that we have integrated for improving results of image retrieval systems for healthcare applications.

Specifically, we investigated the usefulness of high-resolution cubic spline interpolation, level sets and LBF active contour, connectivity-number edge detection algorithm, DFP shape representations, instance-based learning, Gaussian image smoothing and Jensen polynomials to improve retrieval results of an image retrieval system. A robust statistical method was developed to evaluate and test the effectiveness of the algorithms and techniques realized from the use of these methods. We consider very paramount to step-wisely discuss these design issues, beginning from the general image content operation to system evaluation design issues. First, we begin the discussion from image content operation, which is an important step that can be followed to sufficiently describe the content of an image. Next, we consider color-space conversion as a useful process to transform a colored image to grayscale, thereby realizing a robust algorithm for shape extraction. This scheme is effective, because color and shape are two different image features and transformation of a colored image to grayscale image has little or no effect on the shape of the image. Generally, when it comes to shape feature extraction, color feature is not important. Features such as edges are more important than color features in order to effectively describe shapes. Moreover, many medical images such as MRI and x-ray are grayscale and not colored.

Other useful techniques investigated in this study include interpolation functions for scaling images to reasonable sizes. Generally, images come in different sizes such as 256 x 256, 512 x 512, 1024 x 1024, which can be very large for efficient processing. Many steps are involved in image processing and there is the need to reduce image dimensions to manageable sizes so as to speed up processing. We achieved efficient dimension reduction using high-resolution cubic spline interpolation function and vector re-binning. Our interpolation algorithm is able to re-sample images with number of rows different from number of columns, all that is required is to specify the new row and column dimensions as input to the algorithm. An important design issue is image segmentation, which is a central problem in computer vision and image processing. Image segmentation distinguishes objects from the background and separates objects into blobs. There are four approaches for segmenting images into blobs, namely, threshold (Lezoray & Cardot, 2002), edge-based (Jagadish, 1991), region-based (Hu, 1962) and connectivity-preserving relation, sometimes called active contours (Chan & Vese, 2001).

Threshold-based methods make decisions based on local pixel information and they are usually effective when the intensity levels of the object to segment lie outside the range of levels in the background. However, blurred region boundaries can create serious problem in threshold-based methods. Another very important consideration in threshold-based methods is how to efficiently select suitable thresholds. Edge-based methods center on contour detection and they are weak in connecting broken contour lines and thus, prone to failure in the presence of blurring. A region-based method partitions the image into connected regions by grouping neighboring pixels of similar intensity levels. Adjacent regions are then merged under some criteria. However, over-stringent criteria can create fragmentation and lenient ones can overlook blurred edges and over-merge. Connectivity-preserving methods have drawn specific attention in recent years and they are usually referred to as the active contour models. Active contours, sometimes called snakes, moving fonts or deformable models, are computer-generated curves that move within images to find object boundaries. Active contours have their limitations, such as issue of re-initialization. But, they are very attractive, because of their ability to handle protrusious and specific topological effects, thus considered in this study.

4.1. Image Content Operations

An important step that can be followed to sufficiently describe the content of a given image is image-content operations. These operations transform the image data into a spatial data array. This is usually accomplished in three essential units, namely, color, texture and geometry. They can be characterized by the function:

$$f(x) = G \otimes I(x) \tag{4.1}$$

where $I(x)$ is the given image, G is an operator that acts on the image and the resulting image field is $f(x)$. The image content $f(x)$ is extracted by the histogram G that represents the objects in $I(x)$ according to the function given by equation (4.1).

In this study, the content extraction is given by DFP shape representation (Tran & Ono, 2003). But, other shape-based representations such as Fourier descriptors (Lee, et al., 2003) and Bezier curves (Sohel, et al., 2005) can as well be applied. However, an important requirement for using a shape-based representation is that it should be invariant to basic geometrical transformations, such as scaling, translation and rotation. Additionally, the similarity measure for matching two shapes should conform to human perception. Many of these representations do not completely satisfy all the needed requirements and there is the need to modify a given shape representation to suit an image retrieval application. The DFP shape representation satisfies rotation and translation invariant properties, but it is not invariant to scaling, just like many other representations. We achieved scale invariant with DFP shape representation by segmenting all input images re-sampled in the same dimension of 72 x 72 sizes.

4.2. Color-Space Conversion Scheme

The robustness of our algorithms and techniques to process colored images was first achieved by converting all input multi-channel (color) images to grayscale images. It is sometimes desirable to change the color format of an image when processing the image. When a color image is converted to a single channel image, there can be a substantial improvement in efficiency, both in memory storage and in the computational time. Although color is an important image feature, there are areas such as medical applications where color information is not too important. For instance, where shape information is required, edge seems to be more important than color. Moreover, many MRI images are grayscale images and transforming color images to grayscale images is a useful image processing steps. Tests have shown the conversion of color images into grayscale images does not affect performance, but at the same time the running time is reduced from minutes to seconds (Lin, et al., 2006). This way, high computational costs for color image processing is considerably reduced.

The general assumption in converting from RGB color-space images to grayscale images is that noise is homogeneous in RGB color-space and its distribution is Gaussian with the three color coordinates being statistically independent. Then to convert from RGB color-space to grayscale, a point operation is usually applied. Since the transformation from RGB space to grayscale is linear, the assumption of Gaussian noise being homogeneous in grayscale still holds. The grayscale method sets the three color components R, G, B of each pixel (x,y) to the same value $f(x,y)$ using any of the three equations (4.2a), (4.2b) and (4.2c). The first color conversion formula that we consider is based on simple averaging of each color component:

$$f(x,y) = 0.3333R(x,y) + 0.3333G(x,y) + 0.3333B(x,y) \qquad (4.2a)$$

The effect of equation (4.2a) is called de-saturation in Adobe Photoshop and this may likely deteriorate the actual image appearance for images such as those of trademarks where color is considered a relevant feature. The second color space conversion formula popularly used in image processing is the National Television System Committee (NTSC) conversion standard given as:

$$f(x,y)=0.2990R(x,y)+0.5870G(x,y)+0.1140B(x,y) \quad (4.2b)$$

The third color space conversion formula popularly used in image processing is given as:

$$f(x,y)=0.2125R(x,y)+0.7154G(x,y)+0.0721B(x,y) \quad (4.2c)$$

The NTSC color conversion standard is similar to Adobe Photoshop conversion from RGB to grayscale. The NTSC color conversion formula was used in this study to convert a colored image to a grayscale image. The choice of this color conversion was motivated by the fact that it is the first set of standard protocols for television. This standard was introduced in 1941 and is widely used across the world for color conversion from the true RGB color to the equivalent NTSC color-space, whose luminance is the grayscale signal used to display pictures on monochrome televisions and the other components of the color-space carry the hue and saturation information.

4.3. Image Re-sampling using Interpolation Functions

Image re-sampling or image scaling is the process of transforming a discrete image that is defined at one set of coordinate locations to a new set of coordinate points. Re-sampling is used for different purposes in image processing and computer vision. An image can be re-sampled to a finer grid in order to improve its visual appearance or to change its dimension. However, re-sampling an image to a new set of coordinates can result in a loss in image quality. The image can be blurred when one up-samples or stretches to a larger dimensions. But, down-sampling or squeezing of an image can improve its sharpness. Image re-sampling is not a straight forward task and only a few techniques exist. These techniques are based on interpolating functions and each can give more or less good results. The interpolating function to use for re-sampling should be an ideal low-pass filter so as to preserve image quality.

There are five interpolating functions, namely, nearest neighbor, linear, cubic B-spline, high-resolution cubic spline with edge enhancement and high-resolution cubic spline are used for image re-sampling. The nearest neighbor function is the simplest of all interpolation algorithms and it interpolates on the basis of a single point. Usually, the value of a new point is taken as the value of the old point that is located nearest to the new point. Linear interpolation interpolates on the basis of two points. The new point is linearly interpolated between the old points. The other complex functions use four points (two points in each direction). More complicated functions exist that use eight points and so on. Many image processing systems, such as Adobe Photoshop use bi-cubic interpolation, which gives good results for many images, but can as well yield undesirable results for some images, such as medical images. A nearest neighbor function can shift an image up to one-half a pixel. Linear and cubic B-spline interpolations tend to smooth the image, but high-resolution cubic spline function gives the best results (Parker, et al. 1983). The choice of an interpolation function depends on the task to perform, for example, high-resolution cubic spline is a valuable resource for medical images due to its ability to preserve image resolution and to prevent loss of detail. Hence, we applied high-resolution cubic spline interpolation function to re-sample an input image to a fixed dimension before segmentation.

The B-splines (Hou & Andrew, 1978) are convolutions of the rectangular function and a cubic B-spline is four convolutions of a simple rectangular function. B-splines are good low-pass n^{th} order polynomial filters, symmetric piecewise, positive in the interval (0, 2), over-smooth below the cut-off frequency and have good efficiency in the stopband. Mathematically, the general form of a cubic spline function is (Parker, et al. 1983):

$$f(x)=\begin{cases} a_{30}x^3+a_{20}x^2+a_{10}x+a_{00},\ in\ (0,1) \\ a_{31}x^3+a_{21}x^2+a_{11}x+a_{11}\ in\ (1,2) \end{cases} \tag{4.3}$$

A function to be used for interpolation has to satisfy some natural constraints. The original image should be reproducible from the re-sampled image and the function should be continuous at points 0 and 1. These constrains define the cubic spline interpolation function to a constant and using these constraints, equation (4.3) becomes (Parker, et al. 1983):

$$f(x)=\begin{cases} (a+2)x^3-(a+3)x^2+1,\ in\ (0,1) \\ ax^3-5ax^2+8ax-4a,\ in\ (1,2) \end{cases} \tag{4.4}$$

When the constant a in equation (4.4) is negative, the function is positive in the interval (0, 1) and negative in the interval (1, 2). When a increases, the depth of the sidelobe increases in the interval (1, 2). Thus, with the free constant negative, the function is of the general form of a Lanczos re-sampling or windowed-sinc function (Nuttall, 1981). This function (when a is negative) is called a high-resolution cubic interpolating function, because it has a better high frequency performance than the cubic B-spline.

Most applications select $a = -0.5$ (Keys, 1981) for high-resolution cubic spline and $a = -1$ (Simon, 1975) for high-resolution cubic spline with edge enhancement. We selected $a = -0.5$ for high-resolution cubic spline, because, generally Chan & Vese (2001) active contour, which LBF active contour improves using variational level set to eliminate re-initialization does not required edge information. Hence, there is no need to enhance edge information in an image if Chan & Vese active contour or its variant such as region-based LBF is to be used for image segmentation. Chan & Vese active contour was developed to be independent on edge information. Moreover, Keys (1981) showed in the derivation of the family of cardinal splines using a Taylor series approximation of the interpolated signal that a = -0.5 is numerically most accurate. The error of the approximation for this constant goes to zero as the third power of the sampling interval and any second degree polynomial will be exactly reconstructed by the interpolation.

4.4. Image Segmentation using Active Contours

An active contour is a segmentation method used to detect edges in an image by the process of curve evolution. The main idea of an active contour is to start with initial boundary shapes presented in the form of a spline curve and iteratively modify it by applying various shrink or expansion operations according to some energy functional. Active contours are useful methods for image segmentation, but important issues such as initialization, boundary concavities and computational intensiveness can significantly affect segmentation results. However, in spite of issues in contour initialization, edge concavities and high-level computation, active contours are a popular and successful method for segmentation among researchers (Yoon, et al., 2007).

Active contours are attractive because of their ability to handle protrusious and specific topological effects.

There are different kinds of active contours and more are been developed to improve the deficiencies of the current ones. Active contours are generally classified into two classes, namely, edge-based (Kass, et al., 1987; Li, et al., 2005; Pi, et al., 2007) and region-based models (Mumford & Shah, 1989; Tsai, et al., 2001; Chan & Vese, 2001; Vese & Chan, 2005; Paragious & Diriche, 2002; Li, et al., 2007). Edge-based models utilize image gradient to stop the evolving contours on the object edges and they cannot detect objects with interior edges (Pi, et al., 2007). Alternatively, region-based models do not utilize the image gradient and therefore, have better performance for the image with weak edges and they are significantly less sensitive to the location of the initial contours and can detect objects with both interior and exterior edges (Li, et al., 2007).

Intensity in-homogeneity, which occurs in many real images of different modalities, is one of the main reasons for the difficulty in the segmentation of medical. Intensity in-homogeneity in MRI arises from non-uniform magnetic field produced by radio-frequency coils as well as from object susceptibility. The degree of in-homogeneity is worse for higher field imaging. The main motivation of region-based LBF active contour was to overcome the difficulty of segmentation due to the intensity in-homogeneity. The active contour model is able to segment images with intensity in-homogeneity (Li, et al., 2007). This was accomplished through a kernel function that defines a local binary fitting energy in a variational function, so that local intensity information is embedded into a region-based active contour model. Additionally, region-based LBF active contour implicitly uses variational level set to solve the problem of constant re-initialization associated with most active contours. The process of constants re-initialization can complicate segmentation algorithm and diminishes the efficiency of an image retrieval algorithm. Thus, LBF active contour was investigated in this study for image segmentation. Next, we give a brief discussion of variational level set formulation, followed by LBF active contour.

4.4.1. Edge-Based Segmentation using Variational Level Set

The level set formulation of active contours (that is, moving fronts, dynamic curves or deformable models) denoted by $\Gamma(t)$, is represented by the zero level set of a level set function $\varphi(X,t)$ as:

$$\Gamma(t) = \{X \mid \varphi(X, t=0) = 0,\ X \in \mathbb{R}^n,\ n > 0\}$$

The evolution of the level set function can be written as initial value partial differential equation called level set equation (Osher & Sethian 1988; Sethian, 1999; Gomes & Faugeras, 2000):

$$\frac{\partial \varphi}{\partial t} + F \mid \nabla \varphi \mid = 0,\ \varphi(X, t=0) = \varphi_0 \qquad (4.5)$$

In equation (4.5), φ_0 is the initial value of $\varphi(x,y,t)$ at time $t=0$, which is usually a signed distance function for computational efficiency (Osher & Fedkiw, 2003, Zhuang, et. al., 2006). F is called the speed function, which depends on image data $I(x,y) \in \mathbb{R}^2$ and level set function $\varphi(x,y,t)$ for image segmentation problem. In level set methods, periodic re-initialization is conventionally used to avoid the problem of shocks during the process of curve evolution. That is, $\varphi(x,y,t)$ is usually initialized as a signed distance function before the evolution starts and then periodically re-initialized during the evolution. In this way, a stable curve evolution is maintained and a desirable result is ensured. However, the initialization process can be complicated and complex upwind finite difference methods are required for a stable curve evolution. Thus, this makes the overall computation procedure expensive (Li, et. al., 2006).

The general problem of variational level set formulation of active contours can be modeled as that of minimizing certain energy functional so that a function that is closed to a signed distance is forced to evolve. To apply this new method, the total energy functional that corresponds to the sum of internal and external energies is considered. This energy functional model is given as (Li, et al., 2005):

$$\mathrm{E}(\varphi) = \mu \int_{\Omega} \frac{1}{2}(|\nabla\varphi| - 1)^2 \, dxdy + \\ \lambda \int_{\Omega} g\delta(\varphi) |\nabla\varphi| \, dxdy + \nu \int_{\Omega} gH(-\varphi) dxdy \tag{4.6}$$

The internal energy or distance penalizing energy specified by the first integral on the right-hand-size of equation (4.6) characterizes the closeness of the unknown function $\varphi(x,y,t)$ to a signed distance in the domain $\Omega \in \mathbb{R}^2$. The external energy specified by the remaining integrals in equation (4.6) drives the motion of the zero level curve of $\varphi(x,y,t)$. The parameter $\mu > 0$ is the weight of the internal energy term that controls the effect of penalizing the deviation of $\varphi(x,y,t)$ from a signed distance function. The values $\lambda > 0$ and ν are constants, $\delta(x)$ is the univariate Dirac function and $H(x)$ is the Heaviside function respectively given as (Li, et al., 2007):

$$H_\varepsilon(x) = \frac{1}{2}\left(1 + \frac{2}{\pi}\tan^{-1}\left(\frac{x}{\varepsilon}\right)\right) \tag{4.7}$$

$$\delta_\varepsilon(x) = H_\varepsilon^{/}(x) = \frac{\varepsilon}{\pi\left(\varepsilon^2 + x^2\right)} \tag{4.8}$$

The parameter ε is the width of the regularized Dirac function. The edge map or edge indicator function $g(x,y)$ is given as (Sethian, 1996):

$$g(x,y) = \frac{1}{1 + |\nabla(G_\sigma * I(x,y))|^2} \tag{4.9}$$

The function G_σ is the Gaussian kernel (or filter) with standard deviation σ and $G_\sigma * I$ denotes the image convolved with a Gaussian smoothing filter whose characteristic width is σ.

The evolution equation that minimizes the total energy functional E is the gradient flow (Evans, 1998):

$$\frac{\partial\varphi}{\partial t} = -\frac{\partial \mathrm{E}}{\partial\varphi} \tag{4.10}$$

The quantity $\frac{\partial\varphi}{\partial t}$ is the partial derivative of $\varphi(x,y,t)$ with respect to time and $\frac{\partial E}{\partial\varphi}$ is the Gateaux derivative. By calculus of variations, the Gateaux derivative of the energy functional in equation (4.6) can be written as:

$$\frac{\partial E}{\partial\varphi}=-\mu\left(\Delta\varphi-\nabla\bullet\left(\frac{\nabla\varphi}{|\nabla\varphi|}\right)\right)-\lambda\delta(\varphi)\nabla\bullet\left(\frac{g\nabla\varphi}{|\nabla\varphi|}\right)-vg\delta(\varphi) \quad (4.11)$$

Here "•" is the vector dot product and ∇ and Δ are the gradient and Laplacian operators respectively. The function φ that minimizes the functional given by equation (4.6) satisfies the Euler-Lagrange equation $\frac{\partial E}{\partial\varphi}=0$. The steepest descent process for minimization of the functional E is the gradient flow obtained from equations (4.10) and (4.11) as:

$$\frac{\partial\varphi}{\partial t}=\mu\left(\Delta\varphi-\nabla\bullet\left(\frac{\nabla\varphi}{|\nabla\varphi|}\right)\right)+\lambda\delta(\varphi)\nabla\bullet\left(\frac{g\nabla\varphi}{|\nabla\varphi|}\right)+vg\delta(\varphi) \quad (4.12)$$

The update difference equation of level set for solving the evolution equation (4.12) is given as:

$$\varphi_{i,j}^{k+1}=\varphi_{i,j}^{k}+\tau L(\varphi_{i,j}^{k}) \quad (4.13)$$

The implementation of equation (4.13) was given by Chunming Li using the method of weighted area to compute $L(\varphi_{i,j}^{k})$, although the result was not published.

Finally, the variational level set method proposes a non-signed distance function φ_0 for flexible and efficient initialization. The initial level set function φ_0 is defined as:

$$\varphi_0(x,y)=\begin{cases}-c, & (x,y)\in R\\ c, & otherwise\end{cases} \quad (4.14)$$

R is an arbitrary region in image domain, $c>0$ is a constant and a value larger than 2ε can be used. In contrast to signed distance computed from a contour, the function given by equation (4.14) is computed from an arbitrary region R in the image domain Ω. This region-based initialization of level set function is computationally efficient and allows for flexible applications in some situations. Although the initialization procedure of the level set method is region-based, the method itself is an edge-based method, because the contour evolution after initialization stops at the image boundary or edge.

4.4.2. Region-Based Segmentation using Active Contours

To give a summary of active contours, we let $\Omega \subset \mathbb{R}^n$ be the image domain and $I : \Omega \to \mathbb{R}$ be a given image. Mumford & Shah (1989) posited the Mumford-Shah energy functional in which, image segmentation is formulated as a problem of seeking an optimal contour C that divides the image domain into disjoint sub-regions and an optimal function u that fits the original image I and that is smooth within each of the sub-regions. They proposed the energy functional:

$$F^{MS}(u,C) = \int_{\Omega}(I-u)^2 dxdy + v \int_{\Omega \backslash C} |\nabla u|^2 \, dxdy + v\,|C| \qquad (4.15)$$

where $|C|$ is the length of the contour C, thus image segmentation can be performed by minimizing the Mumford and Shah functional over all the contours and the fitting function u. But, this is a difficult task because of the presence of the unknowns C and u and the non-convexity of the functional.

Chan & Vese (2001) proposed one of the most famous active contour methods to the Mumford and Shah problem for a special case where the image u is a piecewise constant function. Given an image $I(x,y)$ on the image domain Ω, they proposed to minimize the energy functional:

$$\begin{aligned} E^{CV}(C,c_1,c_2) = \lambda_1 & \int_{in(C)} |I(x)-c_1|^2 \, dx + \\ & \lambda_2 \int_{out(C)} |I(x)-c_2|^2 \, dx + v\,|C| \end{aligned} \qquad (4.16)$$

The regions inside and outside the contour C are *in*(C) and *out*(C) respectively, c_1 and c_2 are two constants that approximate the image intensity in *in*(C) and *out*(C). Li, et al. (2007) called the first two terms in equation (4.16), Global Binary Fitting (GBF) energy. They argued that such global fitting of image intensities will not be accurate if the image intensities in *in*(C) or *out*(C) are inhomogeneous. In particular, intensity in-homogeneity is often seen in medical images such as X-ray, tomography and MRI, due to technical limitations or artifacts introduced by the object being imaged. As a result, they proposed LBF of energy around the center point x for solving the problems of intensity in-homogeneity and re-initialization. The basic ideal of LBF active contour is to introduce a kernel function to define LBF energy in a variational formulation, so that local intensity information can be embedded into a region-based active contour model. LBF energy functional was further incorporated into a variational level set formulation. Hence, no re-initialization is necessary in LBF active contour. This is a significant advantage, because the process of continuous re-initialization can be overly complex.

Now, consider a given vectors valued image $I:\Omega \rightarrow \mathbb{R}^{D}$ where the domain $\Omega \subset \mathbb{R}^{n}$ is the image domain and $d \geq 1$ is the dimension of the vector $I(x)$. Li, et al. (2007) proposed the eergy functional:

$$\varepsilon(C, f_1, f_2) = \int_{\Omega} \varepsilon_x^{LBF}(C, f_1(x), f_2(x))dx \tag{4.17}$$

For each point $x \in \Omega \subset \Re^{n}$, the following energy functional is defined.

$$\begin{aligned} \varepsilon_x^{LBF}(C, f_1(x), f_2(x)) = \lambda_1 & \int_{in(C)} K(x-y)\,|\,I(y) - f_1(x)\,|^2\,dy + \\ \lambda_2 & \int_{out(C)} K(x-y)\,|\,I(y) - f_2(x)\,|^2\,dy \end{aligned} \tag{4.18}$$

where λ_1 and λ_2 are positive constants, K is a kernel function with a localization property that K(u) decreases and approaches zero as |u| increases, $f_1(x)$ and $f_2(x)$ are two numbers that fit image intensities near the center point x of the integral given by equation (4.18). The LBF active contour is obtained by converting equation (4.17) to an equivalent level set formulation and the resulting LBF equation is the gradient descent flow (Li, et al., 2007):

$$\begin{aligned} \frac{\partial \varphi}{\partial t} = & -\delta_\varepsilon(\varphi)(\lambda_1 e_1 - \lambda_2 e_2) + \nu \delta_\varepsilon(\varphi) \nabla \bullet \left(\frac{\nabla \varphi}{|\nabla \varphi|} \right) + \\ & \mu \left(\nabla^2 \varphi - \nabla \bullet \left(\frac{\nabla \varphi}{|\nabla \varphi|} \right) \right) \end{aligned} \tag{4.19}$$

where δ_ε is the smooth Dirac function given by equation (4.8). The Heaviside function H is approximated by a smooth function H_ε, which is defined as in equation (4.7). The functions e_1 and e_2 are given as (Li, et al. (2007):

$$e_1(x) = \int_\Omega K_\sigma(y-x) \mid I(x) - f_1(y) \mid^2 dy \tag{4.20}$$

and

$$e_2(x) = \int_\Omega K_\sigma(y-x) \mid I(x) - f_2(y) \mid^2 dy \tag{4.21}$$

where

$$f_1(x) = \frac{K_\sigma(x) * [H_\varepsilon(\varphi(x)) I(x)]}{K_\sigma(x) * H_\varepsilon(\varphi(x))} \tag{4.22}$$

and

$$f_2(x) = \frac{K_\sigma(x) * [(1 - H_\varepsilon(\varphi(x))) I(x)]}{K_\sigma(x) * [1 - H_\varepsilon(\varphi(x))]} \tag{4.23}$$

$K(x)$ is the Gaussian kernel function with a scale parameter $\sigma > 0$ and is given by:

$$K_\sigma(x) = \frac{e^{-|x|^2 / 2\sigma^2}}{(2\pi)^{n/2} \sigma^n} \tag{4.24}$$

4.5. Detecting Binary Edges using CNED Algorithm

Edge detection is a useful low level image processing for obtaining a simplified image (Fan, et al., 2001). An edge is a large change in frequency and it is an area with strong intensity contrast. An edge pixel can also be regarded as a pixel where a discontinuity occurs in an image. A well-known edge detector is the Canny (1986) and other edge detectors are Roberts, Marr's Laplacian of Gaussian (LoG) and Sobel (Zhang & Wang, 2005). The 8-connected $CNED_8$ algorithm was used in this study. The $CNED_8$ edges were compared with Canny, Roberts, LoG and Sobel on both binary and grayscale images (Zhang & Wang, 2005). The maximum and mean detection times were used as the performance comparison measures. The $CNED_8$ algorithm spent the least detection time compared to four other detectors. The detection results showed that all the well-known Canny, Roberts, LoG and Sobel edges have distortion of the binary image and so much as they are executed on the grayscale one. Moreover, the $CNED_8$ algorithm has better visual performance such as the horizontal line and the detail of the characters. Thus, $CNED_8$ algorithm spends less time and provides details than the well-known Canny, Roberts, LoG and Sobel edge detection algorithms. The $CNED_8$ algorithm is described as:

Algorithm **$CNED_8$**(BinaryImage F, Row m, Column n)

Step 1: Initializes the output matrix CN[m,n] and a template array f(8)

Step 2: Calculate each foreground pixels f according to the following equation, ignoring outer pixels:

$$\begin{aligned} &f(0)=F(i+1,j), \quad f(1)=F(i+1,j-1), \\ &f(2)=F(i,j-1), \quad f(3)=F(i-1,j-1), \\ &f(4)=F(i-1,j), \quad f(5)=F(i-1,j+1), \\ &f(6)=F(i,j+1), \quad f(7)=F(i+1,j+1) \end{aligned} \tag{4.25}$$

Step 3: Calculates the pixel's CN(i,j) using the quation:

$$CN_n(i,j)=\sum_{i\in\{0,2,4,6\}}\left[f(x_i)-f(x_i)*f(x_{i+1})*f(x_{i+2})\right] \tag{4.26}$$

where $n=4\ or\ 8$ and $x_8=x_0$, $x_0,x_1,...x_7$ are the 8-neighbors of the center pixels. Here $n=8$ was chosen, since $CNED_8$ has better performance than $CNED_4$, Zhang & Wang (2005) contains more detail. Finally, while a simple technique exists to extract the region bounded by a contour, a little effort is needed to extract the actual edge information. This study combines CNED algorithm with active contours to accomplish the task of binary edge extraction from an input image. The combination of these two methods enables edge information to be directly obtained from region information. Conventionally, either edge detection algorithms or edge-based active contours are used for edge extraction.

4.6. Density Histogram of Feature Points Shape Representation

Feature extraction is the process of transforming an input data into a set of features. Usually, these features are represented as a set of numbers that gives relevant information about the data. An important advantage of feature extraction is that the desired task can be efficiently performed using a reduced representation instead of the full size input. Hence, feature extraction is a special form of dimensionality reduction process.

Important features that can be extracted from a given input image include color, texture, shape, edge, corner, junction, movement and face. These features are used in computer vision for object recognition and in CBIR for image indexing and retrieval. Shape representations are generally classified into two main categories, namely, edge-based and region-based. An edge-based representation uses the edge pixels of a shape, while a region-based representation uses the entire pixels of the shape region. The most successful representations for these two categories are Fourier Description (FD) (Lee, et al., 2003) and Moment Invariants (MI) (Mercimek, et al., 2005). FD is based on the Fourier transform and edge transformed using Fourier transformation is used as image feature. It is fast and also good for shape representation. However, it is sensitive to the starting point of the shape edge. Moment invariants are based on probability density functions such as expectation, variance, covariance and skewness. But, they have high computational costs, because the features are computed on the entire region and low discrimination power (Tran & Ono, 2003).

DFP is investigated for shape based image representation, because of its several advantages. Firstly, it is computationally efficient and simple to describe. Secondly, it is histogram-based and histograms are invariant to translation and rotation around the viewing axis and vary slowly with changes of view angle, scale and occlusion (Park, et al., 1999). Moreover, DFP has been shown to be faster than Delaunay triangulation (Fang & Piegl, 1993; Tao, et al., 1999) for large number of feature points (Tran & Ono, 2003). Additionally, DFP is insensitive to small change in the feature points set and thus, conforms well to human vision and is invariant to translation, scale and rotation (Tran & Ono, 2003). An object shape is represented in DFP by a set of feature points. Usually, the object is segmented by a grid $N \times N$ and the bitmap of shape is derived from the grid by assigning 1 to any cell with more than 20% of its pixels belonging to the shape. Each bit 1 in the bitmap is defined as a feature point of shape and the density of feature points is calculated around the centroid of the object shape. The result of this counting is a density histogram of object feature points around the centroid of the object. Since the centroid of an object is invariant under rotation, translation and scaling, DFP is invariant under these operations. Hence, DFP is defined as a vector $v = (v_1, v_2, ..., v_n)$ so that the r^{th} element of v is the number of bit 1 of the m x n bitmap object lying on a rectangle in which (x_0, y_0) is the centroid of the object, $(x_0 - r, y_0 - r)$ is the top left corner, $(x_0 + r\, y_0 + r)$ is the bottom right corner of the r^{th} rectangle and the part of the rectangle outside the bitmap is counted by 0. DFP uses a grid-based method (Sajjanbar & Lu, 1997) for image segmentation. This is questionable, because a slight shape distortion, such as affine transform, can cause significant difference in the similarity measurement (Zhang & Lu, 2001).

An alternative method investigated in this study for image segmentation before applying DFP algorithm is the use of LBF active contour. This segmentation algorithm does not require the severity of normalization as in the grid-based method for shape invariant computation. Moreover, the segmentation method has the advantage of working effectively on images with intensity in-homogeneity, which is often seen in medical images such as X-ray, radiography or tomography and MRI, due to technical limitations or artifacts introduced by the object being imaged. Two DFP representation techniques, here called edge-based DFP and region-based DFP are investigated, because many shape representations reported in the literature use edge pixels for image processing, which is faster than using the entire pixels because few pixels are being processed. The edge information was directly obtained from region information after LBF segmentation. The segmented region is then converted to bitmap objects by assigning 1 to those pixels smaller than 0 and 0 is assigned otherwise. Then CNED algorithm for binary image (Zhang & Wang, 2005) is applied to extract edge information. In the edge-based DFP, density estimation vector is constructed by counting the edge pixels that fall on rectangles placed on the segmented objects, while the entire region pixels are used in region-based DFP representation. It is of interest to know which of these two DFP shape representation techniques will likely give better system performance on a collection of brain MRI.

Additionally, since active contour is used for image segmentation instead of grid method, we do not take rectangles whose parts fall outside the bitmap. Instead, we place a Minimum Bounding Rectangle (MBR) (Chaudhuri & Samal, 2007) on the segmented objects and take a count of pixels lying on rectangles whose sizes are less or equal to that of the MBR. That is, suppose $v_k = 0$ for all $k = 1, 2, ..., \le \max(m,n)$ and let isOnRect(...) denotes a predicate that returns 1 if the pixel (i, j) with value 1 lies on the r^{th} rectangle and 0 otherwise, then it follows that:

$$v_r = \sum_{i=x_1}^{x_2} \sum_{j=y_1}^{y_2} isOn\mathrm{Re}ct(i,\ j,\ x_0 - r,\ y_0 - r,\ x_0 + r,\ y_0 + r) \qquad (4.27)$$

where $r = 1, 2, ..., d+1$, $d \le \max\{x_0 - x_1, x_2 - x_0, y_0 - y_1, y_2 - y_0\}$, (x_1, y_1) and (x_2, y_2) are the top left corner and bottom right corner points of MBR respectively. The value d is the possible number of rectangles on the bitmap that can fit into MBR and this value is usually less than the size of the DFP vector. The remaining components of the vector are filled by 0 according to the initialization process.

The general problem associated with DFP shape representation, especially when images are segmented in the same dimension to achieve scale invariant is that the shape vector representation can be skewed to the left with most of the right components of the shape vector having zero value. As a result, storing a large set of zero values is not necessary. We resolve this problem using vector re-binning technique. Our re-binning algorithm adds those zero components to non-zero components, thereby achieving further 50% dimension reduction. That is, we used a vector of size n to populate a new of size n/2. The components of the original vector at locations 1 and n are translated to the component at location 1 in the new vector. Similarly, the components of the original vector at locations 2 and n-1 are translated to the component at location 2 in the new vector and so on. To define the re-binning algorithm, we let $u = (u_1, u_2, ..., u_{n/2})$ be a new DFP shape vector, our vector space re-binning algorithm is giving as:

$$u_i = \sum_{i=1}^{n/2} (v_i + v_{n-i-1}) \tag{4.28}$$

Hence, our approach to DFP shape representation is exceptionally fast, because only pixels lying within and on the MBR are counted instead of counting the entire pixels of the bitmap. Additionally, possible reduction in feature vector representation by image re-sampling and vector re-binning enables efficient processing.

4.7. Image Smoothing using Gaussian Convolution Kernel

The quality of digital images, especially MRI can be considerably degraded or corrupted as a result of acquisition noise. Image smoothing (Malladi & Sethian, 1996; Yezzi, 1998; Spira, et al., 2003) algorithms are usually applied to reduce noise effect in images and to prepare images for further processing such as image segmentation. In fact, these algorithms are used as pre-processing tools during image processing to suppress the effect of noise.

This study applies Gaussian convolution kernel or filter algorithm to smooth images. The Gaussian filtering is very popular due to its desirable properties like central limit theorem and minimum space bandwidth product. Moreover, it is computationally efficient and has several useful applications in areas like edge detection (see equation 4.9 for instance) and scale space analysis. The Gaussian filter is separable, thus making it efficient to implement. The Gaussian smoothing operator is a 2D convolution and the convolution is performed in the vertical direction, followed by convolution in the horizontal direction and vice versa. The effect of Gaussian smoothing is to blur an image and the formula is given as:

$$G(x, y) = \left(\frac{e^{-\left(\frac{x^2}{2\sigma^2}\right)}}{\sqrt{2\pi}\sigma} \right) * \left(\frac{e^{-\left(\frac{y^2}{2\sigma^2}\right)}}{\sqrt{2\pi}\sigma} \right) \tag{4.29}$$

The degree of smoothing is determined by the standard deviation σ of the Gaussian. A larger standard deviation Gaussian requires a larger convolution kernel in order to have accurate representation.

4.8. Computing Shape Index using Jensen Polynomials

We computed shape index from both geometrical properties and DFP shape representation using Jensen polynomials, by treating an object as a point set that can be infinite. A number of geometrical properties that can be investigated for shape index computation using Jensen polynomials are area, perimeter, convexity, elongation and orientation (Ang, et al., 1995). In this study, we used shape profile, eccentricity and orientation. Moreover, we assumed that the shape of an object is essentially captured by a finite subset of its pixel points. A shape can be represented by a discrete set of points sampled from an internal contour on the object. These points were obtained as locations of the object that lie on the boundaries of rectangles placed on the object, given us a set $F_1 = \{f_1, f_2, ..., f_m\}$. For the shape orientation computation, only edge pixels of the object found by connectivity-number edge detector were used, given us the second set $F_2^l = \{f_1^l, f_2^l, ..., f_n^l\}$. A strong requirement for the shape orientation computation using the higher-order modified principal axes method (Zunic, et al., 2006) is that edge pixels are used. Consequently, $S = F_1 \cup F_2$ gives the set of pixels describing the shape object. Two methods, namely, method of geometric properties and method of scalar projections for shape index computation are described. Our approach is based on the assumption that if shape index can be directly computed from shape properties, then it is possible to realize a unique shape index for an object.

4.8.1. Method of Geometric Properties

In order to apply the Jensen polynomials for computing shape index using the method of geometric properties, we let γ_k be some positive real numbers satisfying the Turan's inequalities (Szego, 1948):

$$\gamma_k^2 - \gamma_{k-1}\gamma_{k+1} \geq 0 \tag{4.30}$$

The shape index γ is then computed as the sum of function values evaluated in an interval $[a, b]$ as:

$$\gamma = \sum_{t\in[a,b]} g_n(t) \tag{4.31}$$

where

$$g_n(t) = \sum_{k=0}^{n} \binom{n}{k} \gamma_k t^k \tag{4.32}$$

is the Jensen polynomials associated with the real entire function of the form:

$$f(x) = \sum_{k=0}^{\infty} \frac{\gamma_k x^k}{k!} \tag{4.33}$$

and $\binom{n}{k}$ is the Binomial combination function given as:

$$\binom{n}{i} = \frac{n!}{(n-i)!i!} \tag{4.34}$$

Specifically, let γ_0, γ_1, γ_2 be three real numbers that correspond to the normalized shape orientation, shape eccentricity and the normalized angle between the horizontal and the vertical profiles respectively. The shape orientation is defined as the angle between the principal axes and the horizontal direction. Shape eccentricity is the ratio of the length of the longest chord of the shape (major axis) to the longest chord perpendicular to it (minor axis). A profile (sometimes called projection) is a useful region-based signature that has been successfully applied in character recognition applications. Vertical profile is the number of region pixels in each column and horizontal profile is the number of region pixels in each row.

Shape orientation computation is a common task in computer vision and image processing, being used for example to define a local frame of reference. It is helpful for recognition and registration, robot manipulation and very important in human visual perception. Orientable shapes can be matched more quickly than shapes with no distinct axis (Palmer, 1999). To compute the shape orientation, the modified high-order principal axes method was applied. The N^{th} higher-order principal axes method works effectively in situations where the standard method fails. For the sake of clarity, the equation for principal axis computation is given as:

$$I_N(\delta,S)=\sum_{i=0}^{N}\binom{N}{i}(-1)^{N-i}(\sin\delta)^{N-i}(\cos\delta)^{i}M_{N-i,i}(S) \qquad (4.35)$$

where $I_N(\delta,S)$ is the principal axis, which is the line that passes through the centroid or center of gravity of the shape S and about which the second moment of S is minimized, δ is the direction of the principal axis (orientation) and the (i,j) moment is $M_{i,j}$. The computation of shape orientation is accomplished using a numerical scheme, because it is computationally difficult to obtain exact solution. The shape orientation $\varepsilon(S)$ is calculated as the ratio of $\max\{I(\delta,S)\mid\delta\in[0,2\pi]\}$ to $\min\{I(\delta,S)\mid\delta\in[0,2\pi]\}$. That is,

$$\varepsilon(S)=\frac{\max\{I(\delta,S)\mid\delta\in[0,2\pi]\}}{\min\{I(\delta,S)\mid\delta\in[0,2\pi]\}} \qquad (4.36)$$

The normalized shape orientation is used to eliminate the effect of dimensionality and is obtained from equation (4.36) when divided by 2π.

Now, suppose that n components horizontal and vertical profiles are H and V respectively. Then shape geometric features γ_0, γ_1, γ_2 are respectively computed as:

$$\gamma_0=\frac{1}{2\pi}\cos^{-1}\left(\frac{\sum_{i=1}^{n}H_iV_i}{\sqrt{\sum_{i=1}^{n}H_i^2}\sqrt{\sum_{i=1}^{n}V_i^2}}\right) \qquad (4.37)$$

$$\gamma_1=\frac{Length\ of\ the\ major\ axis}{Length\ of\ the\ \min or\ axis} \qquad (4.38)$$

$$\gamma_2=\frac{1}{2\pi}\left(\frac{\max\{I(\delta,S)\mid\delta\in[0,2\pi]\}}{\min\{I(\delta,S)\mid\delta\in[0,2\pi]\}}\right) \qquad (4.39)$$

The values of these features clearly satisfy the Turan's inequalities for $n = 2$, because it is always true that $0 \le \gamma_0, \gamma_2 \le 1$ and $\gamma_1 \ge 1$.

4.8.2. Method of Scalar Projections

While the method of geometrical properties compute shape index from eccentricity, orientation and shape profile, the method of scalar projection directly computes shape index directly from DFP shape representation. In vector analysis, the scalar projection of vector $\vec{v}$ onto vector $\vec{u}$, here denoted $\Pr j(\vec{v},\vec{u})$ is defined as:

$$\Pr j(\vec{v},\vec{u}) = \frac{\vec{u} \bullet \vec{v}}{|\vec{u}|}$$

The quantity $\vec{u} \bullet \vec{v}$ is the inner product or scalar product of $\vec{u}$ and $\vec{v}$. Applying this result to shape index computation involves taking the projection of DFP shape representation, which is a vector onto another vector. Three vectors are used to illustrate the possibility of computing shape index from DFP shape representation. These vectors are edge-based DFP, denoted by E, region-based DFP, denoted by R and the difference between R and E, denoted by D respectively. The vector D removes edge information from region information, as a way of deriving a new vector from two given vectors. The normalized shape features $\gamma_0, \gamma_1, \gamma_2$ were obtained by taking projection of R onto D, projection of E onto the R and projection of E onto D respectively. Thus,

$$\gamma_0 = \frac{\sum_{i=1}^{n} R_i D_i}{\sqrt{\sum_{i=1}^{n} R_i^2}\sqrt{\sum_{i=1}^{n} D_i^2}} \qquad (4.40)$$

$$\gamma_1 = \frac{\sqrt{\sum_{i=1}^{n} R_i^2}\sqrt{\sum_{i=1}^{n} E_i^2} + \sum_{i=1}^{n} R_i E_i}{\sqrt{\sum_{i=1}^{n} R_i^2}\sqrt{\sum_{i=1}^{n} E_i^2}} \qquad (4.41)$$

$$\gamma_2 = \frac{\sum_{i=1}^{n} E_i D_i}{\sqrt{\sum_{i=1}^{n} E_i^2}\sqrt{\sum_{i=1}^{n} D_i^2}} \qquad (4.42)$$

The values of these normalized features also satisfy the Turan's inequalities for $n = 2$, because it is always true that $0 \le \gamma_0, \gamma_2 \le 1$ and $\gamma_1 \ge 1$.

To determine without performing statistical test for significance whether there is a significant different between the shape index computed for an image and its derivative using Jensen polynomials approach, equation (4.31) was implemented. The parameters γ_k in equation (4.32) were estimated using equations (4.37) to (4.39) when the method of geometric properties was applied. Each equation was then used for computing a particular parameter. For example, the parameters γ_0, γ_1 and γ_2 can be computed using equations (4.37), (4.38) and (4.39) respectively. Similarly, these parameters were estimated using equations (4.40) to (4.42) when the method of scalar projections was applied. Then using a particular shape index method (geometric properties or scalar projections) the shape index can be computed using the Jensen polynomials given by equation (4.31). To compute the shape index using equation (4.31) the function given by equation (4.32) was evaluated at some points t = 0.1, 0.2,-..., 1.0, here called the evaluation points.

Figure 4.1 shows the Jensen polynomials graphs of shape index versus evaluation point when the method of geometric projections was used to estimate the parameters γ_k. The normalized angle between shape profiles, shape eccentricity and shape orientation were determined for computing shape index values for the image of Alzheimer and its derivative. Chapter 6 gives the description of the image derivation process used in this study, but suffice to mention that a derivative image D(I) of an image I is the image obtained by applying a transformation T to I. The graphs showed that there is no significant difference between shape index computed by Jensen polynomials for an image and its derivative.

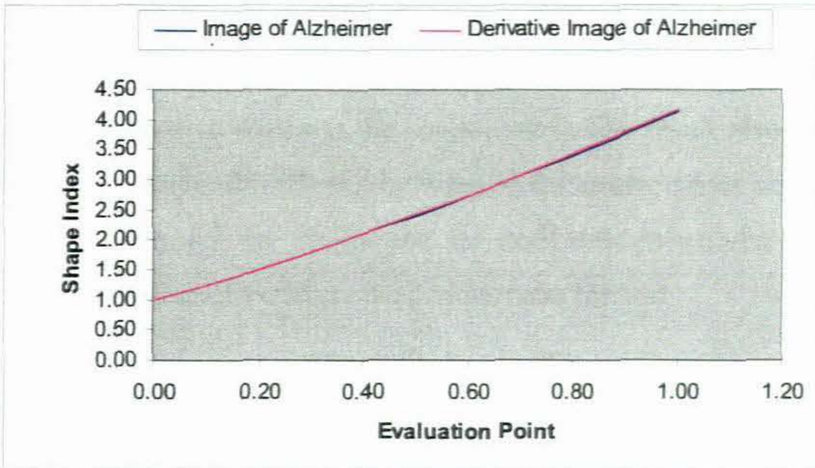

Figure 4.1: Jensen polynomials for the image of Alzheimer using the method of geometric properties

Figure 4.2 shows the graphs of shape index versus evaluation point for the image of AID dementia and its derivative when the method of geometric properties was used to compute the shape index. The result also showed that there is no significant different between shape index values computed by Jensen polynomials for an image and its derivative when another image data (AID dementia) was used to perform the test.

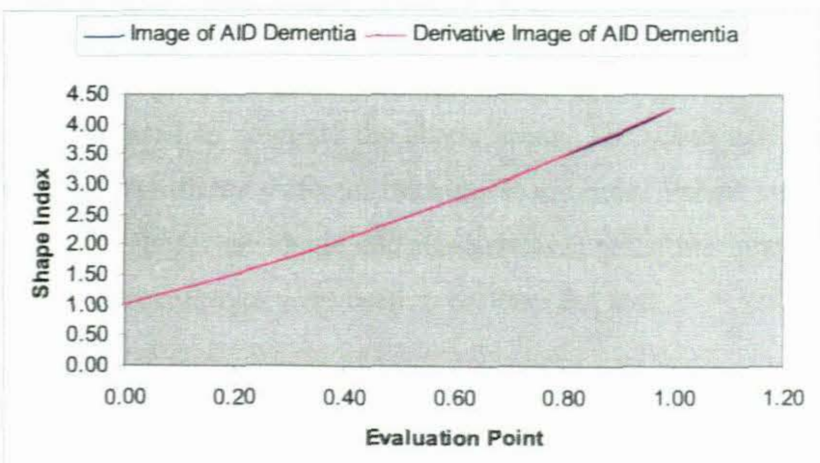

Figure 4.2: Jensen polynomials for the image of AID dementia using the method of geometric properties

Figure 4.3 shows the graphs of shape index versus evaluation point for the image of Alzheimer and its derivative when the method of scalar projections was used to compute the shape index. The result also confirmed that there is no significant different between shape index values computed by Jensen polynomials for an image and its derivative when the images of Alzheimer and its derivatives were used to perform the test.

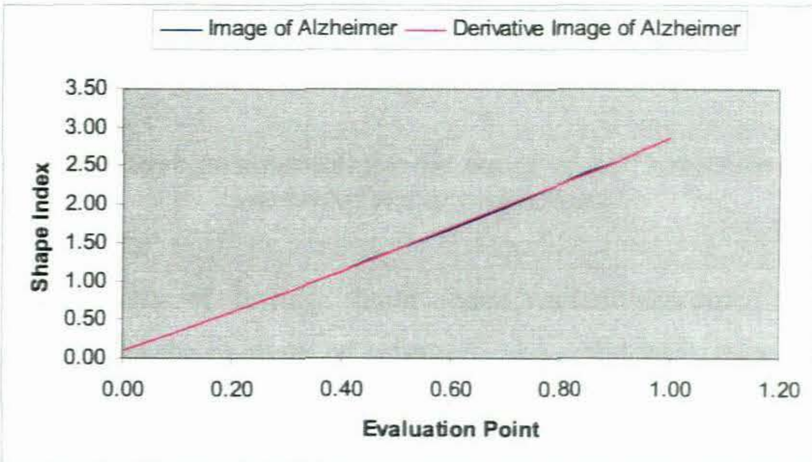

Figure 4.3: Jensen polynomials for the image of Alzheimer using the method of scalar projections

Figure 4.4 shows the graphs of shape index versus evaluation point for the image of AID dementia and its derivative when the method of scalar projections was used to compute the shape index. The result also confirmed that there is no significant different between shape index values computed by Jensen polynomials for an image and its derivative when the images of AID dementia and its derivatives were used to perform the test.

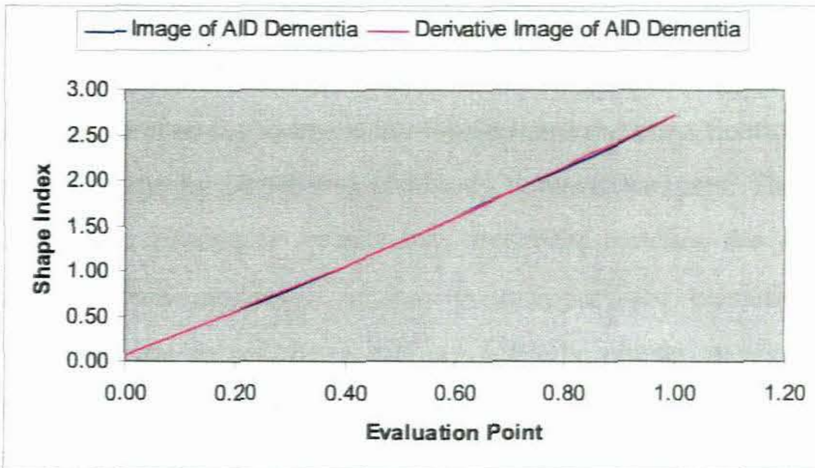

Figure 4.4: Jensen polynomials for the image of AID dementia using the method of scalar projections

The results of testing shape index values computed by Jensen polynomials using the methods of geometric properties and scalar projections generally showed that Jensen polynomials is suitable for shape index computation based on some properties of the image such as shape orientation, eccentricity, angle between shape profiles and DFP vector.

4.9. Image Classification using Instance-Based Learning

Generally speaking, an image classification task is to identify an unknown event e, given a finite set $E = \{e_1, e_2, ..., e_n\}$ of mutually exclusive possible events. The items of E are natural concepts called classes or categories. The classifier receives as input an observation O represented by feature vectors and then outputs a result of the form $\hat{e} \in E$, **where** $\hat{e} \in e_k$, $k = 1, 2, ..., n$. The variable k denotes the index of the class of the event e assumed to be the source of the observation O. If $\hat{e} = e$, the classification result is said to be correct, otherwise it is said to be wrong. The classifier is said to have learned the events set or training samples and used the knowledge acquired during learning to predict the result for a new event.

There are different types of learning techniques, namely, supervised, unsupervised, semi-supervised, reinforcement and multi-agent reinforcement learning. The supervised and unsupervised learning techniques are briefly discussed, because of their immediate relevance to this study. In supervised classification, the training samples are labeled and the classification of a new observation is done by computing similarity between samples. The output of the classification procedure is the class that best matches the observation according to some matching criteria. In unsupervised classification, the training samples are automatically labeled. Usually, clustering algorithms are employed to group similar samples before the classification is performed. The clustering procedure is influenced by some parameters such as the number of clusters to create or the average cluster size specified (Zieren & Canzler, 2006). Thus, the classifier performs the task of labeling the input samples.

Supervised learning is very appropriate for a medical image retrieval system using a classification technique, because the labeling of the training samples can easily be done in the recording process due to the available ground truth in this domain. Instance-Based learning or Reasoning (IBR) was found useful for the task of brain MRI classification, because it gives simple representation of the instances through the use of feature vectors. We used k-NN classifier to perform retrieval image retrieval. Given an integer number k, the k-NN classifier calculates the distances between the new shape feature and shape features in the training dataset and then assigns the new shape feature to a class among its k nearest neighbors based on multiple voting.

An important challenge to address for any classification algorithm is over-fitting. A classifier with a set of parameters p is said to over-fit the training samples T if there exists another set of parameters p' that yields lower performance on T, but higher performance in the actual real-world application (Mitchell, 1997). A good strategy for avoiding over-fitting is to use disjoint sets of samples for both training and testing. This explicitly measures the classifier's ability of generalization and allows including it in the optimization process. The test samples need to be sufficiently distinct from the training samples for this approach to be effective (Zieren & Canzler, 2006).

There are several sampling techniques for avoiding over-fitting problem, namely (a) holdout set method, which is easy to compute, but has higher variance, (b) LOOCV, which is easy to apply for some classifiers and difficult for others, and (c) k-Fold CV, which uses all data for both training and testing. We used 5-Fold CV sampling technique in this study to solve the over-fitting problem. Cross-validation is a useful technique for many tasks often encountered in machine learning, such as accuracy estimation, feature selection or parameter tuning. It consists of partitioning a dataset into n subsets and then running a given algorithm n times, each time using a different training set and validating the results on the dataset (Blockecl & Struyf, 2002). The technique allows all the examples in the database to be used for both training and testing. This can significantly improve system performance, since enough samples are used for both training and testing.

4.10. Retrieval System Performance Evaluation Technique

In this study, we used intuitive-PRECALL to compute the performance of an image retrieval system that uses non-classification technique. The performance of an image retrieval that uses pre-classification technique was also computed using classification accuracy measure. The results are then compared for significance different using a robust statistical method, called analysis of variance (ANOVA) for hypothesis testing.

The process of effective analysis of the performance of an image retrieval system requires that a suitable evaluation method be developed. Generally, precision and recall are two popular measures used to evaluate performance of information retrieval systems as discussed in chapter 3. They are easy to define for a single query and if the retrieval results generated for the query is a linear ordering. However, when the retrieval results are weakly ordered, in the sense that several documents have an identical retrieval status value (i.e. similarity measurement) with respect to a query or when multiple queries are involved, the simple precision and recall formulae discussed in chapter 3 cannot be applied. Conventionally, to facilitate computing means performance over a set of queries, each with a different number of relevant documents, individual query precision values are interpolated to a set of standard recall levels in the interval [0, 1]. The particular rule used to interpolate precision at standard recall x is to use the maximum precision obtained for the query for any actual recall level greater than or equal to x. This particular rule defines a procedure called ceiling interpolation.

Various problems and issues associated with the use of precision and recall as measures of retrieval system performance have long been systematically investigated (Raghavan, et al., 1989). In particular, with ceiling interpolation, the interpretation of precision is difficult and not easily amenable to objective treatment when all the documents in the final rank are not retrieved. As a result, it is difficult to claim that one system is actually better than other only on the basis of determining precision and recall. For the sake of clarity, the precision P(x) as a function of standard recall level x is the PRECALL method given by the expression:

$$P(x)=\frac{r.\lceil x.n\rceil}{r.(\lceil x.n\rceil+j)+s.i} \qquad (4.43)$$

where r is the number of relevant documents, i is the number of irrelevant documents at final rank (lf), j is the number of irrelevant documents in ranks completely needed, s is the number of relevant document desired from lf, x.n corresponds to the number of retrieved relevant documents and n is the total number of relevant documents in response to a query.

To address the deficiency of the PRECALL method, two different improvements for computing precision in the mean sense, namely, Probability of Relevance (PRR) and Expected Precision (EP) were introduced (Raghavan, et al., 1989). Each of these methods was investigated with respect to two distinct stopping criteria, namely, the number of relevant documents that are to be retrieved (NR) and the desired number of retrieved documents (ND). Given a search request in terms of the number of relevant documents desired, the retrieval system begins search from the highest level (rank 1), which contains documents with the highest measure of similarity computation. The search progresses until the final level rank lf at which the stopping criterion is met. Then let, t be the number of documents searched through in ranks 1 through lf-1, tr is the number of relevant documents searched through in ranks 1 through lf-1, j is the number of irrelevant documents searched through in ranks 1 through lf-1, r is the number of relevant documents in rank lf and i is the number of irrelevant documents in rank If. Then PRR as a function of NR, PRR as a function of ND and EP as a function of ND are defined as:

$$PRR(NR) = \frac{NR}{NR + esl_{NR}} \quad (4.44)$$

$$PRR(ND) = \frac{t_r(r+i) + k.r}{ND(r+i)} \quad (4.45)$$

$$EP(ND) = \frac{r.n.ER}{r(n.ER + j) + i(n.ER - t_r)} \quad (4.46)$$

where esl_{NR} is the Cooper's expected search length (Cooper, 1968) and is given as:

$$esl_{NR} = \frac{j(r+1) + i.s}{r+1}$$

and

$$ER = \frac{t_r(r+i) + k.r}{n(r+i)}$$

$$EP = \frac{t_r(r+i) + k.r}{ND(r+i)}$$

The procedure described above is called intuitive interpolation and when PRR(NR) is calculated under ceiling interpolation, NR is simply replaced by n.x in equation (4.44) to obtain the required interpolation ceiling-PRECALL method. It was concluded that ceiling-PRECALL method is not amenable to any reasonable interpretation (Raghavan, et al., 1989). The problem is caused not only by the fact that averaging results for multiple queries is done over NR, but also by the fact that the method of interpolation is ad hoc. Intuitive-PRECALL method yields a graph that can be given a sound interpretation if ND is viewed as the parameter through which precision and recall are defined. It is better for intuitive-PRECALL method for averaging purposes to take precision values over many queries at fixed ND and not NR. EP(ND) coincides with PRR(ND), thus making intuitive-PRECALL defined over ND a candidate choice for evaluating retrieval results for multiple queries and distorted or non-linear ordering. Thus, we used intuitive-PRECALL (equation 4.45) as a performance measure for the retrieval system that uses non-classification technique.

Chapter 5

The BrainSearch Implementation Prototype

This chapter presents the description of a shape-based image retrieval system, called BrainSearch, which is a prototype system to support image retrieval for healthcare applications in our GUISET architecture. The system was developed with a view to improve retrieval results of an image retrieval system. This will then allow for integration of image retrieval services into GUISET to provide healthcare information infrastructure that can enable improved healthcare service provisioning. Among various healthgrid services, brain MRI retrieval services are very important, because useful information that can aid effective diagnosis can be obtained from brain image analysis by studying brain patterns and comparing results with previous cases. Brain image analysis allows for early discovery of useful first-aid information, even for healthy person. Brain MRI retrieval services belong to the ubiquitous access and retrieval management level services (Naseer & Stergioulas, 2006).

The ubiquitous access and retrieval services enable ubiquitous access, storage, retrieval, analysis, management, manipulation and sharing of all types of medical and healthcare specific digital images and medical scans. We give a description of the functional capability of the BrainSearch prototype system in this chapter. This system is then used for the implementation of a series of image retrieval experiments. The purpose of the experiments was to find out if pre-classification of images will improve retrieval results in a CBIR system and to discover whether a combination of LBF active contour and DFP shape representation will be better used for edge-based retrieval or region-based retrieval. The experimental results ultimately provide answers to the research questions as well confirm the achievement of the research aim and objectives. We give detail discuss of the experimental results in chapter 6 that follows. First, in this chapter, we describe the experimental setup and then give the description of the components of the BrainSearch prototype system.

5.1. Experimental Setup

The research experiments designed in this study were implemented on an IBM compatible PC, CPU Intel® Pentium® 4, 2.94GHz, 1.21GB of RAM. The BrainSearch prototype system running on Microsoft Windows XP 2002 was used for the implementation of the research experiments. Brain MRI image modality was used to test the effectiveness of the prototype system and the results are generally appealing. In all the experiments, the value of $[a, b] = [0, 1]$ was used for computing shape index, $t = 0.1$, $\lambda_1 = \lambda_2 = 1.0$ and $\sigma = 1.5$ were used for the image segmentation. The numbers of retrieved images lie in the set $\{1, 2, \ldots, 6\}$. The number of iterations was varied from 5 to 40 for different images to extract regions of interest. The alpha = 0.01 that determine the confidence level was used for the analysis of variance. This confidence level is 100(1-alpha) = 99% indicating strong evidence against null hypotheses. To make the shape properties comparable and to achieve scale invariance in the DFP shape representation, all images were re-sampled to 72 x 72 pixels, ignoring the initial aspect ratio. Then we applied our vector re-binning algorithm to further reduce feature space dimension to half the original size, that is, the final feature vector dimension is of size 36.

Based on the whole brain atlas MRI data, exhaustive experiments were performed using 5-folds cross-validation scheme for system performance evaluation. Each time, a collection of images was used as test images and the remaining image collections were referenced. The mean system performance rate over all permutations was then compared to determine the technique that gives highest effects on system performance. The experiments evolved a k-NN classifier to improve retrieval results of a retrieval system. The evolved k-NN classifier embeds similarity measures for shape features and opts for the image class that gets the most votes over k-references that are closest neighbors to the example image. This is a simple, but effective and useful method to interactively and objectively present retrieval results.

5.2. Overview of the System

This section gives an overview of the BrainSearch prototype system with regards to its image retrieval functional capability. The system was built for implementing our image retrieval experiments. All the functionalities described in chapters 2 and 4 were implemented in our prototype system for experimentation. Thus, the prototype system can be referred to as an experimentation system.

We realized a general architecture of the prototype system based on the mathematical ideals presented in chapters 2 and 4. Later the description of how our prototype system uses the described mathematical models for image retrieval is presented. Accordingly, the BrainSearch system architecture is composed of three core components, namely, feature extraction, similarity measurement and indexing. The feature extraction component has four core elements, namely, dimension reduction, image segmentation, feature vector and feature annotation. Three different algorithmic techniques, namely, Color Space Conversion (CSC), Image Re-Sampling (IRS) and Vector Re-Binning (VRB) are provided for dimension reduction. The CSC algorithm converts colored images to grayscale images so as to generally process any input image. The IRS algorithm reduces 2-dimensional image space to another 2-dimensional image space of manageable size, thereby achieving dimension reduction. The VRB algorithm transforms 1-dimensional feature vector to another 1-dimensional feature vector of lower dimension.

The image segmentation component provides two algorithmic techniques, namely, Contour Evolution (CEV) and Image Binarization (IBI). The CEV uses LBF active contour to extract region of interest and the IBI converts the extracted region of interest to black and white, keeping the image quality. Prior to contour evolution using LBF active contour, the re-sampled image is first enhanced to improve visual quality of the image and the enhanced image goes through a smoothening process to remove noise. The feature vector supports two types of feature representations, namely, edge and region, which may or may not be further reduced or annotated. The feature annotation provides the solution for narrowing the semantic gap by complementing feature vector with high level semantics of an image. If annotation scheme is not applied, conventional image retrieval system is realized. The similarity measurement component implements a number of similarity measures for experimentation. Finally, the indexing component is responsible for shape index computation and algorithms such as Jensen polynomials and principal component analysis are essentially useful for this task, thereby achieving further dimension reduction.

Our prototype system generates two kinds of retrieval results, based on pre-classification and non-classification of images. The outputs of the system when pre-classification technique is used are the class that the example image was predicted to belong and $k' \leq k$ most similar images of the predicted class. Similarly, when non-classification technique is used, the system outputs all k images. The parameter k is the number of retrieved images and is usually supplied by the user, thus making the system interactive. Figure 5.1 shows the overall system architecture of the BrainSearch.

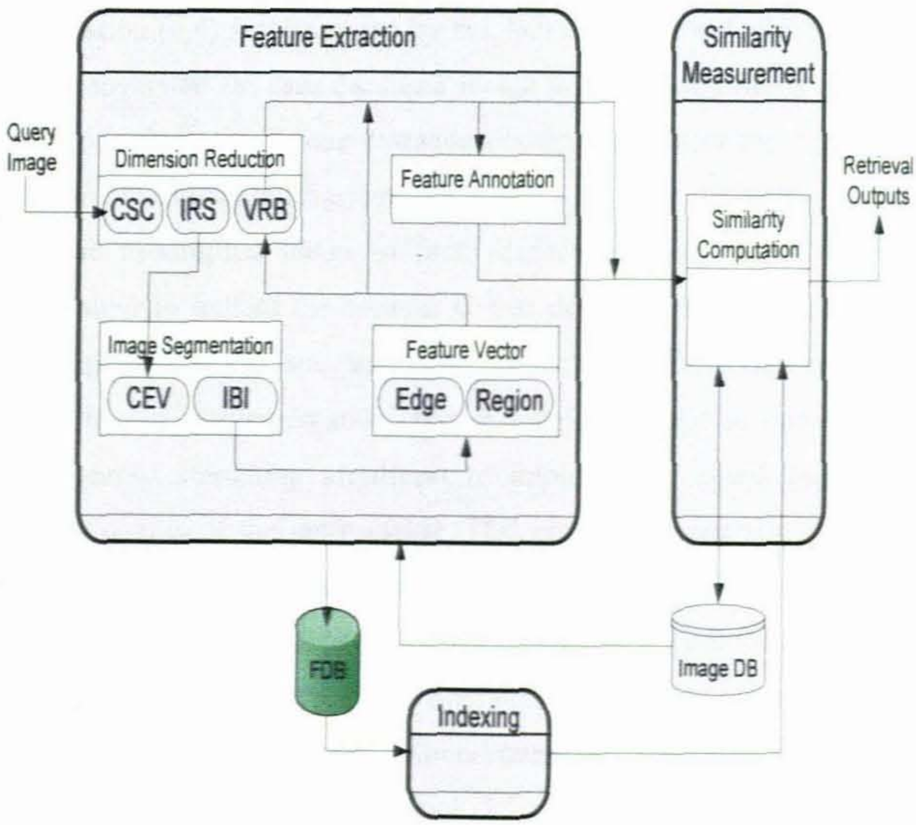

Figure 5.1: The BrainSearch system architecture

Next, we give the description of each component of the BrainSearch with respect to a particular mathematical equation used. The two core steps of the CBIR system are the feature extraction and the similarity computation. The feature extraction process generates a set of features to represent the content of each image. Usually, for shape-based image retrieval, the extracted image feature is an n-dimensional feature vector, which can be regarded as a point in n-dimensional space. The similarity computation process computes the similarity between the query image and each image in the database using their feature vectors. The similarity computation is essentially the determination of the distance between the feature vectors representing the images.

Given an input image $I_{m,n}$ of dimension m x n, if the input image is a colored image, the first step of the feature extraction component converts the color image to a grayscale image. Equation (4.2b) was implemented by the CSC component to accomplish this task. Then the grayscale image is re-sampled to a fixed dimension (for example 72 x 72 in our implementation) using equation (4.4) implemented by the IRS component. Unlike the process of color conversion (in case the input image is a grayscale image, conversion does not occur), in the feature extraction component every input image is re-sampled to achieve scale invariant.

The re-sampled image is then segmented using region-based LBF active contour to extract the contour C that describes the shape of the input image. Equation (4.19) was implemented by the CEV component for this purpose. In our implementation, the re-sampled image is enhanced using simple contrast stretching algorithm to improve the visual appearance or perception quality of the input image. This process is generally called spatial domain enhancement, because the contrast stretching enhancement algorithm operates directly on the image pixels. An alternative enhancement algorithm is the frequency domain method that operates on the Fourier transform of the input image. Spatial domain enhancement is significantly faster than frequency domain enhancement, since for a given image of size n x n, the complexity of 2D spatial domain enhancement algorithm is O(n^2). The 2D discrete Fourier transform enhancement algorithm has complexity O(n^4).

Even if 2-D fast Fourier transform algorithm (O(n^2logn)) was used, spatial domain enhancement is still faster. Moreover, to the best of our knowledge, it has not been reported in the literature, which enhancement algorithm gives the best result. Then we smoothed the enhanced image using Gaussian convolution (Equation 4.29) to remove noise in the input image.

In the implementation of LBF active contour, we computed the functions given by equations (4.22) and (4.23) using convolution operations to solve equation (4.19). The term $\lambda_1 e_1 - \lambda_2 e_2$ in equation (4.19) was written as a linear combination of three convolutions. The terms involving vector dot product ($\bullet$), gradient (∇) and Laplacian (Δ) were expressed as partial derivatives, which were then discretized by simple finite difference scheme. Given a contour C, we extracted the shape I_s of an image $I_{n,n}$ using the given contour as follows. Let i = 0, 1, ..., n-1 and j = 0, 1, ..., n-1 be the row and column indices of the point P(i, j) on C, we have:

$$I_s(i,j) = \begin{cases} 1, \ if \ P(i,j) < 0 \\ 0, \ otherwise \end{cases}$$

The extracted shape of the image has black background (pixel values of 0) and white foreground (pixel values of 1). The edge pixels of the image $I_{n,n}$ were obtained directly from I_s using the CNED algorithm (see equation 4.25 and 4.26), which takes I_s and the dimensions of I_s as arguments. The shape I_s is then converted to a feature vector using the DFP algorithm (equation 4.27). Let $S = \{s \mid s(i,\ j) = 1 \vee s(i,\ j) = 0, \forall\ i, j = 0,1,..,n-1\}$ be a shape space and $V \subset \mathbb{Z}^+$ is a feature space, the conversion function f_c can be specified as:

$$f_c : S \to V^n$$

Assuming the dimension of S is n x n, the dimension of V is n. The feature vector $v \in V^n$ can further be reduced by having its size using the vector re-binning algorithm (equation 4.28). The feature vector may then be classified into one of the brain MRI classes using the k-NN classifier implemented by the feature annotation component. If the feature vector is not classified, we call this technique non pre-classification technique. Both image classification and non classification algorithms generate ranked lists of similar images to the query image. The six similarity measures (equation 3.2, 3.3, 3.5-3.8) were implemented by the similarity computation component for experimentation. Finally, a unique shape index was computed using equation 4.31 after using equations (4.40 to 4.42) to obtain the parameters γ_k. This is the method of scalar projections and the method of geometric properties requires that equations (4.37 to 4.39) be used to determine the parameters γ_k for the Jensen polynomials to compute the shape index.

Table 5.1 shows the summary of the description of important functions implemented in the BrainSearch classes. The prototype CBIR system was written in C++ and has four main classes, namely, vlsSet, vlsImage, vlsObject and vlsContour. The vls prefix nomenclature connotes variational level set. The level set is the fundamental edge-based segmentation method that was originally investigated in this study for Silhouette images. Later a region-based LBF active contour was considered for MRI segmentation.

Table 5.1: Main classes implemented in BrainSearch

Class	Implementation Description
vlsSet	Uses some basic image routines in Borland C++ Builder 6, for reading and writing image files of any format. Additionally, it implements image smoothing, contrast stretching, Gaussian convolution, 4-directional Sobel and CNED edge detectors, some standard similarity measures, region-based LBF active contour, k-NN classifier and performance evaluation algorithms.
vlsImage	Implements the basic image assignment operators and provides a data structure for manipulating digital images.
vlsContour	Implements contour plotting functions, image re-sampling, image un-skewing (rotation transformation) and noise function.
vlsObject	Implements functions for computing geometrical shape properties like, eccentricity, shape profiles, shape orientation and minimum bounding rectangle. Provides the implementations of DFP shape representation and shape index computation using Jensen polynomials.

Figure 5.2 shows a sample of retrieval result when the system used non-classification of images technique (NCI) to search the database for similar images to the query image. The result was generated by matching edge-based shape descriptor of the query image against those of database images and Procrustes shape similarity measure was used for the ranking of similar images. The user requested for 8 similar images to the query image by specifying the value of k to be 8 and the system interactively returned 8 images predicted to be similar to the query image. The system also displayed the DFP Plot (DFPP) for visualizing the distribution of pixels that were on some rectangles placed on the shape object. Additionally, the system gave a search result of similar images in a ranked order, with the first image being the most similar to the query image.

The query image is the image of Alzheimer, which belongs to the degenerative class. Similar images to the query image are the grayscale image of Alzheimer's disease and its derivative at positions 1 and 2 in the image list respectively. Other similar images in the image list are coloured and noisy image of the Alzheimer's disease along with its derivative at positions 3 and 7, image of vascular dementia stroke and its derivative at position 4 and 6, image of chronic subdural hematoma stroke at position 5 and image of herpes encephalitis infectious at position 8 respectively. The shape index for each image is also shown in the image list.

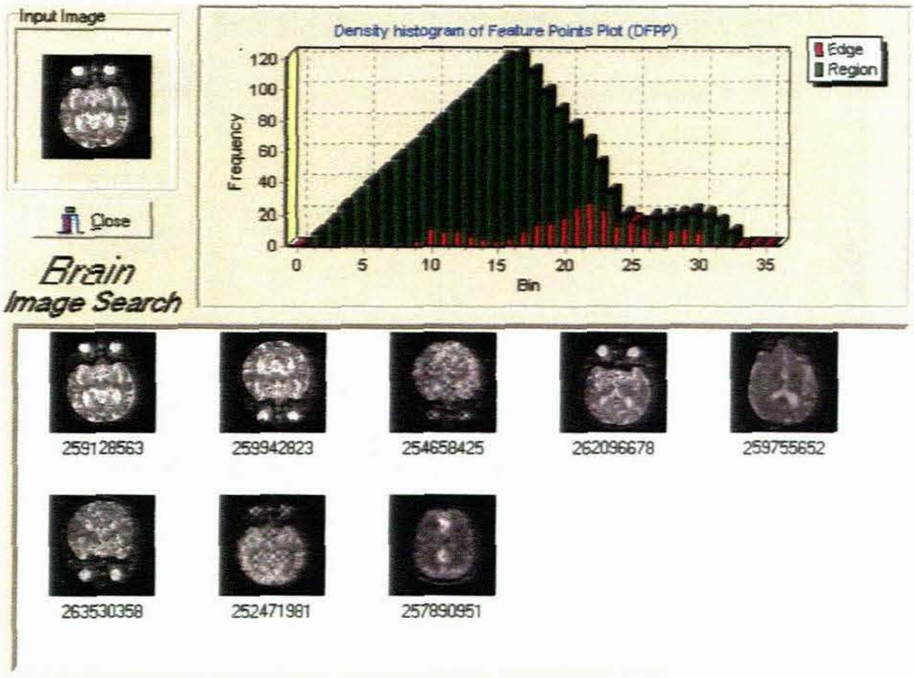

Figure 5.2: NCI-based retrieval of images similar to Alzheimer

Figure 5.3 shows the retrieval result when the user requested for 8 images that are similar to the query image (Alzheimer). The system used pre-classification technique (PCI) to search for similar images in the database. The system correctly predicted that the query image belongs to the degenerative class and returned only those images in the same class as Alzheimer. There are two other images (vascular dementia stroke and its derivative) that are perceptually similar to Alzheimer as shown in Figure 5.2, but because they belong to a different class (stroke), the system does not return these images. This technique follows the objective of a general retrieval system, which requires an effective system to return maximum relevant images and withhold maximum irrelevant images. The system also displayed the diagnostic aid that can be administered to a patient whose brain image was predicted to be similar to the query image. Additionally, the system displayed the previous history of such a disease. This diagnostic information automatically comes up when an image in the image list is clicked.

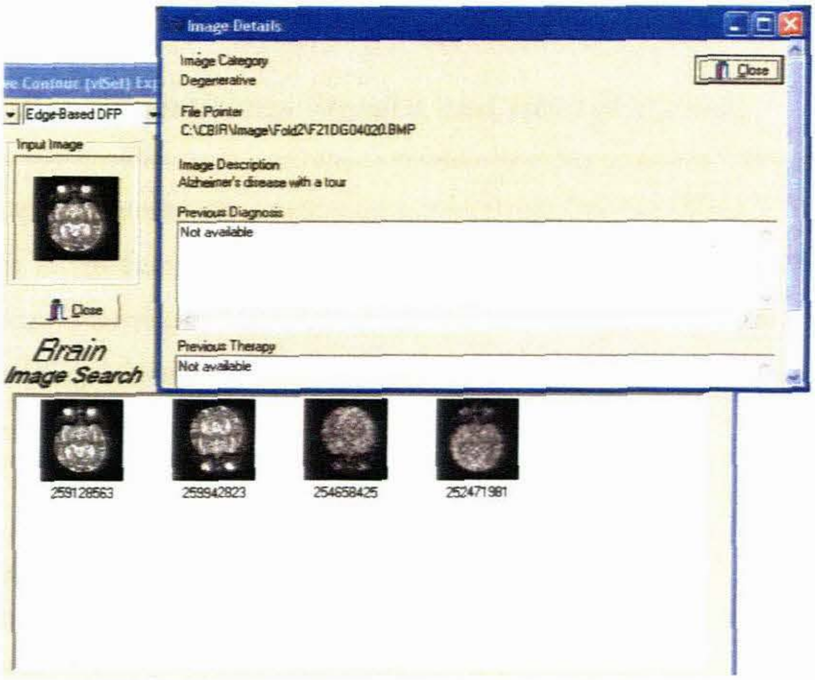

Figure 5.3: PCI-based retrieval of images similar to Alzheimer

Looking at Figures 5.2 and 5.3, it is obvious that k-NN classifier improves retrieval result of image retrieval. In Figure 5.2, the first three images are images of Alzheimer's disease, but the fourth image is the image of vascular dementia stroke, although it is perceptually similar to Alzheimer. In Figure 5.3, out of the eight images requested by the user, only four of the images are Alzheimer's disease degenerative as correctly predicted by the k-NN classifier. This implies that none of the other images (chronic subdural hematoma stroke, vascular dementia stroke and herpes encephalitis infectious) has up to four votes of neighbors. Suppose any of these images has up to four votes, our classification algorithm will still predict degenerative class, until an image with more than four votes is found. This is because the k-NN classifier ranks similar images such that if two ranked images have the same number of votes, the class of the image with the higher rank order will be predicted.

Chapter 6

Evaluation Experiments, Results and Interpretations

This chapter presents our evaluation experiments, results of the experiments and their interpretations. Firstly, we give the analysis of system performance evaluation. Secondly, we give the results of the retrieval experiments and their corresponding interpretations and then show how the results of the retrieval experiments provide answers to research questions.

6.1. Analysis of Performance Evaluation

The general problem of system performance evaluation, which can be approached through experimentations, is how to prove that one system is actually better than the other. Additionally, if one system is better than the other, will it always be better under all conditions? These problems can be approach using the following simple techniques, (a) use two or more test collections of respectable size and observe trends that are consistent across the different data, (b) make sure that the overall performance difference between the systems is relatively large, and (c) perform statistical significance test to claim that the difference was not observe due to chance. A statistical significance test was used to analyze the results of the image retrieval experiments designed in this study. The experiments follow a statistical approach, called 3-way factorial design. The results of the 3-way factorial design experiments are then analyzed using analysis of variance (ANOVA) method provided in MATLAB 7.1 statistical toolbox, which is efficient for analyzing complex N-way factorial designs. ANOVA is used to determine if the means in a set of data significantly differ when grouped by multiple factors. If they do differ, the factors or combinations of factors that are associated with the difference can be determined.

A number of bootstrap hypothesis tests (Sakai, 2007), including t-test bootstrap have been proposed for such analysis to determine, which pairs of means are significantly different and which is not. A procedural analysis called multiple comparisons (Hochberg & Tamhane, 1987) based on ANOVA was used to compare retrieval results. Usually, when a simple t-test bootstrap is used to determine, which means are significantly different, a significance alpha level that determines the cutoff value of the t-test bootstrap is specified. The purpose of the alpha cutoff is to ensure that when there is no real difference, it is possible to incorrectly find a significant difference no more than the cutoff value. If many group means are involved in the analysis, there are also many pairs to compare. If an ordinary t-test is used in this situation, the alpha value would apply to each comparison and therefore, the possibility of incorrectly finding a significant difference becomes high with the number of possible comparisons. To circumvent this problem, we used multiple comparisons technique, instead of t-test bootstrapping. Multiple comparisons are designed to provide an upper bound on the probability that any comparison will be incorrectly found significant. Additionally, a t-test statistics works effectively under the assumptions that the data to test are normally distributed and that they have equal variance. ANOVA test is known to be robust to modest violations of these assumptions and is considered useful in this study than simple t-test statistics. Thus, we used multiple comparison analysis to compare retrieval results.

6.2. Image Retrieval Experiments

The general approach used for the design of the image retrieval experiments reported in this study is comparative. In using a comparative experimentation approach, one needs to plan the experiments to collect data and to make a decision between two or more alternatives. Additionally, one needs to agree on a measurement by which competing alternatives can be compared. Besides, one also needs to generate a sample of data from each alternative and then compare average results to arrive at a decision. The best average response of an experiment is the most preferred solution among possible solutions. We applied experimental design techniques for the design of the image retrieval experiments reported in this study.

A design of experiment or experimental design is defined as a series of trials in which a number of individual experimental units and responses are measured, which can be analyzed to quantify and compare the effects of the treatments (Ress, 1987). It is a structured and organized approach, method and engineering analysis technique of determining the relationship that exists between a set of treatments, predictors or factors $(x_1, x_2, ..., x_n)$ affecting a process and the responding, outcome or response (y) of the process. One of the principal goals of experimental design is to estimate how changes in input factors affect the responses of the experiment (Kelton, 2000). There are good reasons for planning or designing an experiment before its implementation. These include among others, collecting data to make a decision between alternatives and to save time and effort by providing efficient ways to estimate the effect of a change in the factor on its response. Experimentation plays an important role in product realization activities, which consists of new product design and formulation, manufacturing process development and process improvement.

The objective in many cases may be to develop a robust process that is affected minimally by external sources of variability (Montgomery, 2005). The design of an experiment is a critical aspect of research, because the design of an experiment and its implementation can significantly affect the internal validity of the experimental results, which is at the center of all cause-effect inferences. There are several useful stages in designing and implementing an experiment. These include identifying the purpose of the experiment, statistical design, data collection, data scrutiny, data analysis, implementation and interpretation of results. We describe these experimental design stages or techniques as applied to this study.

6.2.1. Purpose of the Experiments

The report of the experiments conducted to evaluate retrieval results in an image retrieval system is presented. The purpose of the experiments was to find out if pre-classification of images will improve retrieval results in a CBIR system and to discover whether a combination of LBF active contour and DFP shape representation will be better used for edge-based retrieval or region-based retrieval. Moreover, the experiments aim to find out whether an image retrieval system $X(t_1(s))$ that uses a retrieval technique $t_1(s)$ is better than an image retrieval system $X(t_2(s))$ that uses a retrieval technique $t_2(s)$ on a collection of MRI data. Here, s is a parameter that represents a shape representation. The design of the experiments involves the following important decisions:

(a) Deciding, which retrieval technique will improve retrieval results?

(b) Deciding, which similarity measure to use for matching two shape representations so as to improve retrieval results?

(c) Deciding, which number of retrieved images in the set $\{1, 2, ..., 6\}$ will improve the matching process so as to improve retrieval results?

(d) Deciding, whether system $X(t_1(s))$ is better than system $X(t_2(s))$ for brain MRI retrieval.

The experiments described follow a statistical approach, called 3-way factorial design and generated an ANOVA. The response variable is the retrieval result, that is, the system performance. The factors are retrieval technique (technique), similarity measure (similarity) and number of retrieved images (retrieved). There are two factor levels for technique, namely, pre-classification (PCI(s)) and non-classification (NCI(s)). There are six factor levels for similarity, namely, Chi-test, Histogram intersection, Pearson correlation, Procrustes shape, Quadratic form and Sorensen. There are also six factor levels for retrieved. In our experiments, k (factor levels) was chosen from $\{1, 2, ..., 6\}$. This is a simple, effective and useful method to present classification results interactively. In general any value of k can be chosen by the user for the query.

The results of the 3-way factorial design experiments are then analyzed using ANOVA. Table 6.1 shows the response, factor and factor level for the brain MRI image retrieval experiments. The response variable for the image retrieval experiments is the retrieval performance. Retrieval performance is measured in terms of classification accuracy and intuitive-PRECALL for PCI(s) and NCI(s) techniques respectively.

Table 6.1: Response, factor and factor level for retrieval experiments

Response: Retrieval performance for different retrieval techniques		
Factor	**Level**	**Level number**
Retrieval technique as a function of shape representation s, (Technique)	pci(s), nci(s)	2
Similarity measurement (Similarity)	chi-test, intersection, pearson, procrustes, quadratic, sorensen	6
Retrieved images (Retrieved)	1, 2, 3, 4, 5, 6	6

Several factors $x_1, x_2, ..., x_n$ are usually involved in measuring retrieval system performance. Some of these factors were screen out using factors screening design experiment, sometimes called inspection of examples and some were controlled throughout the retrieval experiments. For examples, we selected CNED algorithm instead of 4-directional Sobel edge detector, because CNED uses less pixels to approximate edges than 4-directional Sobel algorithm. As a result, 4-directional Sobel algorithm was screen out and CNED was controlled through out the experiments. The LBF active contour segmentation algorithm was also controlled throughout the experiments and variational level algorithm was screen out, because of advantages of region-based segmentation over edge-based segmentation for medical images. Hence, the important factors considered in this study are shape representation (x_1), similarity measurement (x_2), number of retrieval (x_3) and retrieval technique

(x_4). The experimentation function $p_i(x_1, x_2, ..., x_n)$ is therefore, a function of three factor variables. Thus,

$$p_i = f(g_j(x_1), x_2, x_3) \tag{6.1}$$

The function $g_j(x)$ models a retrieval technique when a particular shape representation is applied for system performance computation. The interest is to estimate how a change in a given factor affects the response variable by determining the form of the experimentation function f. The mathematical solution technique to this problem is to apply differential equation by taking the partial derivative of equation 6.1. Unfortunately, the form of this function is unknown and therefore, this solution technique does not work. Another mathematical solution technique to determine the experimentation function is to search through the space of possible factor combinations. This is the solution technique used in this study to determine the effect of changes to factor variables on the response variable.

6.2.2. Experimentation Data

Data collection is an important stage of experimental design, because an experiment cannot be better than its data, that is, the result of an experiment is a function of the data used. The medical images used for the experiments reported in this study are parts of the top 100, 256 x 256 brain structures downloaded from the whole brain atlas of Harvard medical school (Johnson & Becker, 1999). Ten brain images were sampled from each class of the whole brain atlas. A simple random sampling technique (Yates, et al., 2008) was used to select the images so as to avoid classification error and biasness to a certain class. The image classes are normal, degenerative, infectious, stroke and tumor making a total of fifty sampled images.

The images were divided into 5 folds so as to use 5-folds cross-validation sampling technique for the image retrieval experiments. This technique is also called local control or blocking, which has the advantage of lowering the variance of response variables by removing some sources of variability from treatment contrasts. However, folding can increase the complexity of the analysis and interpretation of results as well gives scope for mistakes in the experimental procedure. It is, therefore, advisable to keep the number of folds lower as much as possible. The values of folds proposed in the literature lie between 5 and 10, hence the lowest value of 5 was chosen in this study to minimize mistakes that can occur during an experiment and to effectively manage complexity.

Each fold contains 10 original images and 10 derived images making a total of 20 images per fold. Additionally, 50 images were derived from the original images to test for the robustness of the shape representations to some basic transformations such as rotation. The image derivation follows the standard technique of applying basic transformations such as rotation, scaling, translation and noise contamination. In applying this technique, 50 images were derived from the original 50 images by rotating each original image by 180 degree and then little noise is added to obtain a slight change in the bitmap of shape, but the object shapes in the same groups do not considerably differ in human vision. In all, 100 images were used for the image retrieval experiments reported in this study. The image derivatives were assigned to folds such that an image and its derivative do not belong to the same fold. This allows images to be compared with their derivatives so as to test for robustness of the shape representation to a basic transformation. Appendix "A" shows the names of the 50 whole brain atlas images used for this study, their folds and number of iterations used to segment different regions of interest. Tables 6.2 and 6.3 show the mean classification accuracy for PCI(E) and PCI(R) techniques respectively. Similarly, Tables 6.4 and 6.5 show the mean intuitive-PRECALL for NCI(E) and NCI(R) respectively. The complete data used for system performance computations are shown in Appendix B.

Table 6.2: Mean classification accuracy for edge-based retrieval, PCI(E)

Similarity measure	Number of retrieved images					
	1	2	3	4	5	6
Chi-test	0.84	0.84	0.75	0.71	0.67	0.70
Intersection	0.74	0.74	0.71	0.66	0.63	0.65
Pearson	0.72	0.72	0.66	0.62	0.63	0.58
Procrustes	0.83	0.83	0.77	0.76	0.69	0.68
Quadratic	0.78	0.78	0.65	0.60	0.59	0.63
Sorensen	0.83	0.83	0.79	0.72	0.71	0.67

Table 6.3: Mean classification accuracy for region-based retrieval, PCI(R)

Similarity measure	Number of retrieved images					
	1	2	3	4	5	6
Chi-test	0.87	0.87	0.66	0.65	0.62	0.65
Intersection	0.99	0.99	0.69	0.69	0.66	0.66
Pearson	0.94	0.94	0.69	0.68	0.64	0.63
Procrustes	0.99	0.99	0.69	0.65	0.65	0.66
Quadratic	0.88	0.88	0.65	0.63	0.58	0.61
Sorensen	0.99	0.99	0.65	0.65	0.65	0.64

Table 6.4: Mean intuitive-PRECALL for edge-based retrieval, NCI(E)

Similarity measure	Number of retrieved images					
	1	2	3	4	5	6
Chi-test	0.84	0.76	0.66	0.62	0.59	0.57
Intersection	0.74	0.67	0.58	0.54	0.52	0.50
Pearson	0.72	0.65	0.56	0.53	0.52	0.49
Procrustes	0.83	0.76	0.65	0.60	0.58	0.55
Quadratic	0.78	0.72	0.64	0.59	0.55	0.53
Sorensen	0.83	0.77	0.68	0.62	0.58	0.55

Table 6.5: Mean intuitive-PRECALL for region-based retrieval, NCI(R)

Similarity measure	Number of neighborhood retrievals					
	1	2	3	4	5	6
Chi-test	0.87	0.79	0.68	0.62	0.57	0.54
Intersection	0.99	0.88	0.74	0.66	0.62	0.57
Pearson	0.94	0.85	0.73	0.67	0.62	0.58
Procrustes	0.99	0.87	0.71	0.64	0.60	0.56
Quadratic	0.88	0.77	0.64	0.58	0.54	0.50
Sorensen	0.99	0.86	0.70	0.63	0.58	0.55

6.2.3. Analysis of Image Retrieval Results

The image retrieval experiments performed in this study follow 3-way, 6-by-6-by-2 factorial design and ANOVA was used to analyze the difference between two results. Factorial design is usually used to, (a) identify factors with significant effects on the response, (b) identify possible interactions among factors, (c) identify the factors that have the most important effects on the response, (d) decide whether further investigation of a factor's is justified, and (e) investigate the functional dependence of a response on multiple factors simultaneously.

Factorial designs allow for simultaneous comparisons of the effects of multiple factors on responses. They also allow for a more complete interpretation of main effects, simultaneous manipulation of multiple variables and they are computationally efficient and economical. The main effect of a factor is defined as the average difference in response when the factor moves from its lowest level to its highest level. The interaction between factors measures whether the effect of one factor depends in some way on the level of one or more factors. The 3-way factorial design for the image retrieval experiments has three main effects, namely, retrieval technique (Technique), similarity measurement measure (Similarity) and number of retrieved images (Retrieved).

The null hypothesis, which states that there will be no significant difference between the performance of an image retrieval system X(PCI) that uses pre-classification technique and an image retrieval system X(NCI) that uses non-classification technique deals with comparing the performance of X(PCI) and X(NCI) for statistical significance. Testing for the validity of this hypothesis in healthcare application domain requires the main effect and interaction analyses for six different experimental comparisons, namely, (a) PCI(E) versus NCI(E), (b) PCI(R) versus NCI(R), (c) PCI(E) versus PCI(R), (d) NCI(E) versus NCI(R), (e) PCI(E) versus NCI(R) and (f) PCI(R) versus NCI(E). Additionally, interaction graphs are used to compare two means for statistical significance. Two means are said to be significantly different if their intervals are disjointed and are not significantly different if their intervals overlap. Finally, the means of several groups are compared to test for significant difference using multiple comparison procedure. The analysis and interpretation of the results of the experiments conducted in this study are provided using tables and graphs. The MATLAB sample codes for the image retrieval experiments are given in Appendix C.

6.3. Results of Image Retrieval Experiments

This section describes the results of DFP shape representation experiments to demonstrate visually that our algorithms and techniques yield suitable retrieval results on brain MRI. This was accomplished by plotting the density histogram of feature points (that is, frequency count) against the bin (that is, vector) location $i = 0, 1, 2, \ldots n-1$. The goal was to determine whether there is perceptual similarity between feature vector of an image and the feature vector of the image derivative. The histogram was computed for all region pixels that lie on the boundaries of some rectangles and the technique is called region-based DFP. The histogram was also computed for all edge pixels that lie on the boundaries of some rectangles and the technique is called edge-based DFP. The bins with peak values indicate greater density of points in a particular cell. Thus, it also indicates the distribution of those pixels around the centroid of the object.

Figure 6.1 shows the histogram plot of edge-based DFP (blue color vertical bar) and region-based DFP (red color vertical bar) for the image of

Mild Alzheimer. It is obvious from the graph that region-shape DFP descriptor (large frequency) utilizes more pixel information than edge-shape DFP descriptor (small frequency). To establish an effective comparison using DFP plot, we need to plot similar graphs for at least two derivatives of the image of Mild Alzheimer.

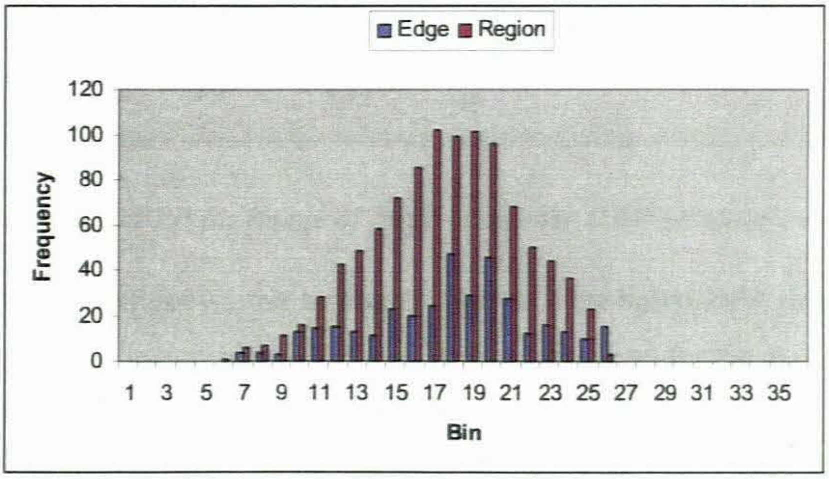

Figure 6.1: DFPP for the image of Mild Alzheimer

Figure 6.2 shows the histogram plot of edge-based DFP (blue color vertical bar) and region-based DFP (red color vertical bar) for the derivative of Mild Alzheimer. The derivative image was obtained by the rotation of the original image through an angle of 180^0 and by the addition of 2% salt and pepper noise to the rotated image. The changes observed in the graphs of the Mild Alzheimer and it derivative were due to the rotation effect and noise contamination. These changes do not significantly affect the retrieval result, because the derivative of the image was effectively retrieved in our experiments.

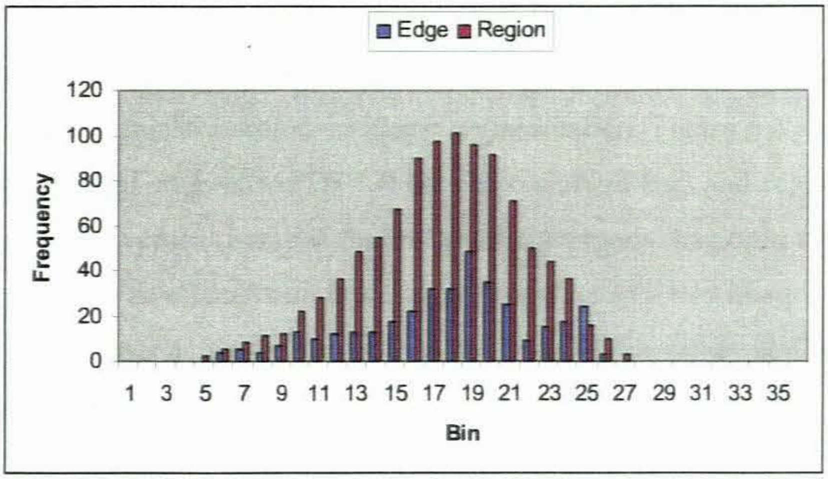

Figure 6.2: DFPP for image of Mild Alzheimer (180^0 rotation + noise)

Figure 6.3 shows the histogram plot of edge-based DFP (blue color vertical bar) and region-based DFP (red color vertical bar) for the derivative of the image of Mild Alzheimer. The derivative image was obtained by the rotation of the original image through an angle of 180^0 without noise contamination to the rotated image. The changes observed in the histogram plots of the Mild Alzheimer and its derivatives were due to the rotation effect. Figures 6.1 to 6.3 show that there is perceptual similarity between the image of Mild Alzheimer and its derivatives as observed in the density histogram plots.

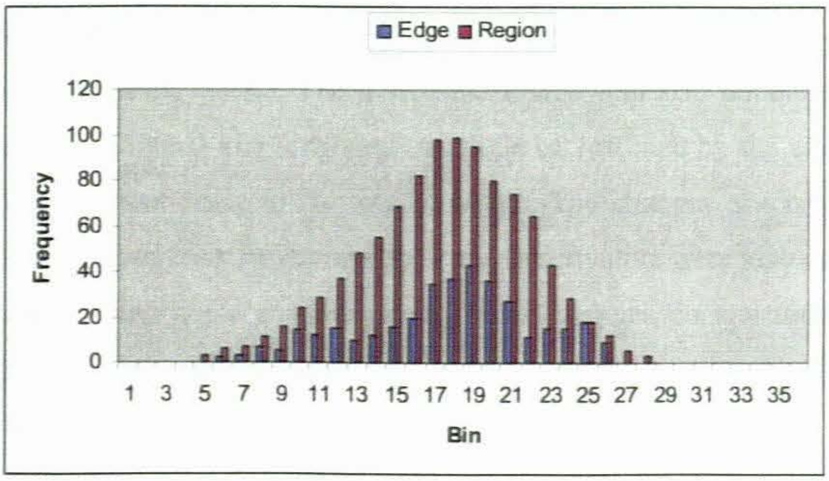

Figure 6.3: DFPP for image of Mild Alzheimer (180^0 rotation only)

The DFP graphs were also plotted for the image of Cavernous Angioma stroke diseases and its derivative images to further investigate the effect of image transformation on shape representation. Figure 6.4 shows the histogram plot of edge-based DFP (blue color vertical bar) and region-based DFP (red color vertical bar) for the image of Cavernous Angioma stroke. To further establish an effective comparison with respect to a new image, we need to plot similar graphs for at least two derivatives of the image of Cavernous Angioma stroke as we did for the image of Mild Alzheimer.

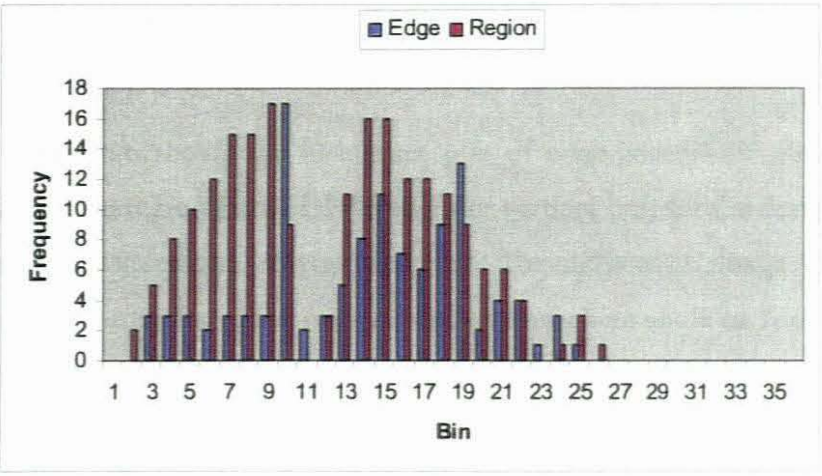

Figure 6.4: DFPP for image of Cavernous Angioma

Figure 6.5 shows the histogram plot of edge-based DFP (blue color vertical bar) and region-based DFP (red color vertical bar) for the derivative of Cavernous Angioma stroke. The derivative image was also obtained by the rotation of the original image through an angle of 180^0 and by the addition of 2% salt and pepper noise to the rotated image. The changes observed in the graphs of the Cavernous Angioma stroke and it derivative were also due to the rotation effect and noise contamination. These changes do not significantly affect the retrieval result, because the derivative of the image was effectively retrieved in our experiments.

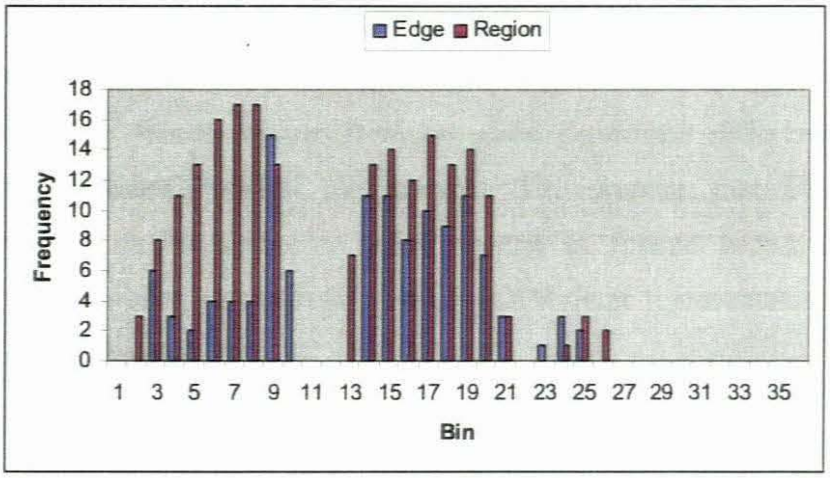

Figure 6.5: DFPP for image of Cavernous Angioma (180^0 rotation + noise)

Figure 6.6 shows the histogram plot of edge-based DFP (blue color vertical bar) and region-based DFP (red color vertical bar) for the derivative of the image of Cavernous Angioma stroke. The derivative image was also obtained by the rotation of the original image through an angle of 180^0 without noise contamination to the rotated image. The changes observed in the histogram plots of the Cavernous Angioma stroke and it derivatives were also due to the rotation effect. Figures 6.4 to 6.6 show that there is perceptual similarity between the image of Cavernous Angioma stroke and its derivatives as observed in the density histogram plots.

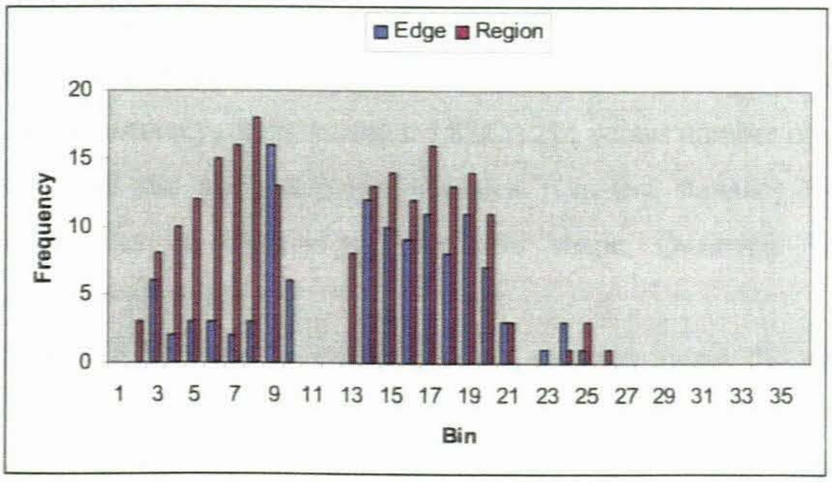

Figure 6.6: DFPP for image of Cavernous Angioma (180^0 rotation only)

Finally, the results of these experiments showed that DFP shape representation is invariant to basic transformation such as rotation. A small change in two feature vectors does not yield significant difference in the similarity measure between the features. This implies that DFP shape representation is insensitive to small change in feature vector. Thus, it conforms well to the human vision, making DFP shape representation suitable for object representation.

6.3.1. Results of Factor Effects

This section reports on the effect of some factors such as shape representation, similarity measures and retrieval technique on retrieval performance. Line graphs were used to present the results of the retrieval system performance evaluation. The goal was to graphically determine without performing statistical test of significance the factors (retrieval technique, similarity measure and number of retrieved images), that will give the best retrieval result. Although this technique is useful for the interpretation of results objectively, it cannot exclude subjectivity inherent in an image retrieval system evaluation. This is because the image classes themselves were classified by humans. However, this technique is usually used for interpreting experimental results. Hence, since line graphs cannot show the generality of specific techniques, mean, standard error, statistical proof, that is, F statistics and p-values and interaction graphs were provided to complement line graphs for results interpretations. The graphs of system performance (mean classification accuracy, mean intuitive-PRECALL) versus number of retrieved images for all the six similarity measures (Chi-test statistic, Histogram intersection, Pearson correlation, Procrustes shape, Quadratic form and Sorensen) were plotted.

Figure 6.7 shows the graphs of mean accuracy versus the number of retrieved images for the six similarity measures. The mean accuracy was generated on the database of brain MRI indexed using the edge-based shape feature when pre-classification technique was used to generate similar images to the query image. It was difficult to draw valid conclusion from the six graphs plotted in the figure, because they form clusters and cross links. However, we can see that the similarity measures have different effect on the retrieval results generated on edge-based shape feature using a pre-classification technique.

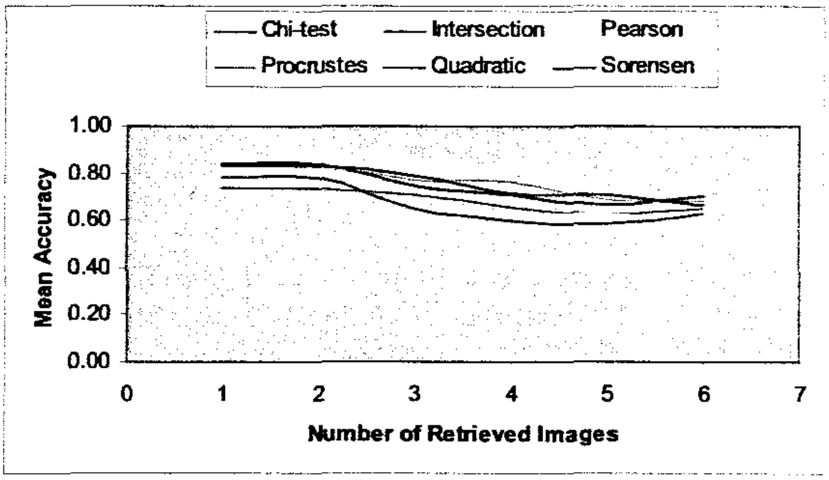

Figure 6.7: Mean classification accuracy for edge-based feature extraction PCI(s=E)

Figure 6.8 shows the graphs of mean accuracy versus the number of retrieved images for the six similarity measures. The mean accuracy was generated on the database of brain MRI indexed using the region-based shape feature when pre-classification technique was used to generate similar images to the query image. Due to the clusters and cross links observed in the graphs, it was also difficult to draw valid. However, we can also see that the similarity measures have different effect on the retrieval results generated on region-based shape feature using a pre-classification technique.

graphs plotted in the figure, because they form clusters and cross links. However, we can see that the similarity measures have different effect on the retrieval results generated on edge-based shape feature using a pre-classification technique.

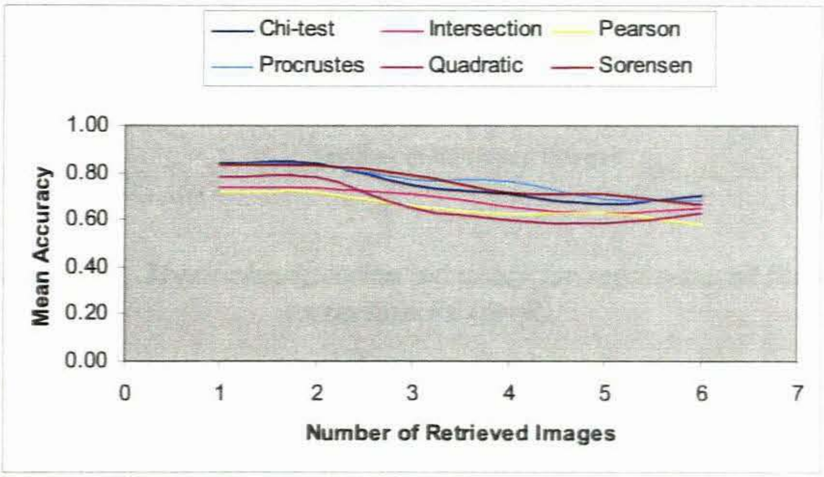

Figure 6.7: Mean classification accuracy for edge-based feature extraction PCI(s=E)

Figure 6.8 shows the graphs of mean accuracy versus the number of retrieved images for the six similarity measures. The mean accuracy was generated on the database of brain MRI indexed using the region-based shape feature when pre-classification technique was used to generate similar images to the query image. Due to the clusters and cross links observed in the graphs, it was also difficult to draw valid. However, we can also see that the similarity measures have different effect on the retrieval results generated on region-based shape feature using a pre-classification technique.

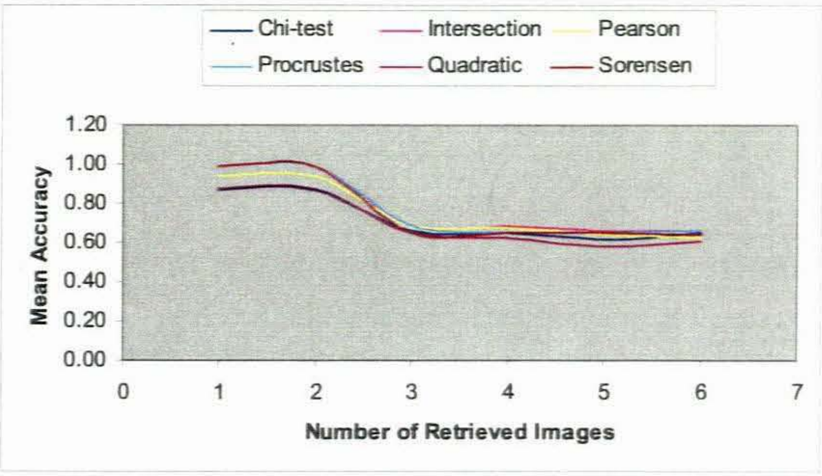

Figure 6.8: Mean classification accuracy for region-based feature extraction PCI(s=R)

Figure 6.9 shows the graphs of mean intuitive-PRECALL versus the number of retrieved images for the six similarity measures. The mean intuitive-PRECALL was generated on the database brain MRI indexed using the edge-based shape feature when non pre-classification technique was used to generate similar images to the query image. A result similar to the case of pre-classification technique was generated and due to the clusters and cross links also observed in the graphs, it was also difficult to draw valid conclusion from the result. However, we can also see that the similarity measures have different effect on the retrieval results generated on edge-based shape feature using a non pre-classification technique.

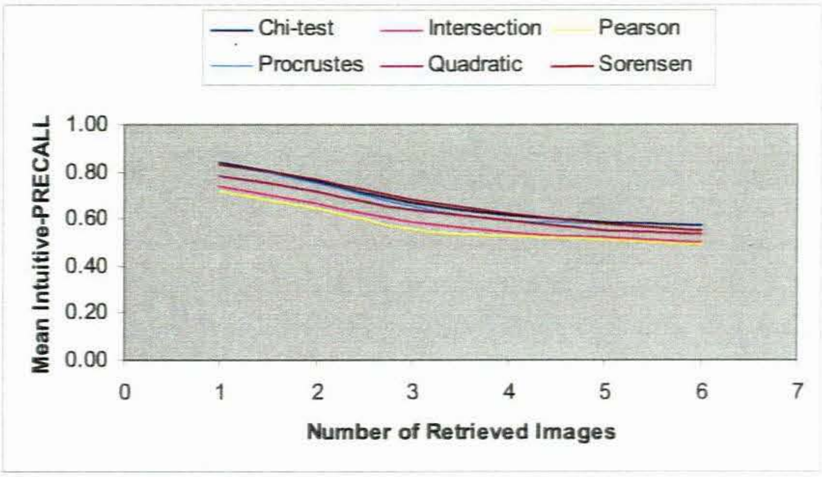

Figure 6.9: Mean intuitive-PRECALL for edge-based feature extraction NCI(s=E)

Figure 6.10 shows the graphs of mean intuitive-PRECALL versus the number of retrieved images for the six similarity measures. The mean intuitive-PRECALL was generated on the database of brain MRI indexed using the region-based shape feature when non pre-classification technique was used to generate similar images to the query image. A result similar to the case of pre-classification technique was also generated and due to the clusters and cross links also observed in the graphs, it was also difficult to draw valid conclusion from the result. However, we can also see that the similarity measures have different effect on the retrieval results generated on region-based shape feature using a non pre-classification technique.

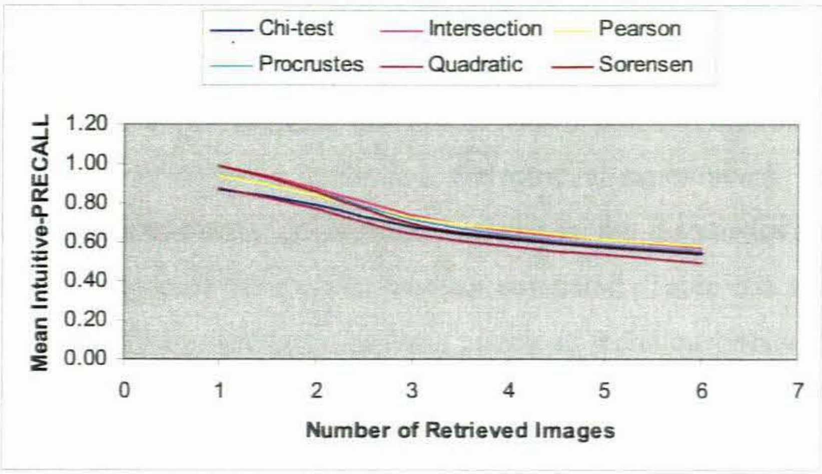

Figure 6.10: Mean intuitive-PRECALL for region-based feature extraction NCI(s=R)

In conclusion, all the graphs (Figures 6.7 to 6.10) showed that the factors investigated have effects on retrieval results. However, it was difficult to directly establish from the graphs the quantitative effects of these factors on retrieval results. It was also difficult to determine whether these effects and possible interactions among factors were significantly different. This is where ANOVA comes into play as a robust statistical analysis technique for determining main effects and interactions among several factors. ANOVA can determine the main effects of factors on retrieval results and as well as interactions among factors. This mechanism is explicitly discussed in the sub-section that follows.

6.3.2. Statistical Analysis of Retrieval Results

A 6 (Retrieved)-by-6 (Similarity)-by-2 (Technique) ANOVA was calculated for retrieval system performance evaluation. Tables 6.6, 6.7, 6.8, 6.9 and 6.10 show the results of ANOVA analysis of the retrieval experiments. Tables 6.6 and 6.7 show the statistical proof statement, that is, the F-statistics and the P-value for each pair of retrieval techniques compared. Table 6.6 shows that there is no significant difference in main effects in technique when PCI(E) is compared to NCI(R). That is, PCI(E) and NCI(R) have equal effects on retrieval results, $F(25, 25) = 1.03$, $p = 0.32 > 0.01$ (very strong evidence that there is no significant difference between the two techniques). However, statistical evidence available from Table 6.6 showed that there are statistical significant differences in main effects for other factors. Similarly, Table 6.7 shows the factors that have no significant difference between first-order interactions and those that have significant difference between first-order interactions. Tables 6.8, 6.9 and 6.10 show the mean and standard error of the effects of technique, similarity and retrieved images on retrieval results.

Table 6.6: Main effects of factors on retrieval performance

Comparison		Source		
t_1	t_2	Technique	Similarity	Retrieved
PC(E)	PC(R)	F(1,25)=398.81, p=0.0	F(5, 25) = 80.21, p=0.0	F(5,25)=286.69, p=0.0
NC(E)	NC(R)	F(1,25)=476.54, p=0.0	F(5, 25) = 26.78, p=0.0	F(5,25)= 930.48, p=0.0
NC(E)	PC(E)	F(1,25)=398.81, p=0.0	F(5, 25) = 80.21, p=0.0	F(5,25)=286.69, p=0.0
NC(R)	PC(R)	F(1,25)=236.07, p=0.0	F(5,25)=103.62, p=0.0	F(5,25)=2209.88, p=0.0
NC(R)	PC(E)	F(1,25)=1.03, p=0.32	F(5, 25) = 20.63, p=0.0	F(5,25)=258.37, p=0.0
NC(E)	PC(R)	F(1,25)=635.16, p=0.0	F(5, 25) = 16.12, p=0.0	F(5,25)=511.53, p=0.0

Table 6.7: First-order interaction between factors

Comparison		Source		
t_1	t_2	Technique x Similarity	Technique x Retrieved	Similarity x Retrieved
PC(E)	PC(R)	F(5, 25) = 5.43, p=0.0	F(5, 25) = 18.82, p=0.0	F(25, 25) = 1.34, p=0.24
NC(E)	NC(R)	F(5, 25) = 60.53, p=0.0	F(5, 25) = 40.70, p=0.0	F(25,25)=1.46, p=0.17
NC(E)	PC(E)	F(5, 25) = 5.43, p=0.0	F(5, 25) = 18.82, p=0.0	F(25,25)=1.34, p=0.24
NC(R)	PC(R)	F(5,25)=2.70, p=0.04	F(5, 25) = 67.05, p=0.0	F(25, 25) = 7.09, p=0.0
NC(R)	PC(E)	F(5, 25) = 19.04, p=0.0	F(5, 25) = 47.39, p=0.0	F(25,25)=0.60, p=0.89
NC(E)	PC(R)	F(5, 25) = 26.88, p=0.0	F(5, 25) = 34.72, p=0.0	F(25,25)=1.14, p=0.37

Table 6.8: Comparison of retrieval techniques

Comparison		Mean (Standard error)	
t_1	t_2	t_1	t_2
PC(E)	PC(R)	0.71 (0.0)	0.75 (0.0)
NC(E)	NC(R)	0.63 (0.0)	0.71 (0.0)
NC(E)	PC(E)	0.64 (0.0)	0.71 (0.0)
NC(R)	PC(R)	0.71 (0.0)	0.75 (0.0)
NC(R)	PC(E)	0.71 (0.0)	0.71 (0.0)
NC(E)	PC(R)	0.64 (0.0)	0.75 (0.0)

Table 6.9: Comparison of similarity measures

Comparison		Similarity Measure					
t	t_i	Chi-test	Histogram	Pearson	Procrustes	Quadratic	Sorensen
PC(E)	PC(R)	0.74 (0.0)	0.73 (0.0)	0.70 (0.0)	0.77 (0.0)	0.69 (0.0)	0.76 (0.0)
NC(E)	NC(R)	0.68 (0.0)	0.67 (0.0)	0.66 (0.0)	0.70 (0.0)	0.64 (0.0)	0.70 (0.0)
NC(E)	PC(E)	0.71 (0.0)	0.64 (0.0)	0.62 (0.0)	0.71 (0.0)	0.65 (0.0)	0.72 (0.0)
NC(R)	PC(R)	0.70 (0.0)	0.76 (0.0)	0.74 (0.0)	0.75 (0.0)	0.68 (0.0)	0.74 (0.0)
NC(R)	PC(E)	0.72 (0.0)	0.72 (0.0)	0.69 (0.0)	0.74 (0.0)	0.66 (0.0)	0.74 (0.0)
NC(E)	PC(R)	0.70 (0.0)	0.69 (0.0)	0.67 (0.0)	0.72 (0.0)	0.67 (0.0)	0.72 (0.0)

Table 6.10: Comparison of number of retrieved images

Comparison		Number of Retrieved Images					
t	t_i	1	2	3	4	5	6
PC(E)	PC(R)	0.87 (0.0)	0.87 (0.0)	0.70 (0.0)	0.67 (0.0)	0.64 (0.0)	0.65 (0.0)
NC(E)	NC(R)	0.87 (0.0)	0.78 (0.0)	0.66 (0.0)	0.61 (0.0)	0.57 (0.0)	0.54 (0.0)
NC(E)	PC(E)	0.79 (0.0)	0.76 (0.0)	0.68 (0.0)	0.63 (0.0)	0.61 (0.0)	0.59 (0.0)
NC(R)	PC(R)	0.94 (0.0)	0.89 (0.0)	0.69 (0.0)	0.65 (0.0)	0.61 (0.0)	0.60 (0.0)
NC(R)	PC(E)	0.87 (0.0)	0.81 (0.0)	0.71 (0.0)	0.66 (0.0)	0.62 (0.0)	0.60 (0.0)
NC(E)	PC(R)	0.87 (0.0)	0.83 (0.0)	0.65 (0.0)	0.62 (0.0)	0.62 (0.0)	0.59 (0.0)

The systematic analysis of the retrieval results is based on interaction graphs, because these graphs allow us to test for the effects of each factor on retrieval results. Interaction graphs also allow us to explicitly test for the population marginal means of groups represented by a symbol and an interval around the symbol. Two means are significantly different if their intervals are disjoint and are not significantly different if their intervals overlap. The evaluation model shows that PCI(R) versus NCI(R) and PCI(E) versus NCI(E) are analyzed for horizontal comparison. Similarly, PCI(E) versus PCI(R) and

NCI(E) versus NCI(R) are analyzed for vertical comparison. Finally, PCI(E) versus NCI(R) and PCI(R) versus NCI(E) are analyzed for cross comparison.

Figures 6.11 to 6.16 show the interaction graphs for horizontal comparisons. Figure 6.11 shows that the population marginal means of groups PCI(R) and NCI(R) are significantly different and thus, PCI(R) has higher effects on retrieval results than NCI(R). Figure 6.12 shows that there are 4 groups of similarity measures having population marginal means significantly different from Histogram intersection. As a result, Histogram intersection and Procrustes shape have the same effects on system performance and thus, better than Chi-test, Pearson correlation, Sorensen and Quadratic form. Figure 6.13 shows that 5 groups of retrieved images have population marginal means significantly different from 1 retrieved, which has the highest effects when PCI(R) and NCI(R) are compared. Figure 6.14 shows that the population marginal means of groups PCI(E) and NCI(E) are significantly different and thus, PCI(E) has higher effects on performance than NCI(E). Figure 6.15 shows that there are 3 groups of similarity measures having population marginal means significantly different from Sorensen. As a result, Sorensen, Chi-test and Procrustes shape have the same effects on system performance and thus, better than Histogram intersection, Pearson correlation, Sorensen and Quadratic form. Figure 6.16 shows that 5 groups of retrieved images have population marginal means significantly different from 1 retrieved, which has the highest effects when PCI(R) and NCI(R) are compared.

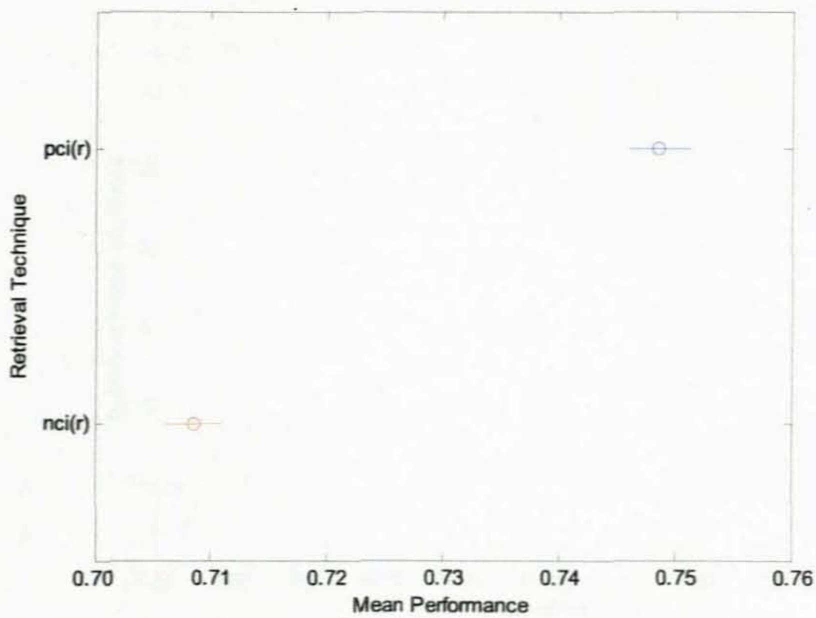

Figure 6.11: Effects of retrieval techniques on system performance, PCI(R) versus NCI(R) comparison

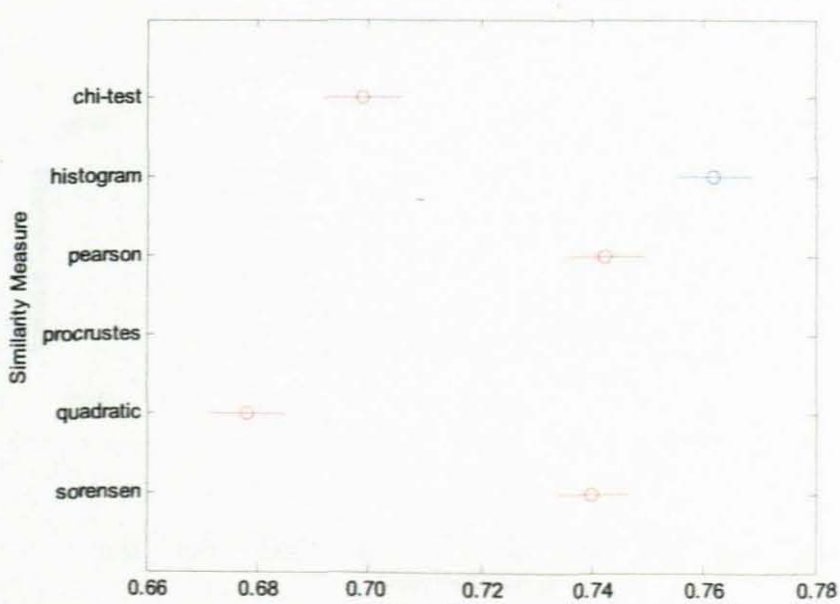

Figure 6.12: Effects of similarity measures on system performance, PCI(R) versus NCI(R) comparison

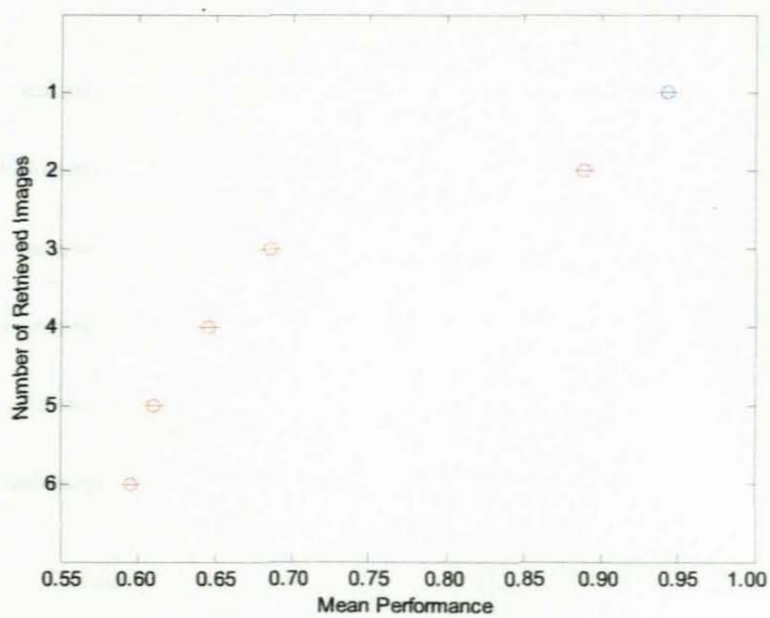

Figure 6.13: Effects of retrieved images on system performance, PCI(R) versus NCI(R) comparison

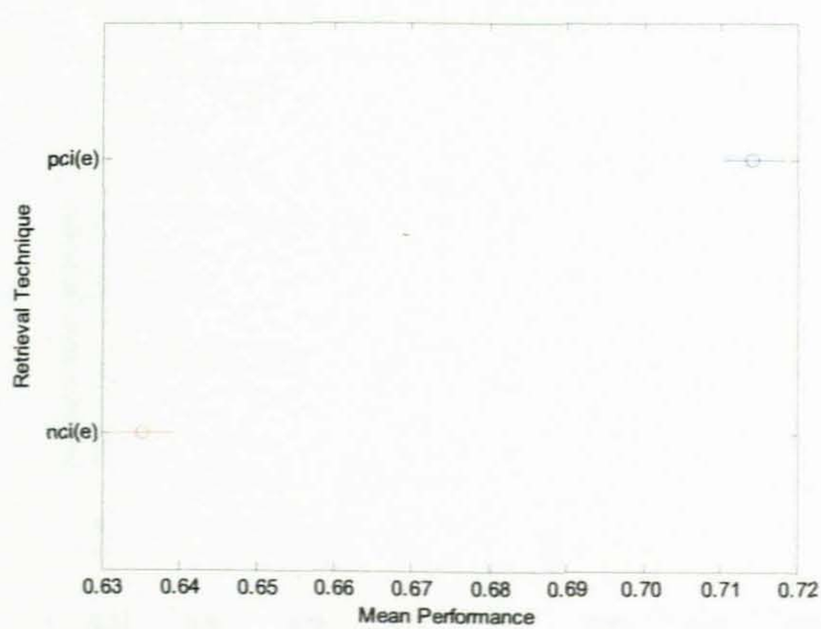

Figure 6.14: Effects of retrieval techniques on system performance, PCI(E) versus NCI(E) comparison

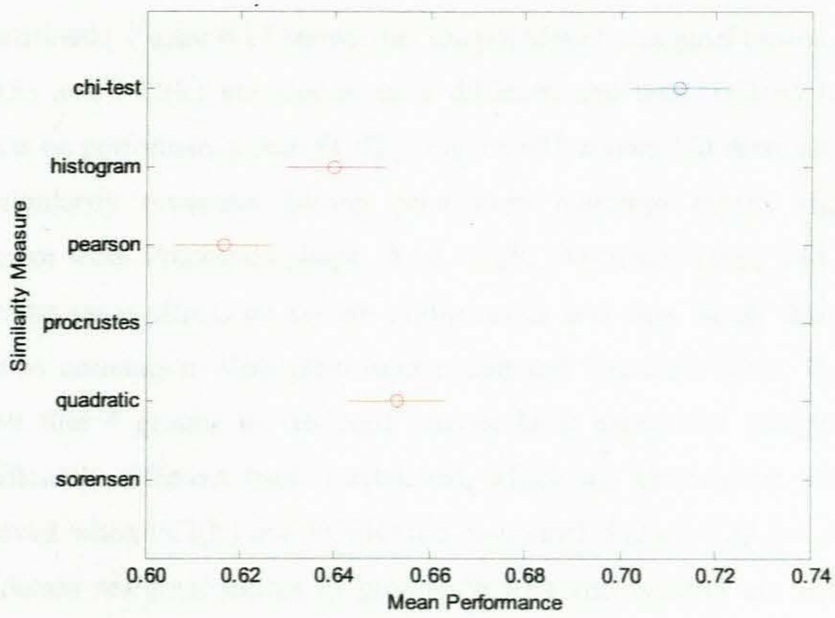

Figure 6.15: Effects of similarity measures on system performance, PCI(E) versus NCI(E) comparison

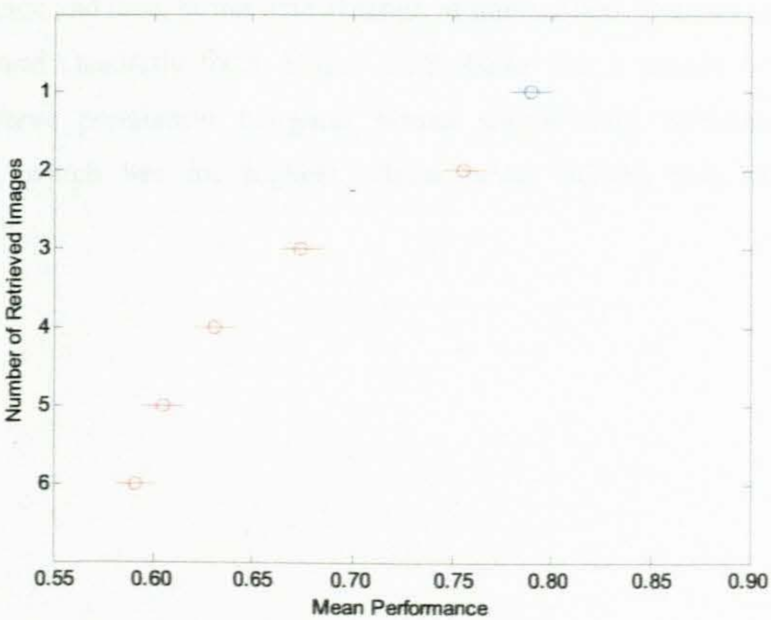

Figure 6.16: Effects of retrieved images on system performance, PCI(R versus NCI(R) comparison

Figures 6.17 to 6.22 show the interaction graphs for vertical comparisons. Figure 6.17 shows that the population marginal means of groups PCI(E) and PCI(R) are significantly different and thus, PCI(R) has higher effects on performance than PCI(E). Figure 6.18 shows that there are 4 groups of similarity measures having population marginal means significantly different from Procrustes shape. As a result, Procrustes shape and Sorensen have the same effects on system performance and thus, better than Chi-test, Pearson correlation, Histogram intersection and Quadratic form. Figure 6.19 shows that 4 groups of retrieved images have population marginal means significantly different from 1 retrieved, which has the highest effects as 2 retrieved when PCI(E) and PCI(R) are compared. Figure 6.20 shows that the population marginal means of groups NCI(E) and NCI(R) are significantly different and thus, NCI(R) has higher effects on performance than NCI(E). Figure 6.21 shows that there are 4 groups of similarity measures having population marginal means significantly different from Procrustes shape. As a result, Procrustes shape and Sorensen have the same effects on system performance and thus, better than Histogram intersection, Pearson correlation, Chi-test and Quadratic form. Figure 6.22 shows that 5 groups of retrieved images have population marginal means significantly different from 1 retrieved, which has the highest effects when NCI(E) and NCI(R) are compared.

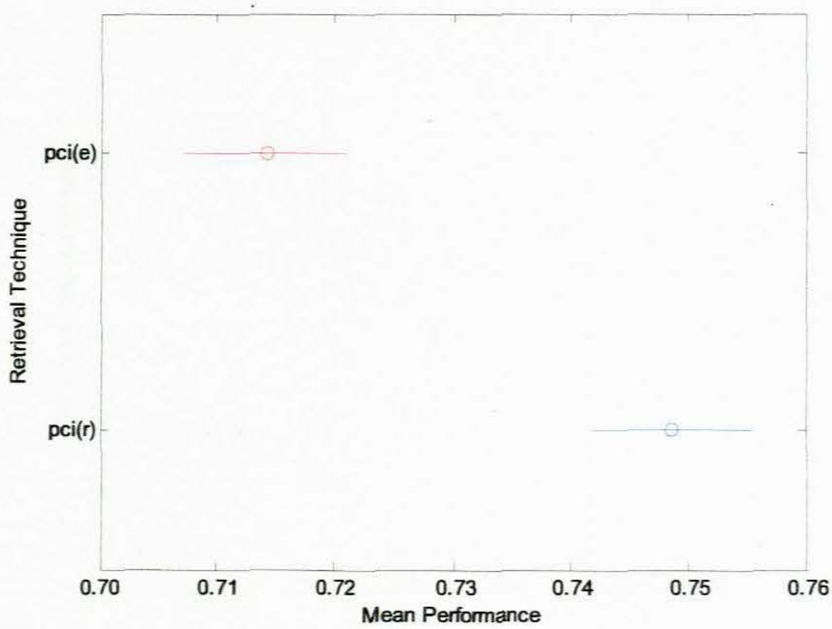

Figure 6.17: Effects of retrieval techniques on system performance, PCI(E) versus PCI(R) comparison

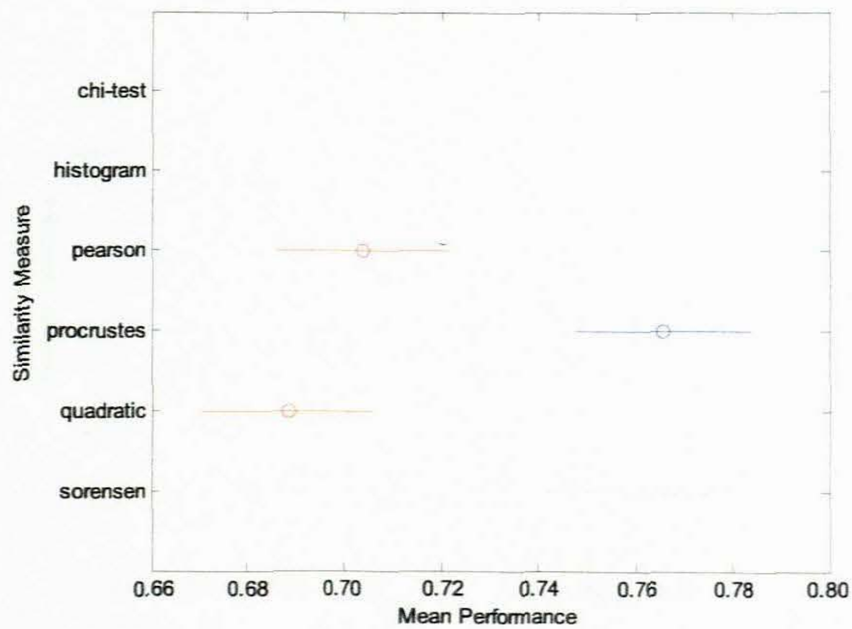

Figure 6.18: Effects of similarity measures on system performance, PCI(E) versus PCI(R) comparison

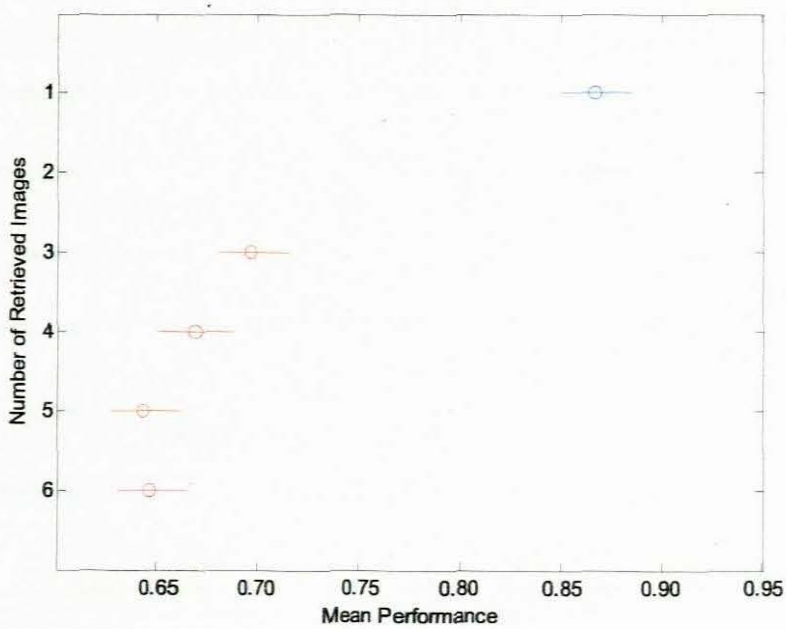

Figure 6.19: Effects of retrieved images on system performance, PCI(E) versus PCI(R) comparison

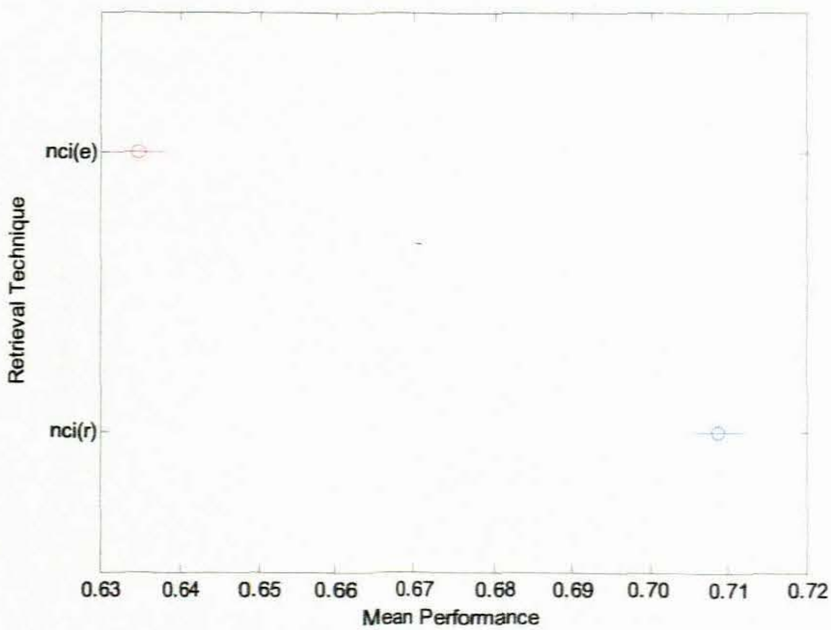

Figure 6.20: Effects of retrieval techniques on system performance, NCI(E) versus NCI(R) comparison

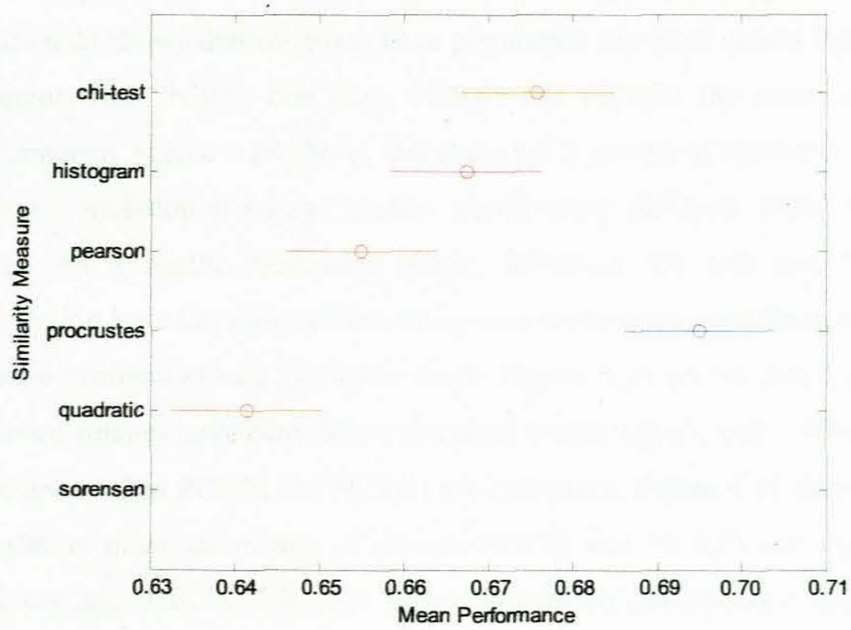

Figure 6.21: Effects of similarity measures on system performance, NCI(E) versus NCI(R) comparison

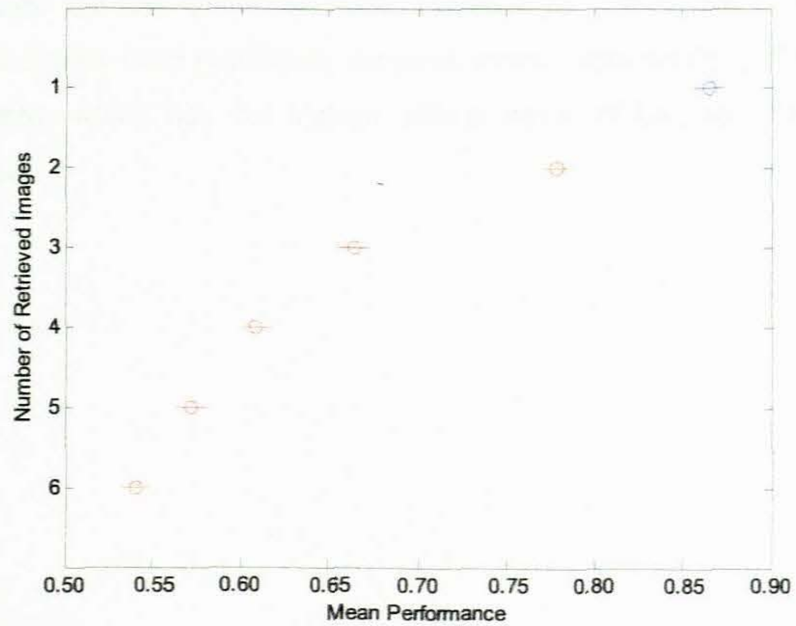

Figure 6.22: Effects of retrieved images on system performance, NCI(E) versus NCI(R) comparison

Figures 6.23 to 6.28 show the interaction graphs for cross comparisons. Figure 6.23 shows that no group have population marginal means significantly different from PCI(E) and thus, PCI(E) and NCI(R) the same effects on performance. Figure 6.24 shows that there are 2 groups of similarity measures having population marginal means significantly different from Procrustes shape. As a result, Procrustes shape, Sorensen, Chi-test and Histogram intersection have the same effects on system performance and thus, better than Pearson correlation and Quadratic form. Figure 6.25 shows that 5 groups of retrieved images have population marginal means significantly different from 1 retrieved when PCI(E) and NCI(R) are compared. Figure 6.26 shows that the population marginal means of groups PCI(R) and NCI(E) are significantly different and thus, NCI(R) has higher effects on performance than PCI(E). Figure 6.27 shows that there are 3 groups of similarity measures having population marginal means significantly different from Procrustes shape. As a result, Procrustes shape, Sorensen and Chi-test have the same effects on system performance and thus, better than Histogram intersection, Pearson correlation, Chi-test Quadratic form. Figure 6.28 shows that 5 groups of retrieved images have population marginal means significantly different from 1 retrieved, which has the highest effects when PCI(R) and NCI(E) are compared.

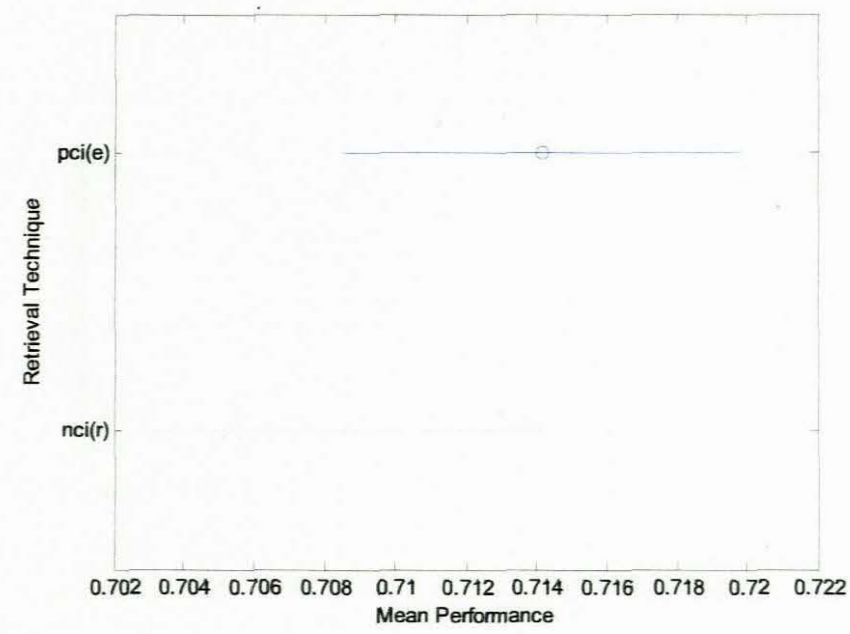

Figure 6.23: Effects of retrieval techniques on system performance, PCI(E) versus NCI(R) comparison

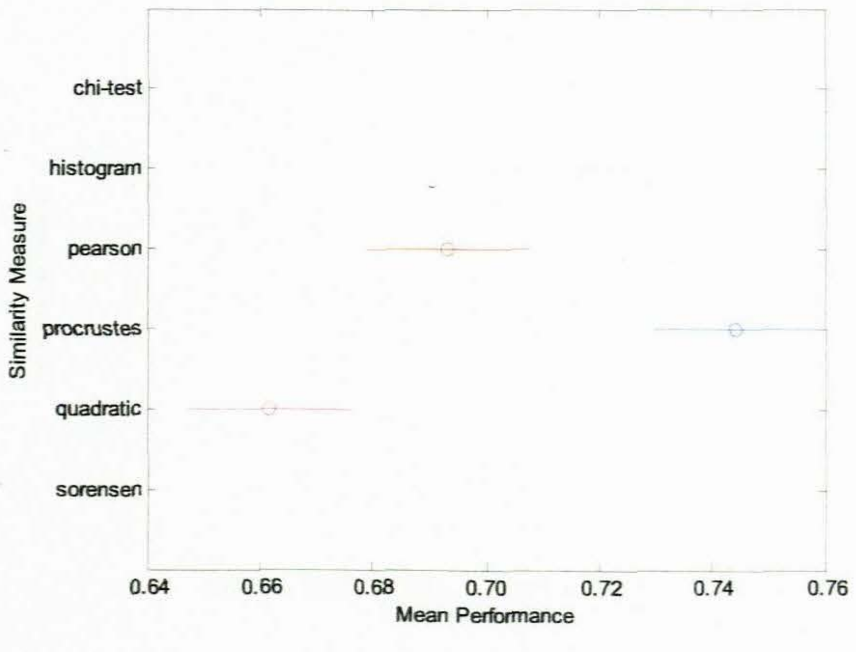

Figure 6.24: Effects of similarity measures on system performance, PCI(E) versus NCI(R) comparison

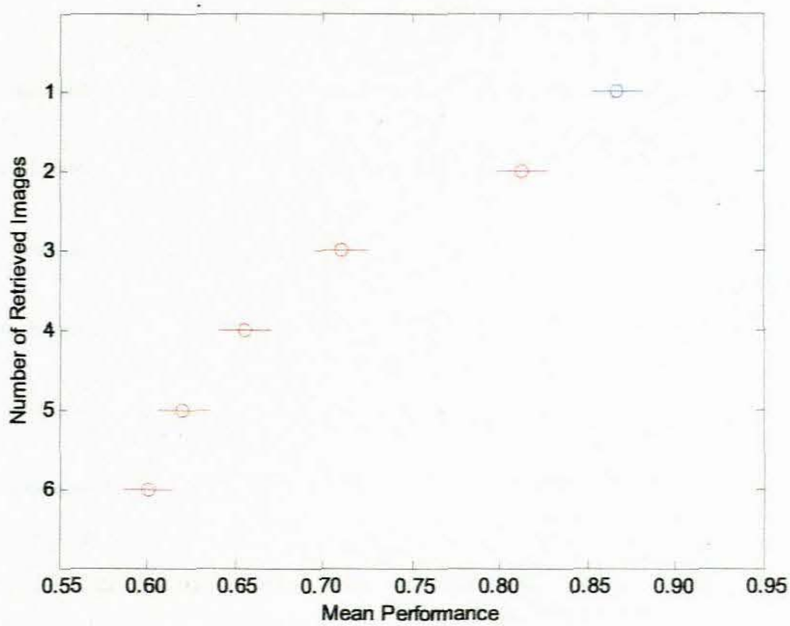

Figure 6.25: Effects of retrieved images on system performance, PCI(E) versus NCI(R) comparison

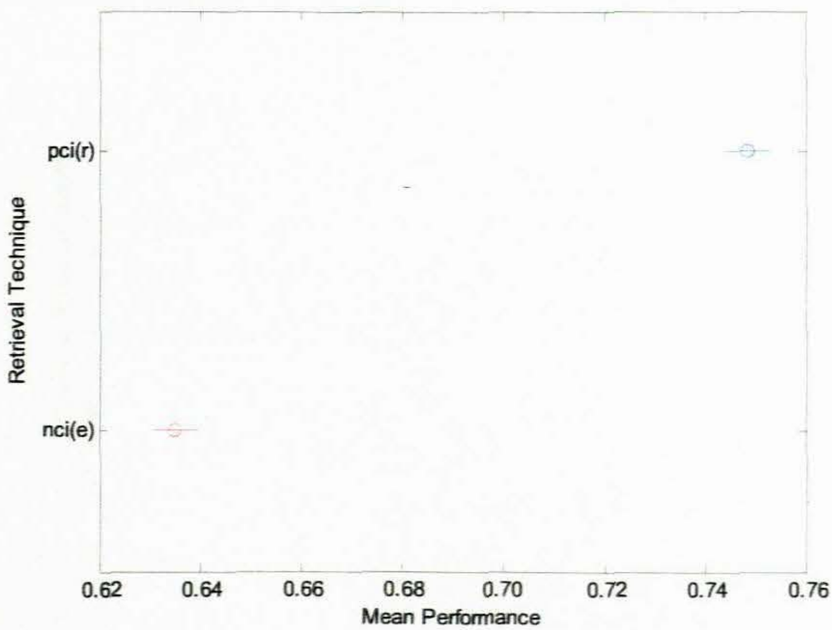

Figure 6.26: Effects of v techniques on system performance, PCI(R) versus NCI(E) comparison

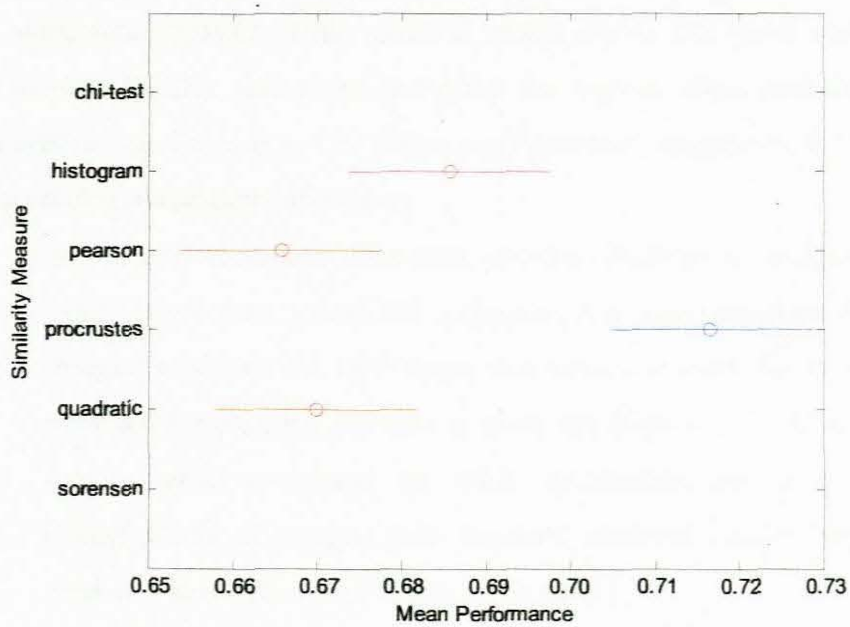

Figure 6.27: Effects of similarity measures on system performance, PCI(R) versus NCI(E) comparison

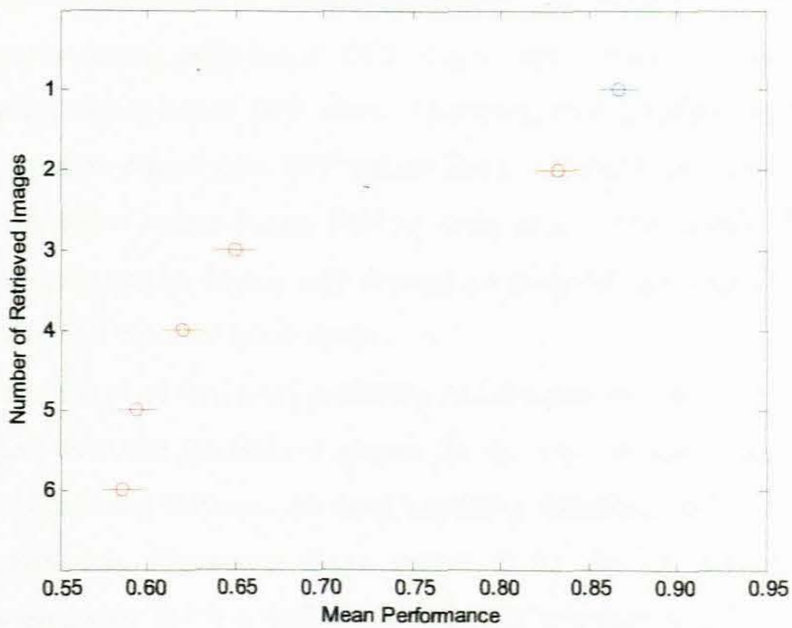

Figure 6.28: Effects of retrieved images on system performance, PCI(R) versus NCI(E) comparison

6.3.3. Summary of the Interpretation of Results

The systematic analysis of the retrieval results shows that in all comparisons that involve PCI(R), this technique gives the highest effect and thus, better than others, see Table 6.8. The following important results can, therefore, be deduced from these comparisons:

(a) A retrieval technique that uses pre-classification of images gives a better result than a retrieval technique that uses non-classification of images, no matter the DFP shape representation used. The best result is obtained for PCI(R), because it gives the highest effects on retrieval results when compared to other techniques. As a result, pre-classification of images will improve retrieval results, which give credence to the results of Wang, et al. (2001).

(b) Region-based DFP shape representation is better than edge-based DFP shape representation, whether pre-classification of images is used or not. This confirms the credibility of the choice of region-based DFP technique used by Tran & Ono (2003).

(c) Pre-classification of images improves performance of a retrieval system using edge-based DFP shape representation to the level of using region-based DFP alone. However, pre-classification technique used with edge-based DFP cannot improve system performance better than when region-based DFP is used alone. This result shows that retrieval results do not only depend on retrieval technique, but also on the shape representation used.

The effects of similarity measures and number of retrieved images can be deduced from the interaction graphs. In the case of similarity measures, there is a dilemma, because the best similarity measures did not come out clearly. Although, Procrustes shape seems to be distinct among all other similarity measures, but it is difficult to conclude whether there is a significant difference when compared to other similarity measures. Analysis of the results of horizontal comparisons showed that (a) Procrustes shape and Histogram intersection measures seem to be the best in one comparison, and (b) Procrustes shape, Sorensen and Chi-test measures seem to be the best in the other comparison. Similarly, analysis of the results of vertical comparisons showed that (a) Procrustes shape and Sorensen measures seem to be the best in both comparisons. Finally, analysis of the results of cross comparisons showed that (a) Procrustes shape, Sorensen, Chi-test and Histogram intersection measures seem to be the best in one comparison, and (b) Procrustes shape, Sorensen and Histogram intersection measures seem to be the best in the other comparison. There is a dilemma, therefore, in our choice of which similarities measures give the best overall performance and whether there is significant difference.

This dilemma was resolved by computing mean effects over all comparisons (Mean of Mean (MoM) effects) using 1-way ANOVA to determine the similarity measures and retrieved images that differ significantly. Figure 6.29 shows that the means of groups, Procrustes shape and Quadratic form are significantly different, but not significantly different from the means of Chi-test, Histogram intersection, Pearson correlation and Sorensen measures. This implies that Procrustes shape, Chi-test statistics, Histogram intersection, Pearson correlation and Sorensen measures have the same effects on retrieval and thus, suitable for brain MRI shape-based retrieval. Obviously, according to Figure 6.29, Quadratic form measure gives the poor result when used for brain MRI shape-based retrieval. Figure 6.30 shows that there are 4 groups having means significantly different from group 1. This implies that 1-NN and 2-NN have the same effects on system performance and thus, evolved for brain MRI retrieval.

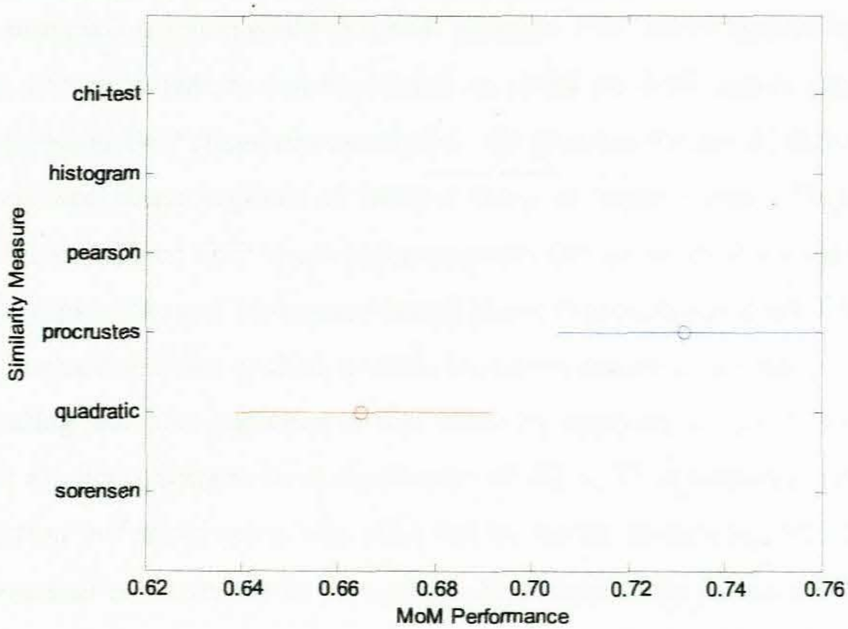

Figure 6.29: MoM effects of similarity measures on system performance

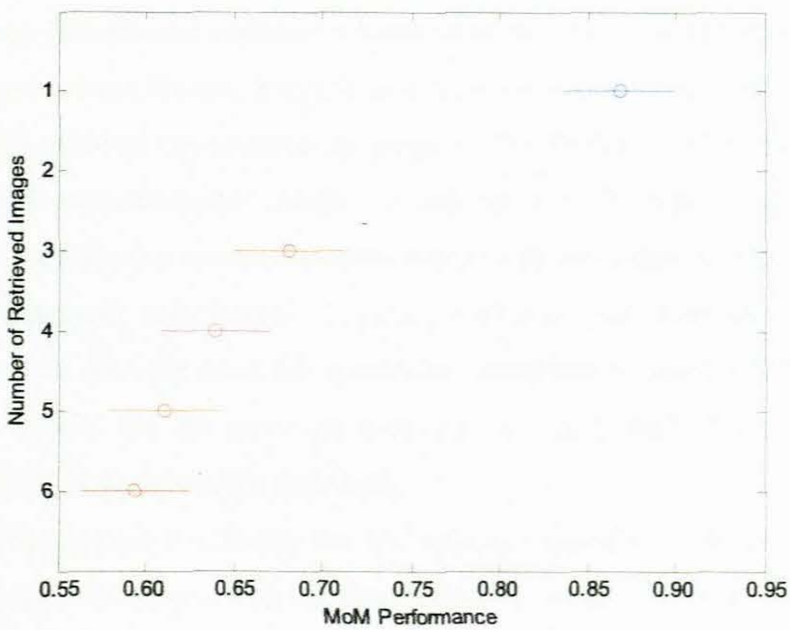

Figure 6.30: MoM effects of retrieved images on system performance

6.4. Providing Answers to the Research Questions

The proposed solution to the research question 1.2a, which has to do with the issue of image pattern representation is based on LBF active contour and region-based DFP shape representation. We propose the use of active contour to segment shape regions of interest from an input image. Then, density estimator, such as DFP shape representation should be used for region-based shape representation. Histogram based shape representations are invariant to basic transformations such as rotation as demonstrated in this study. Invariants to scaling was also achieved in this study by applying image re-sampling to scale all input images to a fixed size of 72 x 72 dimensions and further reduction in feature space was achieved by vector re-binning. The histogram representation according to previous work is inherently translation invariant. The complexity introduced by grid method was eliminated in this study by using active contour, which also makes the algorithms and techniques developed in this study suitable for MRI retrieval.

The proposed solution to the research question 1.2b, which has to do with image features and similarity measures to use for image retrieval is to use region-based shape feature. Shape based retrieval is proposed in this study for brain MRI retrieval applications as proposed for GUISET. The region-based DFP shape representation should be annotated with high level semantic concepts for effective retrieval as demonstrated in this study. Then, Procrustes shape, Histogram intersection, Chi-test, Sorensen and Pearson correlation measures can then be used for similarity computation, but Quadratic form measure should not be used for retrieval of brain MRI due to its poor performance as discovered in this study.

The proposed solution to the research question 1.2c, is that pre-classification of images will improve retrieval results. However, it is also discovered in this study that shape representation and similarity measure used will also affect retrieval results. As a result, pre-classification of images, image representations and similarity measures are three important factors that can affect retrieval results as was confirmed in this study.

6.5. Discussion of Results

This study reports on the effectiveness of LBF active contour, DFP shape representation and k-NN classifier on brain MRI retrieval. To demonstrate this effectiveness, we designed and implemented a series of image retrieval experiments to evaluate the performance of our BrainSearch system that uses different retrieval techniques. The performance evaluation was based on classification accuracy and intuitive-PRECALL to compute retrieval results when pre-classification and non-classification techniques were respectively used.

The results of the retrieval experiments showed that region-based DFP shape representation is better than edge-based DFP shape representation. K-NN classifier was used to improve the performance of the system when edge-based DFP shape representation was used. Although, there was an improvement, but the results obtained was not better than when region-based DFP shape representation alone was used. However, an improvement of the region-based DFP shape representation using k-NN gives the best overall results when compared to other techniques investigated. Six similarity measures, namely, Procrustes shape, Chi-test, Histogram intersection, Pearson correlation, Sorensen and Quadratic form were investigated to improve retrieval results. The mean results showed that there was no significant difference between Procrustes shape, Chi-test, Histogram intersection, Pearson correlation and Sorensen, but Quadratic form gave poor results and thus, not suitable for brain MRI retrieval. Compared to the work reported by Rubner, et al. (2001), which compared nine different families of similarity measures that include Chi-test statistics and Quadratic form, results showed that there was no measure with best overall performance when applied to color and texture features. However, the results of this study for shape based retrieval generally showed that the effects of similarity measures on system performance considerably differ for only Quadratic form measure. As a result, pre-classification of images is not the only factor that can improve retrieval results, shape representation and similarity measures are also important factors that should be considered along with pre-classification for improving retrieval results. The best retrieval result was obtained for region-based DFP (PCI(R)) shape representation.

In general, PCI(R) technique gives retrieval performance of 99% for Procrustes shape and Histogram intersection measures when k = 1 and k = 2 and 66% performance when k = 6. NCI(R) technique gives 99% performance for Procrustes shape and Histogram intersection measures when k = 1, 88% and 87% when k = 2 and 57% and 56% when k = 6. Thus, 1-NN or 2-NN classifier was evolved to improve system performance for brain MRI retrieval, see Tables 6.2 to 6.5. The results of the retrieval experiments do support the hypothesis that pre-classification of images will improve retrieval results in CBIR system (Wang, et al., 2001). Moreover, the review of the literature showed that only very few retrieval systems considered solving image retrieval problem using shape feature alone. Shape is often combined with other features such as texture and color. Additionally, no record of previous studies that use a combination of DFP shape representation and LBF active contour, which is a new method for region-based image segmentation. Where DFP shape representation is being used for experimentation to test for the effectiveness of this technique (Tran & Ono, 2003), grid-base method was used for image segmentation. The possibility of extracting edge information directly from region information using LBF active contour and connectivity-number edge detection algorithm for binary image has also been demonstrated in this study. Conventionally, edge-based active contour and edge detection algorithms are used for the same task of edge extraction. This study has demonstrated that region-based DFP shape representation when combined with active contour and k-NN classifier gives satisfactory results for brain MRI retrieval.

Chapter 7

Conclusions and Further Work

This chapter gives a conclusive summary of the study, highlights the achievements of the research study and makes suggestions for further work. The suggestions derive from the limitations of the study as enumerated in this chapter. We also state how the objectives of the study are perceptibly met.

7.1. Conclusive Summary

We used high-resolution cubic spline interpolation, LBF active contour, CNED edge detection algorithm, DFP shape representation and k-NN classifier to develop algorithms and techniques to improve performance of an image retrieval system in healthcare applications. Jensen polynomial was used to compute a unique shape index directly from DFP shape representation and relational database approach was used for image data management. System performance was respectively computed for NCI and PCI using intuitive-PRECALL and classification accuracy measurements. This way, the two techniques were brought to a common ground for effective comparison to be established.

As an initial step, a modular prototype system, called BrainSearch was implemented and used to show the utility of our algorithms and techniques on brain MRI characterization and their suitability for image retrieval. The system supports retrieval based on shape similarity, a single keyword image annotation and five image classes. The BrainSearch system was realized to make it easy to test retrieval performance and to expedite further algorithm investigation. This was made possible by the implementation of LBF active contour, DFP shape representation and k-NN classifier. The system was used to implement image retrieval experiments designed to determine effects of retrieval technique, similarity measurement and number of retrieved images on system performance as well as to provide solutions to the research questions. Edge-based and region-based density histograms of feature points were investigated for the shape representations. Retrieval results were exhaustively compared, by providing interaction graphs. Statistical evidences are provided, using analysis of variance to validate the research hypothesis and to provide solutions to research questions. Results of the retrieval experiments performed showed that region-based DFP shape representation when combined with k-NN and LBF active contour is promising for brain MRI retrieval in healthcare applications. Thus, our algorithms and techniques are suitable for inclusion into GUISET architecture.

The objectives of this study as stated in chapter 1 have been perceptibly met in the following ways:

(a) We developed algorithms and techniques based on LBF active contour, DFP shape representation and k-NN classifier to improve performance of an image retrieval system. A prototype implementation system was realized from our algorithms and techniques and the prototype was used to implement retrieval experiments on brain MRI. Results showed significant evidence of performance improvement.

(b) We tested and evaluated our algorithms and techniques using the BrainSearch system. We varied shape representations, retrieval techniques, similarity measures and number of retrieved images in a series of retrieval experiments. The results showed that Procrustes shape, Histogram intersection, Chi-test, Pearson correlation and Sorensen measures gave satisfactory results on brain MRI shape-based retrieval. However, Quadratic form gave poor results and thus, not suitable for brain MRI retrieval.

(c) We confirmed by experimentation that pre-classification of images will improve retrieval results of an image retrieval system. The retrieval system generated different results based on pre-classification and non-classification of images. These results were statistically analyzed using a robust multiple comparison analysis of variance and results showed that pre-classification of images improves performance of a retrieval system.

7.2. Limitations of the Study

There are four main limitations of this study, which are enunciated as follows:

(a) A single-phase level segmentation algorithm was investigated in this study. The effects of multiphase level algorithm on retrieval results are not investigated. Although segmentation techniques can improve retrieval efficiency, the advantages that multiphase segmentation would provide over single-phase segmentation in terms of retrieval results was not studied.

(b) The software realization is presently in the prototype form and full-pledged web service components implementation was not considered.

(c) We assumed that images are digitized and stored as BMP files, because of the generality of BMP files. We do not consider extending the study to the newly emerging DICOM file standard.

(d) We focused on image retrieval using classification technique on brain MRI and these results are not tested on different medical image modalities, other than brain MRI.

7.3. Achievements

This study aimed at developing algorithms and techniques to improve performance of an image retrieval system in healthcare applications. As a result, we formulated image retrieval as a classification problem in which similar images are associated with known class labels. The uniqueness of this study lies first in the choice of solution approach, which completely deviates from conventional retrieval approach of text-based retrieval when trying to bridge the semantic gap problem. Rather, we elected the k-NN approach to image retrieval in which a classifier is trained to learn to recognize keywords or class labels of images. Later, this knowledge is used to predict the correct class for a new example image presented as a query. Another uniqueness of this study is that it seeks to produce a hybrid of peculiar algorithms and techniques for shape-based brain MRI retrieval. This then provides the opportunity to add our voice to a recent discovery that shape can be very useful when used for medical image retrieval. The effectiveness of the foregoing choice of approach was demonstrated by a series of experiments and results showed that a hybrid combination of LBF active contour, DFP shape representation and k-NN classifier gives satisfactory results for brain MRI retrieval.

Finally, to support the hypothesis that pre-classification of images will improve retrieval results in image retrieval systems and in ultimately providing answers to the research questions raised the following conclusions of the study constitute significant contributions to knowledge. In the study, we have:

(a) demonstrated that a hybrid combination of LBF active contour, DFP shape representation points and k-NN classifier is promising for brain MRI retrieval,

(b) improved on the existing general image retrieval architecture by adding onto it a new shape-based image retrieval algorithm that works with different image processing methods and techniques,

(c) demonstrated the improve way in which various algorithmic techniques are combined to realize our algorithm for image retrieval,

(d) demonstrated the use of Jensen polynomials for computing shape index directly from DFP shape representation and some geometrical properties such as orientation, eccentricity and image profiles, and

(e) created mechanisms to evaluate a number of similarity measures and then determine effect of these measures on retrieval performance in a BrainSearch implementation prototype. The effectiveness of the whole approach in improving retrieval results was evaluated via the prototype system.

7.4. Suggested Further Work

The experiments reported in this study need to be repeated in future, but using other classifiers like support vector machine or ensemble construction in place of k-NN classifier. Shape representations like shape matrix and shape content need to be investigated and compared with DFP shape representation. A multi-level phase segmentation algorithm needs to be investigated. The results of this study should be tested in other application domains for generalization. The BrainSearch classes need to be implemented within the GUISET architectural framework as grid services and tested in real rural hospital situation. The following steps will help for the extension of this study:

(a) The retrieval experiments can be repeated by re-sampling images to low dimensions, such as 72 x 72, 60 x 60, 48 x 48, 32 x 32 and 24 x 24 and then apply our vector re-binning algorithm. Additionally, active contour segmentation algorithm (Vese & Chan, 2005) can be investigated and compared with LBF active contour used in this study.

(b) Large image database may be investigated and we believe that any of support vector machine, neural network and ensemble-based classifier may be choosing as a suitable classifier to use for large data.

(c) Local database should be replaced by WWW database and bitmap image format should be replaced by DICOM file format. The BrainSearch classes should be converted to grid services. A simple approach to make the system supports DICOM files is to write a separate module that captures DICOM images, convert the images to BMP and vice versa.

(d) Comparing region-based DFP with other shape-based representation such as generic Fourier descriptor, shape matrix and shape content will be a good project. It would be nice to investigate, which of these shape representations would give the best retrieval result.

(e) Another interesting research study is the integration of automatic image classification routine using medical ontology such as Systematized Nomenclature of Medicine (SNOMED) (Spackman, et al., 1997) and Medical Subject Headings (MeSH) (Chevy, 2000) to improve retrieval results.

Appendix A

Brain MRI Images for the Experimentation

The following 50 images were randomly selected from the 100 images downloaded from the Whole Brain Atlas. The interpretations of the symbols used are as follows. Images in a fold (IFold), image derivatives in fold (DFold), degenerative class (D), infectious class (I), normal class (N), stroke class (S), tumor class (T), color image type (C), grayscale image type (G) and iteration (Iter).

Table A1: Brain MRI Images used for the Retrieval Experiments

Code	Image Description	Type	Class	IFold	DFold	Iter
06020	Alzheimerls disease with a tour	C	D	F1	F2	40
13017	Alzheimerls disease	C	D	F1	F2	40
04010	AIDS dementia	C	I	F1	F2	40
01020	Multiple sclerosis with a tour	G	I	F1	F2	40
02020	Normal aging: structure and function	C	N	F1	F2	40
04020	Normal aging: structure and function	G	N	F1	F2	10
28010	Hypertensive encephalopathy	C	S	F1	F2	40
04012	Acute stroke: writes, but can't read, alexia without agraphia	G	S	F1	F2	40
11017	Glioma, TiTc-SPECT	C	T	F1	F2	40
17010	Metastatic bronchogenic carcinoma	C	T	F1	F2	40
10007	Alzheimer's disease with functional MRI	C	D	F2	F3	10
04020	Alzheimer's disease with a tour	G	D	F2	F3	40

05010	AIDS dementia	C	I	F2	F3	40
11020	Herpes encephalitis with a tour	C	I	F2	F3	40
03020	Normal aging: structure and function	C	N	F2	F3	40
07060	Normal aging: coronal plane	G	N	F2	F3	10
26010	Hypertensive encephalopathy	G	S	F2	F3	40
29010	Fatal stroke	G	S	F2	F3	40
01029	Glioma, TiTc-SPECT with a tour	C	T	F2	F3	40
04037	Glioma, TiTc-SPECT with a tour	G	T	F2	F3	40
08007	Alzheimer's disease with functional MRI	G	D	F3	F4	10
21008	Pick's disease	G	D	F3	F4	40
03010	AIDS dementia	G	I	F3	F4	40
06020	Lyme encephalopathy	G	I	F3	F4	40
05020	Normal aging: structure and function	C	N	F3	F4	40
08070	Normal anatomy in 3-D with MRI/PET	G	N	F3	F4	10
12025	Chronic subdural hematoma	C	S	F3	F4	40
11025	Chronic subdural hematoma	G	S	F3	F4	40
09012	Glioma, FDG-PET	C	T	F3	F4	40
19017	Sarcoma	G	T	F3	F4	40
02015	Alzheimer's disease	C	D	F4	F5	40
03015	Mild Alzheimer's disease, FDG-PET and MRI	C	D	F4	F5	40
09020	Herpes encephalitis with a tour	G	I	F4	F5	40

12012	Herpes encephalitis with a tour	G	I	F4	F5	40
06020	Normal aging: structure and function	C	N	F4	F5	40
09070	Normal anatomy in 3-D with MRI/PET	G	N	F4	F5	10
27010	Hypertensive encephalopathy	C	S	F4	F5	40
22010	Hypertensive encephalopathy	G	S	F4	F5	40
10012	Glioma, FDG-PET	C	T	F4	F5	40
18017	Meningioma	G	T	F4	F5	40
12017	Alzheimer's disease	C	D	F5	F1	40
01015	Mild Alzheimer's disease, FDG-PET and MRI	G	D	F5	F1	5
08020	Lyme encephalopathy	C	I	F5	F1	40
13013	Creutzfeld-Jakob disease	G	I	F5	F1	40
01020	Normal aging: structure and function	G	N	F5	F1	40
10051	Normal anatomy in 3-D with MRI/PET	G	N	F5	F1	10
09014	Subacute stroke: loss of sensation	C	S	F5	F1	40
18020	Vascular dementia	G	S	F5	F1	40
16010	Metastatic bronchogenic carcinoma	C	T	F5	F1	40
14016	Metastatic adenocarcinoma	G	T	F5	F1	40

Appendix B

Brain MRI Experimentation Data

This appendix contains the experimental results obtained for classification accuracy and intuitive-PRECALL based retrieval system performance evaluation. The classification accuracy and intuitive-PRECALL determination processes were used to objectively evaluate the retrieval performance of the BrainSearch system. Tables B1 to B5 are the results for classification accuracy determination when the technique of classification was applied to edge-based shape feature for matching similar images. Similarly, Tables B6 to B10 are the results for classification accuracy determination when the technique of classification was applied to region-based shape feature for matching similar images. Equation (3.13) was used to generate the results contained in these tables when 100 brain MRI were trained using k-NN classifier in a 5-Fold cross validation experiment. Each table contains the result when image data in a particular fold was used. Similarly, Tables B11 to B15 show the results for retrieval intuitive-PRECAL computed for the same 100 brain MRI in a 5-Fold cross validation experiment when the number of relevance images was returned by the system for each number of retrieved image in the set {1, 2,...6}. The technique of non classification was applied to generate the results in Tables B11 to B15. Finally, Tables B16 to B20 are the results of the non classification based retrieval for region-based feature extraction.

Table B1: Classification accuracy using images in fold 1

Retrieval Technique: PCI(Edge-Based DFP)			**Fold 1**			
Similarity Measure	**Number of Retrieval**					
	1	**2**	**3**	**4**	**5**	**6**
Chi-test	19	19	16	15	13	12
Pearson	16	16	16	13	13	15
Intersection	14	14	15	13	15	13
Procrustes	17	17	15	15	14	16
Quadratic	15	15	12	11	11	11
Sorensen	18	18	17	13	15	14

Table B2: Classification accuracy using images in fold 2

Retrieval Technique: PCI(Edge-Based DFP)			**Fold 2**			
Similarity Measure	**Number of Retrieval**					
	1	**2**	**3**	**4**	**5**	**6**
Chi-test	15	15	14	12	12	13
Pearson	12	12	12	11	10	11
Intersection	11	11	7	9	9	9
Procrustes	15	15	14	13	11	10
Quadratic	13	13	11	9	8	9
Sorensen	15	15	14	11	12	11

Table B3: Classification accuracy using images in fold 3

Retrieval Technique: PCI(Edge-Based DFP)			**Fold 3**			
Similarity Measure	**Number of Retrieval**					
	1	**2**	**3**	**4**	**5**	**6**
Chi-test	15	15	14	14	14	15
Pearson	15	15	13	14	13	12
Intersection	16	16	15	14	13	11
Procrustes	16	16	17	16	14	14
Quadratic	15	15	14	14	13	13
Sorensen	15	15	14	15	13	13

Table B4: Classification accuracy using images in fold 4

Retrieval Technique: PCI(Edge-Based DFP)				Fold 4		
Similarity Measure	**Number of Retrieval**					
	1	**2**	**3**	**4**	**5**	**6**
Chi-test	18	18	15	15	14	14
Pearson	17	17	17	15	14	14
Intersection	17	17	15	13	12	13
Procrustes	18	18	15	15	14	14
Quadratic	18	18	13	13	14	15
Sorensen	18	18	16	16	15	14

Table B5: Classification accuracy using images in fold 5

Retrieval Technique: PCI(Edge-Based DFP)					Fold 5	
Similarity Measure	**Number of Retrieval**					
	1	**2**	**3**	**4**	**5**	**6**
Chi-test	17	17	16	15	14	16
Pearson	14	14	13	13	13	13
Intersection	14	14	14	13	14	12
Procrustes	17	17	16	17	16	14
Quadratic	17	17	15	13	13	15
Sorensen	17	17	18	17	16	15

Table B6: Classification accuracy using images in fold 1

Retrieval Technique: PCI(Region-Based DFP)					Fold 1	
Similarity Measure	**Number of Retrieval**					
	1	**2**	**3**	**4**	**5**	**6**
Chi-test	17	17	9	10	10	11
Pearson	19	19	14	11	11	11
Intersection	17	17	14	12	11	11
Procrustes	19	19	13	10	12	12
Quadratic	17	17	12	10	9	9
Sorensen	19	19	10	10	10	9

Table B7: Classification accuracy using images in fold 2

Retrieval Technique: PCI(Region-Based DFP)				**Fold 2**		
Similarity Measure	**Number of Retrieval**					
	1	**2**	**3**	**4**	**5**	**6**
Chi-test	17	17	12	12	13	12
Pearson	20	20	12	12	12	11
Intersection	20	20	13	12	11	10
Procrustes	20	20	14	12	11	12
Quadratic	16	16	13	11	12	13
Sorensen	20	20	15	13	11	12

Table B8: Classification accuracy using images in fold 3

Retrieval Technique: PCI(Region-Based DFP)				**Fold 3**		
Similarity Measure	**Number of Retrieval**					
	1	**2**	**3**	**4**	**5**	**6**
Chi-test	17	17	15	14	12	14
Pearson	20	20	15	15	13	14
Intersection	18	18	15	14	13	14
Procrustes	20	20	14	13	12	14
Quadratic	18	18	17	16	14	15
Sorensen	20	20	14	13	14	13

Table B9: Classification accuracy using images in fold 4

Retrieval Technique: PCI(Region-Based DFP)				**Fold 4**		
Similarity Measure	**Number of Retrieval**					
	1	**2**	**3**	**4**	**5**	**6**
Chi-test	18	18	16	15	13	13
Pearson	20	20	13	14	13	13
Intersection	20	20	14	14	13	13
Procrustes	20	20	14	15	15	13
Quadratic	18	18	11	13	12	13
Sorensen	20	20	14	15	15	15

Table B10: Classification accuracy using images in fold 5

Retrieval Technique: PCI(Region-Based DFP)				**Fold 5**		
Similarity	**Number of Retrieval**					
Measure	**1**	**2**	**3**	**4**	**5**	**6**
Chi-test	18	18	14	14	14	15
Pearson	20	20	15	17	17	17
Intersection	19	19	13	16	16	15
Procrustes	20	20	14	15	15	15
Quadratic	19	19	12	13	11	11
Sorensen	20	20	12	14	15	15

Table B11: Retrieval intuitive-PRECALL using images in fold 1

Retrieval Technique: NCI(Edge-Based DFP)				**Fold 1**		
Similarity	**Number of Retrieval**					
Measure	**1**	**2**	**3**	**4**	**5**	**6**
Chi-test	19.0000	16.7500	13.4444	11.1875	10.6000	9.9167
Pearson	16.0000	14.0000	11.5556	10.4375	9.7200	9.5833
Intersection	14.0000	13.2500	12.1111	11.2500	10.8800	10.2222
Procrustes	17.0000	15.5000	13.2222	11.6875	11.6400	11.1111
Quadratic	15.0000	13.5000	11.8889	11.3125	10.1200	9.5000
Sorensen	18.0000	16.2500	13.7778	12.0625	11.0000	10.0000

Table B12: Retrieval intuitive-PRECALL using images in fold 2

Retrieval Technique: NCI(Edge-Based DFP)				**Fold 2**		
Similarity	**Number of Retrieval**					
Measure	**1**	**2**	**3**	**4**	**5**	**6**
Chi-test	15.0000	13.7500	12.0000	10.8125	10.3200	10.4444
Pearson	12.0000	11.2500	10.1111	9.3125	9.1200	8.4722
Intersection	11.0000	10.0000	8.6667	8.0000	7.9600	7.8333
Procrustes	15.0000	13.5000	11.6667	10.7500	9.9600	9.6944
Quadratic	13.0000	12.5000	11.5556	10.3750	9.4800	9.3333
Sorensen	15.0000	14.2500	12.7778	10.8750	9.5200	9.5000

Table B13: Retrieval intuitive-PRECALL using images in fold 3

Retrieval Technique: NCI(Edge-Based DFP)				**Fold** 3		
Similarity Measure	**Number of Retrieval**					
	1	**2**	**3**	**4**	**5**	**6**
Chi-test	15.0000	14.5000	13.8889	13.5000	12.8400	12.1111
Pearson	15.0000	13.5000	11.7778	11.2500	10.8400	10.1389
Intersection	16.0000	13.2500	10.5556	10.6875	10.6800	10.2500
Procrustes	16.0000	14.7500	13.1111	12.3750	12.3200	11.5278
Quadratic	15.0000	14.7500	14.1111	13.0625	12.2400	12.0278
Sorensen	15.0000	14.2500	13.1111	12.3125	12.0400	11.0833

Table B14: Retrieval intuitive-PRECALL using images in fold 4

Retrieval Technique: NCI(Edge-Based DFP)					**Fold 4**	
Similarity Measure	**Number of Retrieval**					
	1	**2**	**3**	**4**	**5**	**6**
Chi-test	18.0000	16.5000	14.6667	13.8750	13.4400	13.0000
Pearson	17.0000	15.7500	14.0000	12.7500	11.8800	11.3056
Intersection	17.0000	15.2500	13.1111	12.1250	11.4000	10.9722
Procrustes	18.0000	16.2500	13.8889	12.5625	12.1600	11.6944
Quadratic	18.0000	15.7500	13.3333	12.7500	12.0000	11.9444
Sorensen	18.0000	16.5000	14.8889	14.3125	13.0800	12.2500

Table B15: Retrieval intuitive-PRECALL using images in fold 5

Retrieval Technique: NCI(Edge-Based DFP)				**Fold 5**		
Similarity Measure	**Number of Retrieval**					
	1	**2**	**3**	**4**	**5**	**6**
Chi-test	17.0000	14.7500	12.4444	12.1875	11.7200	11.5556
Pearson	14.0000	12.5000	10.8889	10.6250	10.4400	10.1944
Intersection	14.0000	12.7500	11.4444	11.1875	10.6400	10.1389
Procrustes	17.0000	15.5000	13.4444	12.2500	11.8800	11.3056
Quadratic	17.0000	15.0000	12.6667	11.8750	11.3200	10.5833
Sorensen	17.0000	15.2500	13.3333	12.8125	12.2400	12.0833

Table B16: Retrieval intuitive-PRECALL using images in fold 1

Retrieval Technique: NCI(Region-Based DFP)				**Fold 1**		
Similarity Measure	**Number of Retrieval**					
	1	**2**	**3**	**4**	**5**	**6**
Chi-test	17.0000	14.5000	11.5556	10.5625	10.2000	10.0278
Pearson	19.0000	16.5000	13.5556	12.4375	11.6400	11.0278
Intersection	17.0000	15.2500	13.1111	12.1875	11.6000	10.8889
Procrustes	19.0000	16.0000	12.5556	11.6250	11.4400	10.9722
Quadratic	17.0000	14.7500	12.2222	11.3125	10.0800	9.2778
Sorensen	19.0000	15.5000	11.4444	10.3125	10.1600	9.6389

Table B17: Retrieval intuitive-PRECALL using images in fold 2

Retrieval Technique: NCI(Region-Based DFP)				**Fold 2**		
Similarity Measure	**Number of Retrieval**					
	1	**2**	**3**	**4**	**5**	**6**
Chi-test	17.0000	15.5000	13.5556	12.3750	11.3200	10.4722
Pearson	20.0000	17.7500	14.7778	12.9375	11.6000	10.8889
Intersection	20.0000	17.7500	14.7778	13.0000	11.8000	10.7778
Procrustes	20.0000	17.2500	13.7778	11.9375	10.7200	10.5556
Quadratic	16.0000	14.5000	12.6667	11.6875	10.6000	9.9444
Sorensen	20.0000	17.0000	13.5556	12.3125	11.0400	10.1667

Table B18: Retrieval intuitive-PRECALL using images in fold 3

Retrieval Technique: NCI(Region-Based DFP)				**Fold 3**		
Similarity Measure	**Number of Retrieval**					
	1	**2**	**3**	**4**	**5**	**6**
Chi-test	17.0000	16.0000	14.5556	13.3125	12.0800	11.3056
Pearson	20.0000	18.2500	15.5556	13.3750	12.2400	11.0556
Intersection	18.0000	16.5000	14.6667	13.5625	12.1200	11.5278
Procrustes	20.0000	18.0000	15.4444	14.0625	12.8400	11.1111
Quadratic	18.0000	16.0000	13.6667	12.6875	11.6000	10.8611
Sorensen	20.0000	18.2500	15.5556	13.3750	12.2000	10.9444

Table B19: Retrieval intuitive-PRECALL using images in fold 4

Retrieval Technique: NCI(Region-Based DFP)				**Fold 4**		
Similarity Measure	**Number of Retrieval**					
	1	**2**	**3**	**4**	**5**	**6**
Chi-test	18.0000	16.7500	14.6667	12.7500	11.8400	11.0833
Pearson	20.0000	17.7500	14.8889	13.3750	12.3200	11.5278
Intersection	20.0000	18.0000	15.4444	14.0000	12.8000	11.8611
Procrustes	20.0000	17.7500	14.6667	12.8750	12.3600	11.6389
Quadratic	18.0000	15.5000	12.3333	10.8750	10.3600	9.7500
Sorensen	20.0000	18.0000	15.3330	13.7500	12.9200	12.4167

Table B20: Retrieval intuitive-PRECALL using images in fold 5

Retrieval Technique: NCI(Region-Based DFP)				**Fold 5**		
Similarity Measure	**Number of Retrieval**					
	1	**2**	**3**	**4**	**5**	**6**
Chi-test	18.0000	16.0000	13.6667	12.7500	11.8800	11.3056
Pearson	20.0000	17.7500	14.8889	13.7500	13.7600	12.6944
Intersection	19.0000	17.0000	14.6667	13.9375	13.6000	12.8056
Procrustes	20.0000	17.5000	14.4444	13.0625	12.1600	11.7222
Quadratic	19.0000	16.5000	13.2222	11.5625	11.0400	10.0833
Sorensen	20.0000	17.2500	14.0000	12.8125	12.1600	11.6670

Appendix C

MATLAB Codes for Image Retrieval Experiments

This is the MATLAB source codes for the ANOVA that was used to analyze the results of the image retrieval experiments. This code generates result for the best comparison and similar code was used to generate other results. The last statement plots the interactive graph.

Listing 1: PCI(R) versus NCI(R) Experiment

```
response=[0.87 0.87 0.66 0.65 0.62 0.65 0.99 0.99 0.69 0.69 0.66 0.66 0.94 0.94 0.69
0.68 0.64 0.63 0.99 0.99 0.69 0.65 0.65 0.66 0.88 0.88 0.65 0.63 0.58 0.61 0.99 0.99
0.65 0.65 0.65 0.64 0.87 0.79 0.68 0.62 0.57 0.54 0.99 0.88 0.74 0.66 0.62 0.57 0.94
0.85 0.73 0.67 0.62 0.58 0.99 0.87 0.71 0.64 0.60 0.56 0.88 0.77 0.64 0.58 0.54 0.50
0.99 0.86 0.70 0.63 0.58 0.55];

g1={'pci(r)' 'pci(r)' 'pci(r)' 'pci(r)' 'pci(r)' 'pci(r)' 'pci(r)' 'pci(r)' 'pci(r)' 'pci(r)' 'pci(r)'
'pci(r)' 'pci(r)' 'pci(r)' 'pci(r)' 'pci(r)' 'pci(r)' 'pci(r)' 'pci(r)' 'pci(r)' 'pci(r)' 'pci(r)' 'pci(r)'
'pci(r)' 'pci(r)' 'pci(r)' 'pci(r)' 'pci(r)' 'pci(r)' 'pci(r)' 'pci(r)' 'pci(r)' 'pci(r)' 'pci(r)' 'pci(r)'
'pci(r)' 'nci(r)' 'nci(r)' 'nci(r)' 'nci(r)' 'nci(r)' 'nci(r)' 'nci(r)' 'nci(r)' 'nci(r)' 'nci(r)' 'nci(r)'
'nci(r)' 'nci(r)' 'nci(r)' 'nci(r)' 'nci(r)' 'nci(r)' 'nci(r)' 'nci(r)' 'nci(r)' 'nci(r)' 'nci(r)' 'nci(r)'
'nci(r)' 'nci(r)' 'nci(r)' 'nci(r)' 'nci(r)' 'nci(r)' 'nci(r)' 'nci(r)' 'nci(r)' 'nci(r)' 'nci(r)' 'nci(r)'
'nci(r)'};

g2={'chi-test' 'chi-test' 'chi-test' 'chi-test' 'chi-test' 'chi-test' 'intersection' 'intersection'
'intersection' 'intersection' 'intersection' 'intersection' 'pearson' 'pearson' 'pearson'
'pearson' 'pearson' 'pearson' 'procrustes' 'procrustes' 'procrustes' 'procrustes'
'procrustes' 'procrustes' 'quadratic' 'quadratic' 'quadratic' 'quadratic' 'quadratic'
'quadratic' 'sorensen' 'sorensen' 'sorensen' 'sorensen' 'sorensen' 'sorensen' 'chi-test' 'chi-
test' 'chi-test' 'chi-test' 'chi-test' 'chi-test' 'intersection' 'intersection' 'intersection'
'intersection' 'intersection' 'intersection' 'pearson' 'pearson' 'pearson' 'pearson' 'pearson'
'pearson' 'procrustes' 'procrustes' 'procrustes' 'procrustes' 'procrustes' 'procrustes'
'quadratic' 'quadratic' 'quadratic' 'quadratic' 'quadratic' 'quadratic' 'sorensen' 'sorensen'
'sorensen' 'sorensen' 'sorensen' 'sorensen'};

g3={'1' '2' '3' '4' '5' '6' '1' '2' '3' '4' '5' '6' '1' '2' '3' '4' '5' '6' '1' '2' '3' '4' '5' '6' '1' '2' '3' '4' '5'
'6' '1' '2' '3' '4' '5' '6' '1' '2' '3' '4' '5' '6' '1' '2' '3' '4' '5' '6' '1' '2' '3' '4' '5' '6' '1' '2' '3' '4' '5' '6'
'1' '2' '3' '4' '5' '6' '1' '2' '3' '4' '5' '6'};

[p,table,stats]=anovan(response,{g1 g2 g3},'model', [1 1 0; 0 1 1; 1 0 1; 1 1 1],
'varnames', {'Retrieval ' 'Similarity' ' Neighbor'},'alpha',0.01)

[p,table,stats]=anovan(response,{g1 g2 g3},'varnames',{'Retrieval' 'Similarity'
'Neighbor'},'alpha',0.01,'model',2)

[c,m]=multcompare(stats, 'dimension',1)
```

Listing 2: 1-Way ANOVA Analysis of Mean Effects

The following MATLAB code produces notched box plot for comparing six similarity measures for retrieval performance using mean effects of all comparisons. This box plot shows that the measures have significant effects on retrieval performance with respect to locations and possible variations.

```
mEffects=[0.74 0.68 0.71 0.70 0.72 0.70 0.73 0.67 0.64 0.76 0.72 0.69 0.70
0.66 0.62 0.74 0.69 0.67 0.77 0.70 0.71 0.75 0.74 0.72 0.69 0.64 0.65 0.68
0.66 0.67 0.76 0.70 0.72 0.74 0.74 0.72];

Similarity={'chi-test', 'chi-test', 'chi-test', 'chi-test', 'chi-test', 'chi-test',
'histogram', 'histogram', 'histogram', 'histogram', 'histogram', 'histogram',
'pearson', 'pearson', 'pearson', 'pearson', 'pearson', 'pearson', 'procrustes',
'procrustes', 'procrustes', 'procrustes', 'procrustes', 'procrustes', 'quadratic',
'quadratic', 'quadratic', 'quadratic', 'quadratic', 'quadratic', 'sorensen' 'sorensen'
'sorensen' 'sorensen' 'sorensen' 'sorensen'};

[p,table,stats]=anova1(mEffects, Similarity)
```

Bibliography

Adigun, M.O. (2006). Zululand University: on our way to wireless grid computing. *Presentation at University of Syracuse, USA.*

Aisen, A.M., Broderick, L. S., Winer-Muram, H., Brodley, C. E., Kak, A. C., Pavlopoulou, C., Dy, J., Shyu, C.R. & Marchiori, A. (2003). Automated storage and retrieval of thin-section CT images to assist diagnosis: system description and preliminary assessment. *Radiology.* 228, 265-270.

Ang, Y.H., Li, Z. & Ong, S.H. (1995). Image retrieval based on multidimensional feature properties. In *Proceedings of IS&ISPIE Conference on Storage and Retrieval for Image and Video Database III.* 2420, pp. 47-57.

Antani, S., Long, L.R. & Thomas, G.R. (2002). A biomedical information system for combined content-based retrieval of spine x-ray images and associated text information. In *Proceedings of the Indian Conference on Computer Vision, Graphics and Image Processing.* 242-247.

Antania, S., Leeb, D.J., Longa, L.R. & Thoma, G.R. (2004). Evaluation of shape similarity measurement methods for spine x-ray images. *Journal Visual Communication and Image Research.* 15, 285–302.

Arkin, E.M., Chew, L.P., Huttenlocher, D.P., Kedem, K. & Mitchell, J.S.B. (1991). An efficient computable metric for comparing polygon shapes. *IEEE Trans. On Pattern Analysis and Machine Intelligence.* 13(3), 209-216.

Belongie, S., Malik, J. & Puzicha, J. (2002). Shape matching and object recognition using shape contexts. *IEEE Transactions on Pattern Analysis and Machine Intelligence.* 24(4), 509-522.

Bloackecl, H. & Struyf, J. (2002). Efficient algorithms for decision tree cross-validation. *Journal of Machine Learning Research.* 3, 621-650.

Bober, M. (2001). MPEG-7 visual shape descriptors. *IEEE Transactions on Circuits and Systems for Video Technology.* 11(6), 716-719.

Boissel, J.P., Cucherat, M., Amsallem, E., Nony, P., Fardeheb, M., Manzi, W. & Haugh, M.C. (2003). Getting evidence to prescribers and patients or how to make EBM a reality. *Studies in Health Technology and Informatics (95). 554-559.*

Bui, A.A.T., Taira, R.K., Dionision, J.D.N., Aberle, D.R., El-Sadam, S. & Kangarloo, H. (2002). Evidence-based radiology. *Academic Radiology.* 9(6), 662-669.

Bustos, B., Keim, D.A., Saupe, D., Schreck, T. & Vranic, D.V. (2005). Feature-based similarity search in 3D object databases. *ACM Computing Surveys.* 37(4), 345-387.

Cai, W. Feng, D. & Fulton, R. (2001). Web-based digital medical images. *IEEE Computer Graphics and Applications.* 21, 44-47.

Canny, J. (1986). A computational approach to edge detection. *IEEE Transactions on Pattern Analysis and Machine Intelligence.* 8, 679-714.

Carson, C., Belongie, S., Greenspan, H. & Malik, J. (2002). Blobworld: image segmentation using expectation-maximization and its application to image querying. *IEEE Transactions on Pattern Analysis and Machine Intelligence.* 24(8), 1026-1038.

Chan, T. & Vese, L. (2001). Active contours without edges. *IEEE Transactions on image Processing.* 10(2), 266-277.

Chaudhuri, D. & Samal, A. (2007). A simple method for fitting of bounding rectangle to closed regions. *Pattern Recognition.* 40, 1981-1989.

Chevy, C. (2000). Historical notes: medical subject headings. *Bull Medical Library Association.* 88(3), 265-266.

Cihlar, J., Xiao, Q., Chen, J., Beaubien, J., Fung, K. & Latifovic, R. (1998). Classification by progressive generalization: a new automated methodology for remote sensing multispectral data. *International Journal of Remote Sensing.* 19, 2685–2704.

Congalton, R.G. (1991). A review of assessing the accuracy of classification of remotely sensed data. *Remote Sensing of Environment.* 37, 35–46.

Cooper, W.S. (1989). Expected search length: A single measure of retrieval effectiveness based on the week ordering action of retrieval systems. *AM. Document.* 19, 30-41.

Csordas, G., Varga, R.S. & Vincze, I. (1990). Jensen polynomials with applications to the Riemann ς - Function. *Journal. Math Anal. Appl.* 153, 112-135.

Dean, K. & Solomonides, T. (2004). HealthGrid - a summary. *Cisco White Paper.* http://whitepaper.healthgrid.org/30260HealthgridWPv5.pdf.

Dimov, D. (2003). Fast, shape based image retrieval. *International Conference on Computer Systems and Technology (CompSysTech 2003).* 296-302.

Evans, L. (1998). Partial differential equations. *American Mathematical Society, Providence.*

Fan, J., Aref, W.G. & Hacid, M.S. (2001). An improved automatic isotropic colour edge detection technique. *Pattern Recognition Letters.* 22, 1419-1429.

Fang, T.P. & Piegl, L.A. (1993). Delaunay triangulation using a uniform grid. *IEEE Computer Graphics and Applications.* 13(3), 36-47.

Flicker, M., Sawhney, H., Nibleck, W., Ashley, J., Huang, Q., Dom, B., Gorkani, M., Hafner, J., Lee, D., Petkovic, D., Steele, D. & Yanker, P. (1995). Query by image and video content: The QBIC system. *IEEE Computer.* 28(9), 23-32.

Frankewitsch, T. & Prokosch, U. (2001). Navigation in medical internet image databases. *Medical Informatics.* 26 (1), 1-15.

Funt, B.V. & Finlayson, G.D. (1995). Color constant indexing. *PAMI.* 17(5), 522-529.

Gomes, J. & Faugeras, O. (2000). Reconciling distance functions and level sets. *Journal Visual Communication and Image.* 11, 209-223.

Goutte, C. (1997). Note on free lunches and cross-validation. *Journal of Neural Computation.* 9, 1211-1215.

Greenes, R. A. & Brinkley, J. F. (2000). Imaging systems. In: *Medical Informatics: Computer Applications in Healthcare, 2nd Edition, New York: Springer.* 485-538.

Guild, M.O., Keysers, D., Deselaers, T., Leisten, M., Schubert, H., Ney, H. & Lehmann, T.M. (2004). Comparison of global features for categorization of medical images. *Proceedings of SPIE.* 5371, 211-222.

Hafner, J., Sawhney, H.S., Equitz, W., Flicker, M. & Niblack, W. (1995). Efficient color histogram indexing for quadratic form distance functions. *IEEE Transactions on Pattern Analysis and Machine Intelligence.* 17(7), 729-736.

Han, J. & Kamber, M. (2006). Data mining concepts and techniques. 2nd Ed., *Morgan and Kaufmann.*

Hochberg, Y. & Tamhane, A.C. (1987). Multiple Comparison Procedures. *New York: Wiley.*

Hornak, J.P. (2007). The basic of MRI. *Textbook Revolution.*

Horsch, A. & Thurmayr, R (2003), How to identify and assess tasks and challenges of medical Image processing. *Stud Health Technol Inform. 95, 281-285.*

Hou, H.S. & Andrew, H.C. (1978), Cubic splines for image interpolation and digital filtering. *IEEE Trans. Acoust, Speech, Signal Processing,* ASSP-26, 508-517.

Hripcsak, G. & Rothschild, A.S. (2005). Agreement, the F-measure, and reliability in information retrieval. *Journal of America Medical Informatics Association.* 12(3), 296-298.

Hu, M. K. (1962). Visual pattern recognition by moment invariants. *IRE Trans. Information Theory. 8, 178-187.*

Iqbal, Q. & Aggarwal, J. K. (2002). Retrieval by classification of images containing large manmade objects using perceptual grouping. *Pattern Recognition.* 35(7), 1463-1479.

Jacobsen, C., Zscherpel, U. & Perner, P.A. (1999). Comparison between neural networks and decision trees. *Pattern Recognition.* 144-158.

Jagadish, H. V. (1991). A retrieval technique for similar shapes. *Proceedings of International Conference on Management of Data, SIGMOID'91.* 208-217.

Johnson, K.A. & Becker, J.A. (1999). The whole brain Atlas, http://www. med.harvard.edu/AANLIB/home.html.

Kass, M., Witkin, A. & Terzopoulos, D. (1987). Snakes: active contour models. *International Journal of Computer*. 1, 321-331.

Katehakis, D.G & Tsiknakis, M. (2006). Electronic health record. *Wiley Encyclopedia of Biomedical Engineering.*

Kelton, W.D. (2000). Experimental design for simulation. *Proceedings of the 2000 Winter Simulation Conference*. 32-38.

Kendall, D.G. (1984). Shape manifolds, procrustean metrics and complex projective spaces. *Bull London Math. Society*. 16, 81-121.

Keys, R.G. (1981). Cubic convolution interpolation for digital image processing. *IEEE Trans. Acoustics, Speech, and Signal Processing,* ASSP-29(6), 1153-1160.

Keysers, D., Dahmen, J., Ney, H., Wein, B. B. & Lehmann, T. M. (2003). A statistical framework for model-based image retrieval in medical applications. *Journal of Electronic Imaging*. 12(1), 59-68.

Kherfi, M.L., Ziou, D. & Bernardi, A. (2004). Image retrieval from the World Wide Web: issues, techniques and systems. *ACM Computing Surveys*. 36(1), 35-67.

Khludov, S. Vorwerk, L. & Meinel, A. (2000). Internet-orientated medical information system for DICOM-data transfer, visualization and revision. *13th IEEE Symposium on Computer-Based Medical Systems (CBMS'2000)*, 293 - 296.

Kim, W.K. & Sung, Y. (2000). A region-based shape descriptor using Zernike moments. *Signal Process and Image Communication.* 16, 95-102.

Kulikowski, C., Ammenwerth, E., Bohne, A., Ganser, K., Haux, R., Knaup, P., Maier, C. Michel, A., Singer, R. & Wol, A. C. (2002). Medical imaging informatics and medical informatics: opportunities and constraints. *Methods of Information in Medicine.* 41, 183-189.

Kuo, W.J., Chang, R.F., Lee, C.C., Moon, W.K. & Chen, D.R. (2002). Retrieval technique for the diagnosis of solid breast tumors on sonogram. *Ultrasound in Medicine and Biology.* 28(7), 903-909.

Lee, D.J., Antani, S. & Long, L.R. (2003). Similarity measurement using polygon curve representation and Fourier descriptors for shape-based vertebra image retrieval. *Image Processing.* SPIE 5032, 1283-1291.

Lehmann, T.M., Wein, B., Dahman, J., Bredno, J., Vogelsang, F. & Kohnen, M. (2000). Content-based image retrieval in medical applications: a novel multi-step approach. *Proceedings of SPIE.* 3972, 312-320.

Lehmann, T.M., Guld, M.O., Thies, C., Fischer, B., Spitzer, K., Keysers, D., Ney, H., Kohnen, M., Schubert, H. & Wein, B.B. (2003). The IRMA project: a state of the art report on content-based image retrieval in medical applications. *Proceedings of Korea-Germany Joint Workshop on Advanced Medical Image Processing.* 161-171.

Lehmann, T.M., Guld, M.O., Thies, C., Fischer, B., Spitzer, K., Keysers, D., Ney, H., Kohnen, M., Schubert, H. & Wein, B.B. (2004). Content-based image retrieval in medical applications. *Methods Inf. Med.* 43, 354-361.

Lehmann, T.M., Guld, M.O., Deselaers, T., Keysers, D., Schubert, H., Spitzer, K., Ney, H. & Wein, B.B. (2005). Automatic categorization of medical images for content-based retrieval and data mining. *Computerized Medical Imaging and Graphics.* 29, 143-155.

Lezoray, O. & Cardot, H. (2002). Histogram and watershed based segmentation of color images. *Proceedings of CGIV'2002.* 358-362.

Li, C., Xu, C., Gui, C. & Fox, M.D. (2005). Level set evolution without re-initialization: a new variational formulation. *IEEE Conference on Computer Vision and Pattern Recognition (CVPR).* 1, 430-436.

Li, C., Xu, C., Konwar, K.M. & Fox, M.D. (2006). Fast distance preserving level set evolution for medical image segmentation. IEEE International Conference on Control, Automation, Robotics and Vision (*ICARCV' 06).* 1-7.

Li, C., Kao, C.Y., Gore, J.C. & Ding, Z. (2007). Implicit active contours driven by local binary fitting energy. *IEEE Conference on Computer Vision and Pattern Recognition (CVPR).* 1-7.

Li., J. & Wang, J. (2003). Automatic linguistic indexing of pictures by a statistical modeling approach. *IEEE Transactions on Pattern Analysis and Machine Intelligence.* 25(10), 1-14.

Lin, M.W., Tapamo, J.R. & Ndovie, B. (2006). A texture-based method for document segmentation and classification. Joint Special Issue-Advances in end-user data-mining techniques. *ARIMA & SACJ,* 23, 49-56.

Lin, P., Yang, Y., Zhang, C. & Gu, J. (2004a). An efficient automatic framework for segmentation of MRI brain image. *Proceedings of the 4^{th} IEEE International Conference on Computer and Information Technology (CIT'04).* 896-900.

Lin, P, Yang, Y. & Zheng, C. (2004b). An efficient brain magnetic resonance image segmentation method. *Proceedings of the 3rd International Conference on Machine Learning and Cybernetic.* 2757-2760.

Long, F., Zhang, H.J. & Feng, D.D. (2003). Fundamental of content-based image retrieval. In: Feng, D. (Ed.), Multimedia Information Retrieval and Management, *New York: Springer-Verlag.* 1-26.

Lowe, H. J., Antipov, I., Hersh, W. & Smith C. A. (1998). Towards knowledge-based retrieval of medical images. The role of semantic indexing, image content representation and knowledge-based retrieval. *Proceedings of the Annual Symposium of the America Society for Medical Informatics (AMIA).* 882-886.

Lu, D. & Weng, Q. (2007). A survey of image classification methods and techniques for improving classification performance. *International Journal of Remote Sensing.* 28(5), 823–870.

Ma, W. Y. & Manjunath, B. S. (1997). Edge flow: a framework of boundary detection and image segmentation. *IEEE International Conference on Computer Vision and Pattern Recognition.* 744-749.

Ma, W. Y. & Manjunath, B. S. (1999). Netra: a toolbox for navigating large image databases. *Multimedia Systems.* 17(3), 184-198.

Malladi, R. & Sethian, J.A. (1996). A unified approach to noise removal, image enhancement and recovery, *IEEE Transactions on Image Processing.* 5(11), 1554-1568.

Mercimek, M., Gulez, K. & Mumcu, T.V. (2005). Real object recognition using moment invariants. *Sadhana.* 30(6), 705-775.

Mitchell, T.M. (1997). Machine learning. *New York: McGraw-Hill.*

Mojsilovis, A., Gomes, J. (2002). Semantic based image categorization, browsing and retrieval in medical image databases. *IEEE International Conference on Image Processing (ICIP' 02)*. 145-148

Mokhtarian, F., Abbasi, S. & Kitter, J. (1996). Efficient and robust retrieval by shape content through curvature scale space. *Proceedings of International Workshop on Image Database and Multimedia Search*. 35-42.

Montgomery, D.C. (2005). Design and analysis of experiments. 6th ed., New *York: John Wiley and Sons. Inc.*

Muller, H., Squire, D. M., Muller, W. & Pun, T. (1999). Efficient access methods for content-based image retrieval with inverted files. In: S. Panchanathan, S.F. Chang, C.C. J. Kuo (Eds.), multimedia storage and archiving systems IV (VV02). *Proceedings* of *SPIE*. 3846, 461-472.

Muller, H., Michoux, N., Bandon, D. & Geissbuhler, A. (2004). A review of content-based image retrieval systems in medical application-clinical benefits and future directions. *International Journal of Medical Informatics*. 73(1), 1-23.

Muller, H., Rosset, A., Garcia, A., Vallee, J.P. & Geissbuhler, A. (2005). Benefits of content-based visual data access in radiology. *Radio Graphics*. 25, 849-858.

Mumford, D. & Shah, J. (1989). Optimal approximation by piece-wise smooth functions and associated variational problems. *Commun. Pure Appli. Math*. 42, 577-685.

Naseer, A., Stergioulas, L.K. (2006). Discovering healthgrid services. IEEE *International Conference on Service Computing (SCC'06)*. 301-306.

Nuttall, A.H (1981). Some windows with very good sidelobe behavior", *IEEE Transactions on Acoustics, Speech, and Signal Processing* ASSP-29:1, 84–91.

Ogiela, M.R. & Tadeusiewicz, R. (2001). Semantic-oriented syntactic algorithms for content recognition and understanding of images in medical databases. *Proceedings of the 2nd International Conference on multi-media and exposition. IEEE Computer Society.* 621-624.

Ojo S.O., Olugbara O.O., Ditsa G., Adigun M. O. & Xulu S.S. (2007). Formal model for e-Healthcare readiness assessment in developing country context. *IEEE 4th International Conference on Innovations in Information Technology, Innovations Apo. 07, Dubai, UAE,* 41-45.

Olugbara, O.O., Adigun, M.O., Ojo, S.O. & Mudali, P. (2007a). Utility grid computing and body area network as enabler for ubiquitous rural e-Healthcare service provisioning. *Proceedings of IEEE 9th International Conference on e-Health Networking, Application and Services. 19-22 June, 2007, Taipei, Taiwan,* 202-207.

Olugbara, O.O., Ojo, S.O. & Adigun, M.O. (2007b). Requirements engineering framework for information utility infrastructure for rural e-Healthcare service provisioning. *IRMA, International Conference, Vancour, Canada,* 1644-1647.

Olugbara, O.O., Ojo, S.O., Adigun, M.O., Emuoyibofarhe, O.J. & Xulu, S.S. (2007c). An architectural framework for rural e-Healthcare information infrastructure with Web service-enabled middleware support. *HELINA Conference 2007: eHealth in Africa,* Bamako, Mali, http://www.sim.hcuge.ch/ helina/6.pdf.

Olugbara, O.O., Adigun, M.O., Ojo, S.O., Adewoye, T.O. (2007d). An efficient heuristic for evolving an agent in the strategy Game of Ayo. *ICGA Journal.* 30(2), 92-96.

Osher, S. & Sethian, J.A. (1988). Fronts propagating with curvature dependent speed: algorithm based on Hamilton-Jacobi formulations. *Journal of computational Physics*. 79, 12-49.

Osher, S. & Fedkiw, R. (2003). Level set methods and dynamic implicit surfaces: motion in the normal direction. *Springer-Verlag, New York.*

Palmer, S.E. (1999). Vision science: photons to phenomenology, *Cambridge, M.A: MIT Press*, 1999.

Paragions, N. & Deriche, R. (2002). Geodesic active regions and level set methods for supervised texture segmentation. *International Journal of Computer*. 46, 223-247.

Park, D., Park, J., Kim, T.Y. & Han, J.H. (1999). Image indexing using weighted color histogram. *Proceedings of the 10th International Conference on Image Analysis and Processing (ICIAP' 99)*. 909-914.

Park, M., Jin, J.S. & Wilson, L.S. (2003). Detection of abnormal texture in chest x-rays with reduction of Ribs. *VIP*. 71-74.

Parker, J.A., Kenyon, R.V. & Troxel, D.E. (1983). Comparison of interpolating methods for image re-sampling. *IEEE Transactions on Medical Imaging*. M1-2(1), 31-39.

Persoon, E & Fu, K. (1977). Shape discrimination using Fourier descriptors. *IEEE Trans. Syst. Man and Cybernatics*. SMC-7(3), 171-181.

Pham, D.L. & Prince, J.L. (1999). Adaptive fuzzy segmentation of magnetic resonance images. *IEEE Transactions on Medical Imaging*. 18(9), 737-752.

Pi, L., Fan, J. & Shen, C. (2007). Color image segmentation for objects of interest with geodesic active contour method. *Journal of Math Imaging Visualization*. 27, 51-57.

Prokop, R. J. & Reeves, A. P. (1992). A survey of moment-based techniques for unoccluded object representation and recognition. *CVGIP Graphical Models and Image Processing*. 54(5), 438-460.

Pun, T., Gerig, G. & Ratib, O. (1994). Image analysis and computer vision in medicine. *Computerized medical imaging and graphics*, 18 (2), 85-96.

Puzicha, J., Hofmann, T. & Buhmann, J. (1999). Histogram clustering for unsupervised segmentation and image retrieval. *Pattern Recognition Letter*. 20(9), 899-909.

Raghavan, V.V., Jung, G.S. & Bollmann, P. (1989). A critical investigation of recall and precision as measures of retrieval system performance. *ACM Transactions on Information System*. 7(3), 205-229.

Rees, D.G. (1987). Foundation of statistics. 1st Ed., *Chapman and Hall*.

Rogulin, D., Estrella, F., Hauer, T., McClatchey, R. & Solomonides, T., (2004), A grid information infrastructure for medical image analysis. http:// arxiv.org/ftp/cs/papers/0405/0405087.pdf.

Rubner, Y., Puzicha, J., Tomasi, C. & Buhmann, J.M. (2001). Empirical evaluation of dissimilarity measures for color and texture. *International Journal of Computer Vision and Image Understanding*. 84, 25-43.

Rucklidge, W.J. (1997). Efficiently locating objects using Hausdorff distance. *International Journal of Computer Vision*. 24(3), 251-270.

Rui, Y., Huang, T.S. & Mehrotra, S. (1997). Content-based image retrieval with relevance feedback in MARS. *Proceedings of International Conference on Image Processing*. 2, 815 -818.

Safar, M., Shahabi, C. & Sun, X. (2000). Image retrieval by shape: A comparative study. *IEEE International Conference on Multimedia and Expo*, 141-144.

Sajjanhar, A. & Lu, G. (1997). A grid based shape indexing and retrieval method. Special Issue of *Australian Computer Journal on Multimedia Storage and Archiving Systems*. 29(4), 131-140.

Sakai, T. (2007). Evaluating information retrieval metrics based on bootstrap hypothesis tests. *IPSJ Digital Courier*. 3, 625-642.

Sarvazyan, A. P., Lizzi, F. L., & Wells, P. N. T. (1991). A new philosophy of medical imaging. *Medical Hypotheses*. 36, 327-335.

Sclaroff, S. & Pentland, A. (1995). Model matching for correspondence and recognition. *IEEE Trans. on Pattern Analysis and Machine Intelligence (PAMI)*, 17(6), 545-561.

Selvarani, A.G. & Annadurai, S. (2008). Content-based image retrieval for medical images using generic Fourier descriptor. *Journal of Computational Intelligence in Bioinformatics*. 1(1), 65-72.

Sheikholeslami, G., Chang, W. & Zhang, A. (2002). SemQuery: semantic clustering and querying on heterogeneous features for visual data. *IEEE Transaction of Knowledge Data Engineering*. 14(5), 988-1002.

Shen, D. & Ip, H. S. (1998). Discriminative wavelet shape descriptors for recognition of 2-D patterns. *Pattern Recognition*, 32(2), 151-165.

Sheng, C. & Xin, Y. (2004). Shape-based image retrieval using shape matrix. *International Journal of Signal Processing*. 1(3), 163-166.

Sethian, J. A. (1996). Theory, algorithms and applications of level set methods for propagating interfaces. *Acta Numerica*. 309-396.

Sethian, J. A. (1999). Level set methods and fast marching methods. Cambridge: *Cambridge University Press*.

Shyu, C.R., Brodley, C. E., Kak, A. C., Kosaka, A., Aisen, A. M., Broderick, L. S.(1999). ASSERT: a physician-in-the-loop content-based retrieval system for HRCT image databases. *Computer Vision and Image Understanding* special issue on content-based access for image and video libraries, 75 (1/2), 111-132.

Simon, K.W. (1975). Digital image reconstruction and resampling for geometric manipulation. In *Proceedings of IEEE Symp. Machine Processing of Remotely Sensed Data*. 3A-1-3A-11.

Sinha, U. & Kangarloo, H. (2002). Principal component analysis for content-based image retrieval. *Radio Graphics*. 22 (5), 1271-1289.

Smeulders, A.W.M., Worring, M., Santini, S., Gupta, A. & Jain, R. (2000). Content-based image retrieval at the end of the early Years. *IEEE Transactions on Pattern Analysis and Machine Intelligence*. 22(12), 1349-1380.

Sohel, F.A., Karmakar, G.C. & Dooley, L.S. (2005). A generic shape descriptor using Bezier curves. *Proceedings of the International Conference on Information Technology: Coding and Computing, ITCC'05*. 2(2), 95-100.

Spackman, K.A., Campbell, K.E. & Cote, R.A. (1997). SNOMED RT: a reference terminology for healthcare. *Proceedings of AMIA Annual Fall Symposium*. 640-644.

Spiegel, M.R. (1972). Shaum's outline series, theory and problems of statistics. *McGraw-Hill Company*.

Spira, A., Sochen, N. & Kimmel, R. (2003). Efficient Beltrami flow using a short time kernel. *Proceedings of Scale Space 2003, Lecture Notes in Computer Science*. 2695, 511-522.

Squire, D. M., Muller, W., Muller, H. & Pun, T. (2000). Content-based query of image databases. In-17 *Aspirations from Text Retrieval, Pattern Recognition Letters*, B.K. Ersboll, P. Johansen, Eds., 21 (13-14), 1193-1198.

Stehman, S.V. & Czaplewski, R.L. (1998). Design and analysis for thematic map accuracy assessment: fundamental principles. *Remote Sensing of Environment*. 64, 331–344.

Stewart, B.K. & Langer, S.G. (1998). Integration of DICOM images into an electronic medical record using thin viewing clients. *Proceedings of AMIA Annual Symposium*. 902-906.

Stricker, M. & Swain, M. (1994). The capacity of color histogram indexing. In *IEEE Conference on Computer Vision and Pattern Recognition (CVPR94)*, 704-708.

Su, M.J., Chen, H.S., Yang, C.Y., Chen, S.J., Lee, W.J., Cheng, P.H., Yip, P.K., Liu, H.M., Lai, F.P. & Racoceanu, D. (2007). A preliminary study of medical image distributed intelligent access integrated with electronic medical records system for brain degenerative disease. *Proceedings of IEEE 9th International Conference on e-Health Networking, Applications and Services*. 19-23.

Su, Z., Zhang, H., Li, S. & Ma, S. (2003). Relevance feedback in content-based image retrieval: Bayesian framework, feature subspace and progressive learning. *IEEE Transaction on Image Processing*. 12(8), 924-937.

Sun, Y. & Ozawa, S. (2005). Efficient wavelet-based image retrieval using coarse segmentation and fine region feature extraction. *IEICE Transaction of Information and Systems*. Vol. E88-D, 1021-1030.

Swain, M.J. & Ballard, D.H. (1991). Color histogram indexing. *International Journal of Computer Vision*. 7(1), 11-32.

Szego, G. (1948). On an inequality of P-Turan concerning Legendre polynomials. *Bull American Math Society*. 54, 401-405.

Tao, Y., Grosky, W.I. & Delaunay, B. (1999). Delaunay triangulation for image object indexing: a novel method for shape representation. *Proceedings of the 7th SPIE Symposium on Storage and Retrieval for Images and Video Databases*. 631-642.

Teh, C. & Chin, R. T. (1988). On image analysis by the method of moments. *IEEE Trans. on Pattern Analysis and Machine Intelligence*, 10(4), 496-513.

Topel, T., Neumann, J. & Hofestadt, R., A. (2007). A medical case-based reasoning component for the rare metabolic diseases database Ramedis, *20th IEEE International Symposium on Computer-Based Medical Systems (CBMS'07)*. 7-11.

Traina, A.J.M., Castarion, C.A.B. & Traina, Jr. C. (2003). MultiwaveMed: a system for medical image retrieval through wavelets transformations. In *Proceedings of 16th IEEE Symposium on Computer-Based Medical Systems*. 150-155.

Tran, D.C. & Ono, K. (2003). Content-based image retrieval: object representation by the density of feature points. In *Proceedings of RIVF*. 213-218.

Tsai, A., Yezzi, A. & Willsky, A.S. (2001). Curve evolution implementation of the Mumford-Shah functional for image segmentation, denoising, interpolation and magnification. *IEEE Transactions on Image Processing*. 10, 1169-1186.

Tsai, C. & Hung, C. (2008). Automatically annotating images with keywords: a review of image annotation systems. *Recent Patents on Computer Science*. 1, 55-68.

Urban, J., Jose, J.M. & Rijsbergen, C.J.V. (2003). An adaptive approach towards content-based image retrieval. In *Proceedings of the 3rd International Workshop on Content-Based Multimedia Indexing*.

Vailaya, A. Figuiredo, M.A.T., Jain, A.K. & Zhang, H.J. (2001). Image classification for content-based indexing. *IEEE Transactions on Image Processing*. 10(1), 117-130.

Van Rijsbergen, C.V. (1979). Information Retrieval. *London, Boston. Butterworth, 2nd Ed.*

Vese, L. & Chan, T. (2005). A multiphase level set framework for image segmentation using the Mumford and Shah Model. *International Journal of Computer Vision*. 50(3), 271-293.

Voorhees, H. & Poggio, T. (1998). Computing texture boundaries from images. *Nature*. 333, 364-367.

Wang, J.Z., Li, J. & Wiederhold, G. (2001). SIMPLIcity: semantic-sensitive integrated matching for picture libraries. *IEEE Transactions on Pattern Analysis and Machine Intelligence*. 23(9), 947-963.

Wong, W. & Hsu, S. (2006). Application of SVM and ANN for image retrieval. *European Journal of Operation Research*. 173: 938-950.

Yates, D.S., Moore, D.S. & Starnes, D.S. (2008). The practice of statistics, 3rd Ed. *Freeman*.

Yezzi, A. J. (1998). Modified curvature motion for image smoothing and enhancement. *IEEE Transactions on Image Processing*. 7(3):345-352.

Yoon, S.W., Shin, H.S., Min, S.D. & Lee, M. (2007). Medical endoscopic image segmentation with multi-resolution deformation. *Proceedings of the IEEE 9th International Conference on e-Health Networking, Application and Services*. 256-259.

Zhang, J., Hsu, W. & Lee M.L. (2001). Image mining: issues, frameworks and techniques. In *Proceedings of the 2nd International Workshop on Multimedia Data Mining (MDM/KDD'2001)*. 232-242.

Zhang, D.S. & Lu, G. (2001). Content-based shape retrieval using different shape descriptors: a comparative study. *IEEE International Conference on Multimedia and Expo*. 317-320.

Zhang, D.S. & Lu, G. (2002). Shape-based image retrieval using generic Fourier descriptors. *Signal Processing: Image Communication*. 17, 825-848.

Zhang, W.M. & Wang, S.A. (2005). An efficient connectivity-number-based edge detection method for binary images. *Proceedings of the 4th International Conference on Machine Learning and Cybernetics*. 5324-5329.

Zhu, L., Zhang, A., Rao, A. & Srihari, R. (2000). Keyblock: an approach for content-based image retrieval. *ACM Multimedia*. 157-166.

Zhuang, A.H., Valentino, D.J. & Toga, A.W. (2006). Skull-stripping magnetic resonance brain images using a model-based level set. *Neuroimage*. 32(1), 79-92.

Zieren, J. & Canzler, U. (2006). Non-intrusive acquisition of human action in advanced man-machine interaction. *Signals and Communication Technology*, Kraiss, K.F. (ed.), 7-94.

Zunic, J., Kopanja, L. & Fieldsend, J.E. (2006). Notes on shape orientation where the standard method does not work. *Pattern Recognition*. 39, 856-865.